UNIVERSITÀ DI PISA

Scuola di Dottorato in Ingegneria "Leonardo da Vinci"

Corso di Dottorato di Ricerca in
Ingegneria Chimica e dei Materiali

Tesi di Dottorato di Ricerca

Polymer Modified Asphalt Nanocomposites (PMAN)

M.S. Sureshkumar

Anno 2011

UNIVERSITÀ DI PISA

Scuola di Dottorato in Ingegneria "Leonardo da Vinci"

Corso di Dottorato di Ricerca in
Ingegneria Chimica e dei Materiali

Tesi di Dottorato di Ricerca

Polymer Modified Asphalt Nanocomposites (PMAN)

Autore:

M.S. Sureshkumar

Relatori:

Prof. Giovanni Polacco, DICCISM, University of Pisa

Anno 2011

UNIVERSITÀ DI PISA

Scuola di Dottorato in Ingegneria "Leonardo da Vinci"

Corso di Dottorato di Ricerca in
Ingegneria Chimica e dei Materiali

Tesi di Dottorato di Ricerca

Polymer Modified Asphalt Nanocomposites (PMAN)

Autore:

M.S. Sureshkumar _____

Relatori:

Prof. Giovanni Polacco _____

Anno 2011

Abstract

Asphalt one of the versatile materials of antique, inspite of its compositional variations and complexities, widely employed in various applications like water proofing, paving etc. Due to the complex physical and chemical nature, Asphalt seldom performs well, without any modification. Amidst other materials, polymers found to be most suitable for modifying asphalt to suit the application demands. Nanomaterials, particularly invention of nanoclays, have enhanced the properties of polymers manifold when introduced in polymer. Polymer Nanocomposites thus obtained emerge with innovative properties which are not available with existing polymers. Similar to the effect of nanoclay in polymer, polymers improve the properties of asphalt. The hypothesis behind this work is to combine the advantages of nanoclay in polymer and polymer in asphalt by introducing, polymer and nanoclay in asphalt. Two different nanoclays, Cloisite 20A and Dellite 43B, were introduced along with EVA by different methods such as Physical Mixing and Melt Blending. This gave rise to Polymer Modified Asphalt Nanocomposites (PMAN) a new class of material. Thermal, morphological, structural and rheological properties were studied. Based on the above studies, fuel resistance PMAN with EMA, EVA and SBS developed. Also, flammability of PMAN was studied by developing new test method using Limiting Oxygen Index equipment. From this research work, new class of materials (PMAN) based on polymer and nanoclay with improved rheological and performance properties, fuel resistance were developed.

Sommario (in Italiano)

Il bitumen è un material molto versatile, utilizzato per pavimentazioni ed impermeabilizzazioni, sin da tempi molto antichi. Sino a pochi decenni orsono, il bitumen veniva impiegato prevalentemente tal quale. Poi, però, la necessità di prestazioni sempre più importanti ha portato alla introduzione, nel bitume, di agenti modificanti di varia natura. Fra questi, i materiali polimerici rappresentano sicuramente la categoria più importante. Più o meno contemporaneamente, sono nati i nanocompositi polimerici, nei quali un additivo di dimensioni nanometriche risulta disperso nella matrice polimerica. Rispetto agli additivi convenzionali ,di dimensioni micrometriche, i nanocompositi possono garantire prestazioni paragonabili anche con aggiunte molto modeste di additivo. L'idea di base di questa tesi è quella di combinare la modifica del bitumen con polimeri e dei polimeri con additive nanometrici. Sono stati quindi preparati dei materiali innovativi, battezzati "polymer modified asphalt nanocomposites" (PMAN) le cui proprietà sono state studiate nel corso dei 3 anni di dottorato. Questi materiali sono quindi dei sistemi ternari le cui componenti sono il bitume, un polimero ed un argilla organomodificata, che rappresenta la "nano componente".

Come materiali si sono utilizzati principalmente due polimeri, il copolimero styrene-butadiene-stirene (SBS) ed il copolimero etilene-vinilacetato (EVA), e due argille, la Cloisite 20A e la Dellite 43B. Queste ultime sono state aggiunte al sistema in due diverse maniere. La prima è un normale miscelamento fisico, nel quale polimero ed argilla sono aggiunte indipendentemente al bitume. La seconda invece prevede un pre-miscelamento di polimero ed argilla, con formazione di un nanocomposito polimerico classico, e quindi l'aggiunta di quest ultimo al bitume.
Le proprietà termiche, morfologiche e reologiche di questi materiali sono state quindi studiate, per confrontarle con quelle dei bitumi modificati "classici". Inoltre, sono state valutate le proprietà di resistenza a solventi idrocarburici, nonché la infiammabilità di questi materiali. Infine, è stata fatta una valutazione di questi materiali secondo la normativa americana SHRP.

Acknowledgments

daivattan oNTyOs phurnaa
menik yattan miLin hono
diyyo miLnattak kaamasko
hOnaa kai puurti, sattama.

- In, Sourashtra Niiti Sambhu, Verse 3, 1900,
By, Sourashtra Medhavi (Scholar) T.M Rama Rai.

(Oh, Great souls, Grace alone is not enough, it is fully realized when you put all your efforts)

With the above words, I realized grace when I blessed with an opportunity to undertake my research work at the University of Pisa, Pisa, Italy from Prof. Dr. Ing. Giovanni Polacco. Since the day I sent my first communication to till date I am showered with his kindness and simplicity, along with systematic guidance to my research degree.

I am highly indebted to Dr. Ing. Dario Biondi who took me into the world of asphalts, where I learned the fundamental about the handling of asphalt from processing to characterization, etc. I offer my sincere gratitude to Dr.ssa.Sara Filippi for her instrumental support and making some memorable moments.

Thanks are also to Prof. Dr. Ing. Massimo Paci for providing computer, and other necessary facilities whenever in need.

Amidst the above team members, I am indebted to the administrative and technical staff of University of Pisa, Pisa, Italy for the smooth flow of official proceedings.

When my stay at Italy was taken care by the good hearts, I had an opportunity to witness not only a new country but also a new dimension in my research work through Prof. Ludo Zanzotto, Chairman, Bituminous Materials, University of Calgary, Calgary, Canada. I offer my sincere thanks to Prof. Ludo Zanzotto for generous funding and great work.

Prof. Jiri Statsna plays a vital role in introducing me into the 'asphalt rheology' and a colorful stay at Canada.

I thank Dr. Igor Kazatchov for his esteemed presence and guidance during my experiments at Calgary, Canada.

I am highly indebted to Dr. Pavel Kriz and Dr. T. Lakshan J. Wasage who invested their invaluable time in training me with the rheological facilities at Bituminous Materials Lab., Calgary amidst their thesis work and I thank Dr. Mauricio Reeves for his friendship and care.

Thanks are also to Eva, Zuzana, Ryan, Dr. Susanna of Bituminous Materials Lab., Calgary, for their kindness and analytical support.

It is time to honour countless teachers/masters/professors, from my childhood to till date who carved this stone into a good shape and without whom I may not able to write this page. On this occasion, it is high time to thank the organizers of various Conferences for providing me with an opportunity to present this work and also to the Faculty members who blessed me with the invitation to present this work at their holistic academic premises.

Above all my parents blessing who not only dreamed about my research dimension but prepared to die-heard to fill the voids created by me when I started for a long-term career.

Whatsoever, I have done could not have completed nicely without my wife Kavitha (meaning of the name: poem) who converted my life lines as poems and prepared to spend the days in loneliness and permitted to 'fly away' for Ph. D., by side-lining her tears smoothly and silently.

It is very difficult to list the friends from whom I have received lots and lots of help, leaving me as a big lender. Though these pages may look big, but still I feel tiny in front of your tremendous and timely help. Instead of thanking you, I beg you to leave me with an opportunity to show my kindness and love.

With all these I was able to realize the omni-presence,

With love,

എം. എസ്. സുരേഷ്കുമാർ
M.S. Sureshkumar

Pisa, Italy, Apr 06, 2011

Dedicated to

My Mother

ಎಸ್. ಯು. ಉಷ

S. U. Usha

and my Father

ಎಸ್. ಕೆ. ಸುಬ್ರಮಣಿಯನ್

S. K. Subramanian

Contents

List of Figures

List of Tables

Chapter 1

1.1 PREFACE

Asphalt one of the oldest engineering material is widely employed for pavements amidst other applications. Asphalt due to its complex chemical and physical properties is not suitable for application without modification. Various materials were employed for modification of asphalts and polymers were identified as suitable candidates among them. Due to the ever increasing number of vehicles and amount of materials transported, the service demands of modern day pavements increase day-by-day. Apart from this, the changes in climatic condition pose a big challenge in maintaining pavements. This opens a new avenue from civil engineers to chemists to address the issue. Recent breakthrough in materials with the introduction of nano materials or nano clays specifically embodied asphalts too.

1.2 STATEMENT OF THE PROBLEM

For the past two decades Polymer Nano composites emerged as an innovative material with new properties after the discovery of nano clay. Nanoclays are the materials employed in asphalt for modifying the asphalt properties. At the same time, the presence of nano clays along with polymers was seldom available in the literature. The introduction of nano clay and the method of introduction of nano clay in the asphalt along with polymer anticipated to have significant impact in the performance and other properties of asphalt. This thesis records the thermal, rheological, morphological, performance properties of asphalt upon addition of polymer/nano clay.

1.3 HYPOTHESIS

Nano clays improve the properties of polymers, in the similar fashion polymers improve the properties of asphalt. Though these are different aspects, the common material involved in this different process is polymer. By harnessing the advantages of the presence of nano clay in polymer and polymer in asphalt,

attempt has been made to obtain a new class of material called Polymer Modified Asphalt Nanocomposites (PMAN) having the synergism of both the systems. Based on this new class of pavement materials using different polymers have been prepared.

1.4 OBJECTIVE

The main objective of the thesis:

- To obtain PMAN with different polymers
- To study the performance and rheological properties of PMAN
- To prepare PMAN with fuel resistance to meet the special requirement of pavements at airport filling stations, industries
- To study the flammability of PMAN

1.5 ORGANIZATION OF THE THESIS

The thesis summarizes the research work carried out during January 2008 to December 2010 at the Department of Chemical Engineering, Industrial Chemistry and Materials Science (DICCISM), University of Pisa, Pisa, Italy, and Bituminous Materials Laboratory, Schulich School of Engineering, University of Calgary, Calgary, Canada.

Chapter 2 describes the detailed literature about the modification of asphalt with special emphasis to nano material modification of asphalt. Preparation and detailed rheological studies of ethylene vinyl acetate asphalt nanocomposites (EVAN) obtained using ethylene vinyl acetate (EVA) and different nano clays are described in Chapter 3. In Chapter 4, fuel resistance PMAN obtained using different polymers such as EVA, ethylene methacrylate (EMA) and styrene-butadiene-styrene (SBS). Flammability property of PMAN and a new method for obtaining the flammability are provided in Chapter 5. Chapter 6 describes the SHARP analysis of developed PMAN for Performance Grading. Further scope of research follows chapter 6, with the Award received in this thesis work and List of Publications as final part.

Chapter 2

2.1 INTRODUCTION TO ASPHALTS

Asphalt is used as a road carpeting material throughout the world. Asphalt is a black or dark brown solid or semi-solid thermoplastic material possessing water-resistant and adhesive properties. Asphalt is obtained while processing naturally available ground oil (always referred as 'crude oil') and is a complex combination of high molecular weight organic compounds containing a relatively high proportion of hydrocarbons having carbon numbers greater than C25 with a high carbon to hydrogen ratio. It also contains trace amounts of metals such as nickel, iron or vanadium [1, 2]. According to the Oxford English Dictionary [3], asphalt is, "A bituminous substance, found in many parts of the world, a smooth, hard, brittle, black or brownish-black resinous mineral, consisting of a mixture of different hydrocarbons". ASTM [4] definitions for bitumen and asphalt are: (Bitumen are) Mixtures of hydrocarbons of natural or pyrogeneous origin, or combinations of both, frequently accompanied by their non-metallic derivatives, which may be gaseous, liquid, semisolid, or solid, and which are completely soluble in carbon disulphide and (Asphalt is a) Black to dark-brown solid or semi solid cementitious materials which gradually liquefy when heated, in which the predominating constituents are bitumens, all of which occur in the solid or semi-solid form in nature or are obtained by refining petroleum, or which are combinations of the bitumens mentioned with each other or with petroleum or derivatives thereof". Though asphalt and bitumen defined differently, still the exact framers are unclear. So, a tenable position is not arrived. Moreover the definition varies regionally, in Asia and Europe it is called as Bitumen and in American continent it is called as Asphalt. Asphalt / Bitumen are employed synonymous in the thesis. Owing to its complexity, Asphalts could be considered as mixtures of an indefinitely large number of chemical individuals of mainly of hydrocarbon nature, but varying in the structure of the hydrocarbon (eg., in aromaticity and branching) in the presence of other elements (apart from carbon and hydrogen) such as oxygen, sulfur, nitrogen with varying molecular weight components [5]. Naturally occurring asphalts called Lake asphalt discovered in 1595 by Sir Walter Raleigh in Trinidad. Rock asphalt is extracted from mines or quarries depending on the type of deposit. Rock asphalt occurs when bitumen,

formed by the same concentration processes as occur during the refining of oil, becomes trapped in impervious rock formations. The largest deposits in Europe were found at Val de Travers in Switzerland, Seyssel in France and Ragusa in Italy, all of which were mined in underground galleries. Another variety of natural asphalt is Gilsonite, discovered as vertical deposits in the 1860s by Samuel H Gilson in 1880 used as waterproofing agent for timber. Due to the labor intensive nature of the mining process, Gilsonite is relatively expensive. This makes this material unattractive for wide-spread use in paving materials [6].

'Tar' is the generic word which have been employed for the liquid obtained when natural organic material such as coal or wood are carbonized or destructively distilled in the absence of air. Though it sounds synonymous with asphalt or bitumen, the major difference is asphalt is the product obtained from the vacuum distillation of natural ground oil.

2.2 NOMENCLATURE

Asphalt appears to have been used practically in every civilization since thousand decades. Several subtle distinctions depending on the source, usage, type of application, etc., were found in Prakrit (naturally evolved language existed in pre-writing period), Sanskrit, the refined form of the language spoken in the Bharada Kandam (or Indian sub-continent/Indian peninsular region) [7] that predates much before present day or Gregorian record of time. Apart from twenty terminologies in Sanskrit [8], Forbes [9, 10] and others [11] have compiled the related terminologies from Latin, Greek, Sumerian, Assyrian, Egyptian, Turkish, etc.

2.3 APPLICATIONS OF ASPHALT

Naturally available materials were used diversely since the existence of mankind. Asphalt/Bitumen has its usage from the Hummailan period estimated as 1,80,000 B.C., as per Gregorian calendar [12, 13]. Irrespective of the difference in opinion [14-16] about the period, the great Bhaaratian (Indian) epic Mahabhaaratha, having its existence since primitive period, mentions a house build with bitumen, among other construction materials, with the specific intention of consigning the residents of fire by of the nature of the construction material. Excavations in the Indus Valley (northwestern region of Bhaarada Kandam) revealed asphalmastic composed of a mixture of asphalt, clay, gypsum and organic matter between two brick walls as well as on the outside of walls and beneath the floor of a bathing pool used for ritualistic cleansing. The age of the mixture dated about 3000 B.C., prewriting period of India. This mastic was also used for inlaid decorations, as an adhesive for the application of ornaments to statues, and as a protective coating for woodwork. Seepages of liquid asphalt, as well as many rock asphalt deposits, exist today on the Basti River in Kashmir as well as near Hotien, Xinjiang, China [17, 18]. Some historical applications of bitumen obtained from Forbes [10] are provided as Figures 2.1 to 2.4.

Figure 2.1 *Excavations of Mohenjadaro showing water tank in front of the temple where walls sealed with Bitumen (a) Water tank, (b) Close look of wall.*

Figure 2.2 *Bitumen mortar of Corbel vaulted chamber*

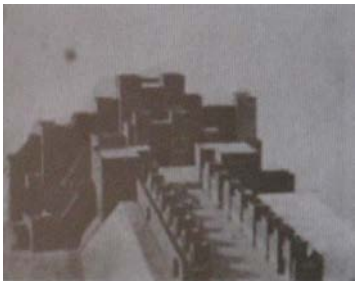

Figure 2.3 *Model Road – Aibur shabu of Babylon*

Account of asphalt applications is described by Abraham [19]. Connan [20] lists the use and trade of bitumen in antiquity and pre-history. Table 2.1 provides some of the ancient applications referred by Connan [19]. The Shell Bitumen Handbook [6] lists over 250 known current uses for bitumen in agriculture, construction, hydraulics, erosion control, automobile industry, electrical industry, railways, paving industry, etc. Few applications that are available [21, 22] including the use of asphalt in electrical appliances and the issues related to it [23-29] are consolidated by Murali Krishnan and Rajagopal [7]. Apart from this, Bitumen is also used to store and contain low and moderate radioactive wastes [7].

Figure 2.4 *Mastic covered toilet seat*

2.4 CHEMISTRY AND STRUCTURE OF ASPHALT

Asphalt consists of tens of thousands different chemical species [30]. The whole scale of molecules ranges from non-polar fully saturated linear alkanes to highly polar polycyclic porphyrins or hetero-hydrocarbons [31]. The chemistry of asphalt is still not completely understood due to the large variety of its chemical compounds. In general, asphalt consists of hydrocarbons, which differ significantly in molecular structure, molecular weight or polarity.

Table 2.1 Ancient applications of Asphalt (Bitumens)

Use of Bitumen	Examples	Excavations with example studied
mortars in construction building	temples, palaces, terraces, doors, ziggurats,	door threshold, courtyard of Mari, Babylon, Larsa, Har
waterproofing agent	mats, baskets, jars, water reserves, bathrooms, water pipes, cisterns, boats, sarcophagi	Tell es-Sawwan, Tell el'Oueili, Qal'at al-Bahrain, Saar, Bagh
adhesive and glue sickles	tool handles, statues, jars, decoration (game, lyre, temple, pillar, ostrich egg)	Tell Atij, Netiv Hagdud, Umm El Tlel,Mari, Tell Halula, Ras Shamra, Susa
domestic artefacts	spindle whorls, balls, dice, wall cones	Tell el'Oueili, Failaka, Saar, Qal'at al-Bahrain, Susa, Tell Brak
jewellery	bead, ring, gold badges on clothing or for horse harnesses	Umm al-Qaiwwain, Ulu Burun, Susa, Saar
sculpture	sculpture, cylinder and stamp seal of Susa in bitumen mastic	Susa
mummication	mixed with conifer resin, beeswax, grease to prepare mixtures for embalming	Egyptian mummies from the Queen valley and from several Museums (Lyon, Hannover, Paris)

Asphalts composed of aliphatic straight chain alkanes (paraffins), branched chain hydrocarbons (iso-alkanes), saturated, cyclic hydrocarbons with one or more rings (naphthenic rings) or aromatic hydrocarbons with single or condensed aromatic rings. Although molecules are composed predominantly of carbon and hydrogen, most molecules contain one or more of the heteroatoms such as sulphur, nitrogen, and oxygen. Also the trace metals such as vanadium and nickel are present in asphalts, predominantly in its heavy parts, mostly in the form of porphyrins. The

heteroatoms significantly contribute to the polarity of asphalt [32]. Asphalt components can be separated and evaluated by using various methods such as: solvent extraction, adsorption by finely divided solids and removal of unadsorbed solution by filtration, chromatography and molecular distillation used in conjunction with one of the above techniques. Irrespective of several techniques, it is possible only to separate asphalt into two broad chemical groups called Asphaltenes and Maltenes. The maltenes can be further divided into saturates, aromatics and resins . Polarity is the separation of charge within a molecule due to an imbalance of electrochemical forces within the molecule that produce a dipole [33].

.

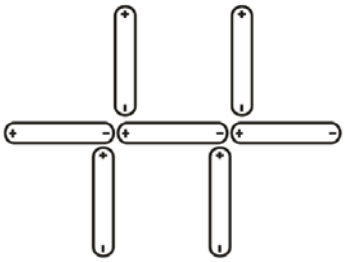

Figure 2.5 *Asphalt Polar Molecule Associations [33].*

According to Robertson [33], the polarity can be considered as a major contributor to the characteristics of asphalt performance. Robertson reports that polar molecules tend to associate into the matrix (Figure 2.5), which is dispersed in a non-polar continuous medium. This matrix is composed of associated polar molecules that give the asphalt its elastic character, while the non-polar phase provides asphalt with its viscous character.

According to this theory, excessive association and structuring (high initial heteroatom content or increased content of heteroatoms because of oxidative aging) can lead to hard and brittle binders that are prone to cracking, while poor structuring can lead to easily deformable materials. Elemental analysis proved to be a valuable tool in the determination of elemental composition of asphalts, especially in terms of heteroatoms. According to Moschopedis and Speight [34], the elemental composition of asphalts may be used as a guide to the changes in composition taking place during air blowing (oxidation) of the materials. Oxidation reactions usually cause an increase in the amount of present oxygen. Also some reactions leading to the elimination of sulphur or nitrogen atoms may occur and this change of chemical composition can help us to understand the changes of physical properties of these materials.

2.5 COLLOIDAL CHARACTERISTICS OF ASPHALTS

Asphalt has been historically modeled as a colloidal system consisting of asphaltenes which are dispersed in maltenes and where resins act as a peptizing agent (Figure 3-7). From the colloidal standpoint asphalts have been classified as

sol and gel types [35] (Figure 2.6). Sol type asphalts are characterized by low content of asphaltenes and exhibit purely viscous (Newtonian) flow, high temperature susceptibility and higher ductility. In gel type asphalts the content of asphaltenes is relatively high and asphalts exhibit non-Newtonian flow, lower temperature susceptibility and ductility. Sol type asphalts are considered as compatible and gel type as incompatible asphalts [35]. In general, the boundaries between these two systems are not clear and therefore the asphalts with their properties between sol and gel asphalts are called the sol-gel asphalts.

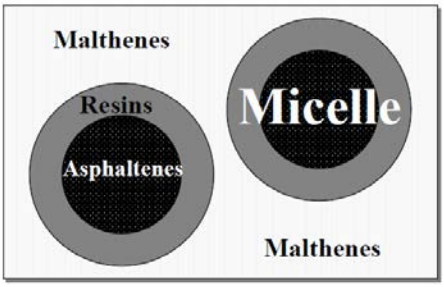

Figure 2.6 *Schematic traditional representation of asphalt as a colloidal system.*

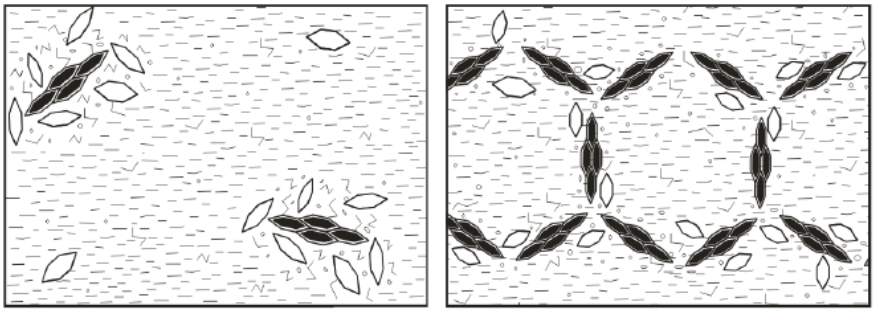

Figure 2.7 *Schematic representation of Sol (left) and Gel type (right) asphalt [36].*

According to an absolute majority of authors and experimental evidence, asphalt is a multi-disperse micellar system. The study of the internal working of this system is made extremely difficult by the very high viscosity of asphalt and complexity of its components. For the macrostructure of asphaltenes, Yen [37-40] unisotropic structure of mesomorphic liquid in which many individually oriented clusters are suspended and randomly distributed within lower molecular weight homologues. The individual clusters are ordered and consists in a number of planar aromatic molecules stacked in layers via π- π association. He suggests a unit sheet mass of 1000 to 4000, a cluster or particle mass of 4000 to 10,000 and a micelle mass of 40,000 to 40,000,000. The macrostructure of petroleum derived asphaltene as proposed by Yen is shown in Figure 2.8.

Yen estimated the molecular weight of petroleum asphaltenes to be between 800 and 2500, and proposed a hypothetical formula (figure 2.9) of asphaltene molecule

by considering asphaltenes as multipolymers, polycondensated substances with different repeating blocks, associated by inter and intramolecular interactions within the structure.

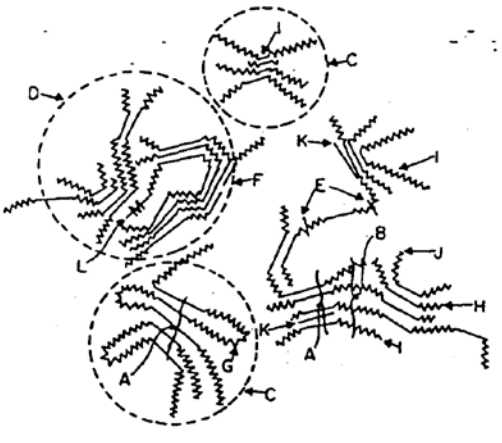

Figure 2.8 *General feature of macrostructure of asphaltene and related components.*

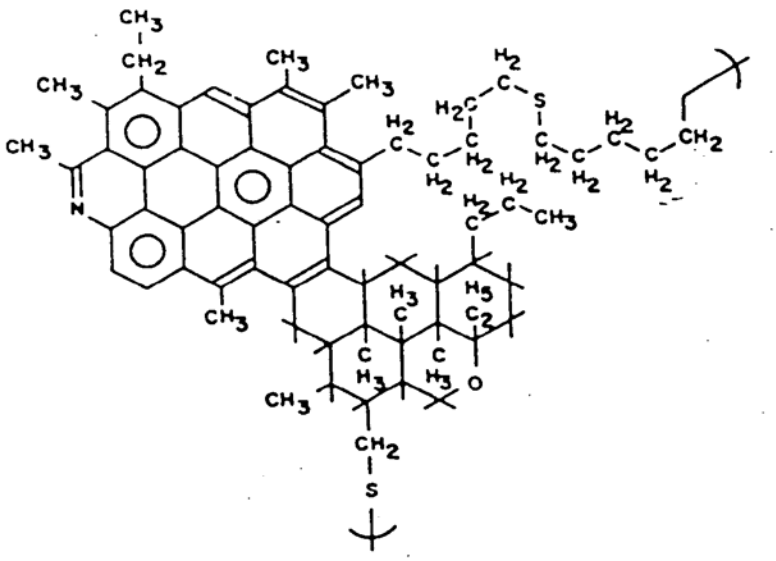

Figure 2.9 *Hypothetical structure of Asphaltene [18]*

In the 1930s, Nellensteyn described asphaltenes as a micelles consisting of microcrystalline graphite particles [41]. In the 1940s, Pfeiffer and Saal [42] suggested that asphaltenes are probably composed of aromatic hydrocarbons of high molecular weight. Since then the molecular character of asphaltenes has been subject of numerous investigations using various techniques such as X-ray diffraction (XRD) [43-46] nuclear magnetic resonance (NMR) [47-50] or infrared spectroscopy (FTIR) [51-54] which defined asphaltenes as a complex polyaromatic structures bearing long aliphatic and alicyclic substituents with heteroatoms (O, N, and S) as a part of the aromatic system and trace metals (V, Ni) as porphyrins (figure 2.10).

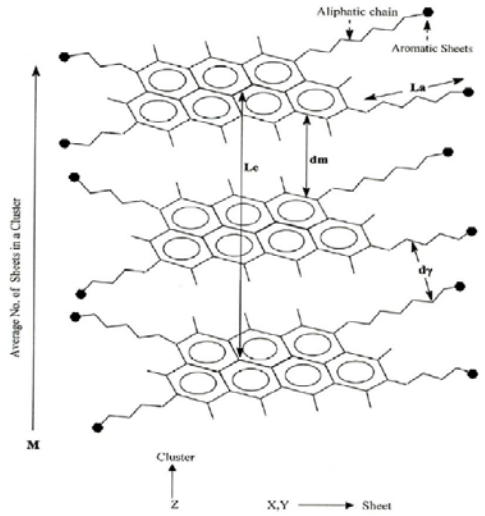

Figure 2.10 *Cross-section of Asphaltene model illustrating the group types that gives rise to the XRD peaks* [55].

Yen [55] used XRD technique for characterization of asphaltenes in crude oil. Based on XRD data he proposed a model for macrostructure of asphaltenes (see Figure 2.11). The XRD method is able to provide information about the aromaticity and crystalline parameters of asphaltenes such as distance between aromatic sheets, layer diameter, height of the unit cell, and the number of the sheets contributing to the unit. Decroocq et al. [56] used XRD to investigate and observe structural transformations (change in peak position, intensity of bands) in asphaltenes and resins during heat treatment. Those transformations are being used in assessing the changes in structure of asphaltenes on aging.

The investigations of structural parameters of asphaltenes were accompanied by investigations of asphaltene aggregation phenomenon. Asphaltene molecular weights have been determined by using various techniques (ultracentrifuge, ebullioscopic, cryoscopic method, vapour pressure osmometry etc. [57]) and obtained molecular weights significantly varied from 1000 up to 300 000 g/mol. It is

now recognized that major source of such discrepancies lies in the formation of asphaltene aggregates due to intermolecular associations [58]. As reported in the literature, the strength of the interaction among asphaltene molecules increases with increasing polarity of the sample, decreasing temperature and decreasing polarity of the solvent [59]. Many researchers have studied the colloidal particles in crude oil or bitumen [60-63]. Various techniques have been employed to investigate the size of colloidal particles, including scanning electron microscopy [63, 64], high resolution transmission microscopy [65], and small angle X-ray scattering [62]. Loeber [66] used microscopic techniques and observed asphaltene aggregates of 100-200 nm in size. Similarly, Baginska and Gawel [63] using scanning electron microscopy observed asphaltene aggregate particles in size from 110-260 nm. According to Dickie [64] the size of individual asphaltene particles varies from 4 to 10 nm and that of asphaltene micelles ranges between 15 and 30 nm.

Recently a dispersed polar fluid model (DPF) developed during the SHRP research has been proposed as an alternative to already existing traditional micellar model. The DPF model does not consider the asphalt as a two phase colloidal system consisting of continuous low polar phase and dispersed asphaltene phase but essentially as a single-phase system. The DPF model explains asphalt microstructure as a continuous three-dimensional association of polar molecules (generally referred to as "asphaltenes") dispersed in a fluid of non-polar or relatively low-polarity molecules (generally referred to as "malthenes") [67]. Model is based on the fact that the molecules are able to form dipolar intermolecular bonds of varying strength. However, since these intermolecular bonds are much weaker than the bonds in hydrocarbons they break first and govern the asphalt behaviour. Physical properties of asphalts are therefore result of forming, breaking and reforming these weak dipolar intermolecular bonds [67]. Masson [68, 69] used atomic force microscopy (AFM) to detect new phases such as catana, peri, para and sal in asphalt. Recently, DE Moraes [70] et. al., have studied the phase morphology of 30/45 pen grade asphalt with high temperature AFM.

2.6 INDUSTRIAL CLASSIFICATION OF ASPHALT/BITUMEN

Apart from the chemical and structural aspect, asphalt/bitumen is classified on the basis of production or industrial manufacturing.

Penetration Grades – are usually produced from naturally available (crude) petroleum oil atmospheric distillation residues by using further processing such as vacuum distillation, thermal conversion, partial oxidation (air rectification/semi-blowing) or solvent precipitation. A combination of these processes can be used to make different grades which are normally classified by penetration value specifications. They are principally used for road surfacing and in roofing.

Hard Bitumen (asphalt) – are manufctured using similar processes to penetration grades but have lower penetration values and higher softening points, i.e., they are harder and more brittle. The main use is in the manufacture of bitumen paints and

enamels. They are normally classified by a softening point specification and designed by a prefix H (hard) or HVB (high vacuum bitumen).

Oxidized bitumens (Air Blown Asphalt) – are produces by passing air through a bitumen feedstock under controlled conditions. This produces higher softening point bitumen with reduced susceptibility to change with temperature and greater resistance to imposed stresses. Applications include use in roofing materials, waterproof papers, electrical components and many other building and industrial products. Classification is normally by both penetration value and softening point specifications.

Bitumen(asphalt) derivatives – are proprietary fromulations classified as: Cutback Bitumens, Fluxed Bitumens, Bitumen Emulsions and Modified Bitumens.

2.7 ASPHALT MODIFICATION

Asphalt binder constitutes only a small but crucial part of any paving mix. Thermo-mechanical properties of asphalt are determined by its complex internal structure that is not quite known, yet. Phenomenologically, asphalt can be characterized as a low molecular weight viscoelastic material with strong temperature susceptibility. At higher temperatures asphalt behaves as a viscoelastic liquid and at low temperatures it is a brittle viscoelastic material prone to cracking even at moderate loads. Moreover, at low temperatures asphalt can stay at non-equilibrium thermodynamic state for extended periods of time. This is the effect of its complex internal structure. Such a complex behavior create problems in engineering applications of asphalt binder in paving mixes. Therefore, asphalt modification, with various types of materials, has been attempted to overcome, or at least delay, the above-described problems.

Asphalt modification date backs to four decades [72]. Some of the common materials used for asphalt modification are sulphur [73-75], organic polymers [76-78], copolymers [79, 80], polymer blends [81], modified polymers [82-84], pyrolitic carbon black [85], maleic anhydride, dicarboxylic acid [86], phosphazenes [87], lime [88], etc. Ray provides a concise account on the history and development of modified bitumen [89]. An outline of the materials used for modifying asphalt is tabulated by Isaccson [90, 91]. Yue summarizes the usage of recycled solid waste materials employed in asphalt pavement [92].

2.8 POLYMER MODIFIED ASPHALTS (PMA)

Irrespective of various materials employed for modifying asphalt, polymers are the preferred materials to tailor the asphalt for various applications for the following host of reasons:

- To obtain softer blends at low service temperatures and reduce cracking

- To reach stiffer blends at high temperature and reduce rutting
- To reduce viscosity at layout temperatures
- To improve stability and strength of mixtures
- To improve the adhesion resistance of blends
- To improve fatigue resistance of blends
- To improve oxidation and aging resistance
- To reduce structural thickness of pavements
- To reduce life cost of pavements

Polymers are added to asphalt to increase its toughness and viscosity. There are two important category of Polymer Modified asphalt: one is mixtures which are said to be simple where, no chemical reaction occurs between the asphalt and polymer. In this case the polymer is considered as filler only. Another is complex due to the possible chemical reaction occurs between the components present which is not going to be discussed in the thesis.

This is explained schematically, using styrene-butadiene-styrene as example (figure 2.12). Primarily polymer (SBS) molecules trapped in the bitumen mass and a network is formed enclosing the asphalt. In such blends, nodules of the styrene and butadiene copolymer aggregate forming micelles which are bound to each other by butadiene chains. The structure is predicted below (figure). The result is the formation of a network in which the bitumen is embedded.

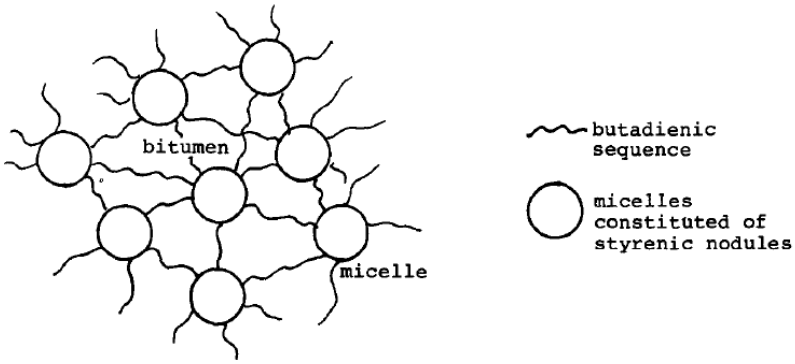

Figure 2.11 *Schematic representation of Polymer Modification in Asphalt.*

Apart from the polymers cited above, various polymeric materials such as thermoplastics like polyethylene [93], chlorinated polyethylene [94], ethylene vinyl acetate (EVA) [95, 96], low density polyethylene (LDPE), high density polyethylene (HDPE) [97-100], different types of polyethylene [101] and elastomers such as natural rubber (NR) [102-104] and NR latex [105, 106], styrene butadiene styrene (SBS) [107], styrene-butadiene random copolymers (SBR), styrene isoprene styrene (SIS), polybutadiene, ethylene propylene diene rubber (EPDM) [82-84], blend of HDPE/EPDM [94], styrene ethylene/butylene styrene (SEBS) [108], crumb rubber [82], chlorothio phenol devulcanized rubber [108], hydrogenated SBS [109] have been investigated as polymers for modifying bitumen. Also,

copolymers such as alkyl(meth)acrylate-maleic anhydride [79], various copolymer containing arene polymer end block, one conjugated diene mid block and (ethylene-propylene) styrene copolymer [110] and SBS tri block copolymer [80], glycidylmethacrylate functionalized polymer [111] has been studied for modifying bitumen.

Irrespective of virgin polymers, waste/recycled polymeric materials also have been identified as a suitable polymer material for asphalt modification. A comprehensive account of recycled polymer used in the asphalt modification is provided by Murphy [112]. As polymer modification of asphalt is ever expanding with new approach [113], it is very difficult to present the complete account of current scenario in asphalt modification.

From the above studies, it is evident that polymers are the suitable material to modify asphalts, which in turn increases (a) *the high temperature stiffness* (b) reduces the low temperature stiffness (c) *improves fatigue resistance* (d) improves age hardening resistance (e) *facilitates the preparation of stiffer hot-mixes* as compared to base (i.e., neat or unmodified) asphalt. The associated advantages with the improvement in these properties respectively are: (a) *resistance to rutting bleeding and flushing* (b) prevention of thermal cracking (c) *prevention of ravelling and cripping* (d) increase in durability and (e) *possibility of thinner lifts* [114].

2.9 POLYMER MODIFIED ASPHALT NANOCOMPOSITES (PMAN)

Thus, the modification of asphalts by polymers has become a common method to improve the performance properties of binders for pavements. Since the invention and the subsequent production of layered silicates in nanometer (nm) range in 1985 at Toyota Central R & D laboratory, a great interest has been generated in the academic and industrial communities, leading to the invention and innovation of materials that contain nanomaterial as one of the component. Polymer nanocomposites basically consist of a blend of one or more polymers with various nanomaterials like nano clays, carbon nano tubes, etc.

The modification of asphalt using polymer/nanoclay [115-119] has generated a new class of materials, viz., polymer modified asphalt nanocomposite (PMAN). PMAN is a ternary blend of polymer/nano clay prepared by adding the nano clay and polymer to the asphalt, either separately or in the form of a pre-mixed master batch [117, 118]. Recent investigations revealed that the method of incorporation of nano clay into the asphalt has significant effect on the blend morphology, dispersion and rheological properties [117, 118]. PMAN obtained with different polymers found to possess excellent fuel resistance [120]. Thus, PMAN is emerging as a new class of pavement materials with synergism of properties obtained from polymer nanocomposites and polymer modified asphalt.

Chapter 3

3.1 INTRODUCTION

Since the rediscovery of nano materials in 1985 at the Toyota Central R & D laboratory [121] and the subsequent development of polymer nanocomposites, such materials have generated a great deal of interest in the academic and industrial communities. Polymer nanocomposites basically consist of a blend of one (or more) polymer with various nanomaterials like nanoclays, carbon nanotubes, etc. Polymer–clay nanocomposites (layered silicate nanocomposites) are basically filled polymers in which at least one dimension of the dispersed phase is on a nanometer scale [122, 123]. Three types of structural arrangements are possible in layered silicate nanocomposites [124]: immiscible, where the polymer does not penetrate the bundle of silicate layers; intercalated, where the polymer chains penetrate the bundles of silicate layers without destroying the stacking layers; exfoliated (delaminated), where individual silicate layers are dispersed in the polymer. Polymer–clay nanocomposites are studied because of their superior thermo-mechanical properties even at low concentrations of clay [125]. Generally, the exfoliated nanocomposites (individual layers are irregularly delaminated and dispersed in a continuum polymer matrix) are materials with better physical properties when compared with intercalated nanocomposites [126]. Traditionally, the structure of nanocomposites is investigated by X-ray diffraction (XRD), transmission electron microscopy (TEM) and by differential scanning calorimetry (DSC) [122-125]. Lately, dynamic mechanical analysis (DMA) and other rheometric flows have been used in the study of nanocomposites. According to Krishnamoorti and Yurekli [124], rheological studies showed a transition from liquid-like to solid-like behavior with little difference between intercalated and exfoliated nanocomposites. The time–temperature superposition principle was quite frequently used when studying the dynamic properties of nanocomposites [124, 125, 127]. Some examples of nanocomposite systems that are not rheologically simple were given [127]. The creep study of polypropylene nanocomposites [128], showed a decrease of creep compliance, thus confirming the solid-like behavior of these systems. The ability of shear deformation, with large amplitudes, to orient nanocomposites was also studied [129-133]. In many cases the layered silicate nanocomposites behave like anisotropic materials i.e. the silicate layers orient in the shear direction. On the other hand some studies

reported the perpendicular orientation of at least some fraction of silicate layers, [134-136]. Naturally the orientation of silicate layers will determine the properties of various material functions. When studying the polypropylene–clay nanocomposites by rheological methods it was shown that the effect of flow can lead to break down of the aggregate network, and possibly, the aligning of the structural elements [137]. This resulted in time and shear history dependence of rheological properties. Vermant [137] et al., introduced a combination of transient flow protocols in order to separate the effects of flow on the aggregate structure and on the orientation of nanoclay domains.

The degree of exfoliation was determined from the low frequency viscoelastic behavior and the high frequency behavior of dynamic moduli allowed estimation of the quality of dispersion. From an engineering point of view, an ideal asphalt binder should be resistant to permanent deformation at higher temperatures (in order to decrease the rutting potential of asphalt paving mixes), it has to be stable in storage and at low temperatures it should be less prone to the developments of cracks. The ultimate goal of modification of asphalt by polymers is to satisfy these requirements. Despite of many investigations these goals were not reached and moreover an unambiguous characterization of these systems is not known, yet. The use of ternary systems, asphalt/polymer/nanocomposite, is a novel approach to the asphalt modification and our intention was at first to study the properties of such individual systems before any suggestions can be made for practical use of these systems as binders in paving mixes. The present chapter follows a previous study where the effect of the addition of clay as a third component in polymer-modified asphalt was investigated [117]. The main idea is, therefore, to combine the effects induced on the polymer properties by the addition of nanoclay, with the asphalt modification. The ternary blend can be defined as polymer-modified asphalt nanocomposites (PMAN). In the first paper [117], the asphalt was modified by using poly(styrene–butadiene–styrene) block copolymer (SBS). After a preliminary investigation on the binary asphalt/clay and polymer/clay blends, the ternary blends were prepared by adding the clay and polymer to asphalt, either separately or in the form of a premixed master batch. Intercalated nanocomposites with comparable interlayer distances and glass transition temperatures were obtained in both cases; however, the results showed that the mixing procedure significantly affected the final rheological properties. Here, a similar procedure is followed by using poly(ethylene–vinyl acetate) (EVA) as a main part of EVA-organoclay modifiers of a conventional asphalt.

EVA is a thermoplastic material, that resembles elastomers in softness and flexibility, which is commercially available with the percentage of vinyl acetate varying from 10% to 40% depending on the requirements. After SBS, EVA is probably the most important polymeric modifier for asphalts and an abundant literature is already available, both for the virgin [139-142] and recycled [143–148] polymer. At the same time, EVA copolymers were intensively investigated for the preparation of nanocomposites [122, 124, 149-151]. For example, EVA nanocomposite [152] was prepared by melt intercalation with various concentrations of bentonite organoclay. The dynamic and steady shear material functions showed a remarkable difference when compared with those of pure EVA

copolymer. It was also shown [152] that extensional viscosities were increasing with the content of silicate and strain hardening was observed. At higher strains, silicates have only a small effect on the extensional viscosities. In contrast with the behavior of pure EVA copolymer, systems with higher content of silicate showed a rapid shear thinning.

The thermal degradation and rheological properties of EVA-montmorillonite nanocomposites were studied by Riva et al. [151]. An increase of the storage and loss moduli was observed in nanocomposites when compared with those in pure EVA copolymer. At high temperatures, the difference between elastic moduli of various nanocomposites was also observed. The thermal behavior of EVA-layered silicate nanocomposites was studied by Zanetti et al. [150]. A slower thermal degradation and delayed weight loss were observed in these materials. Tensile properties of EVA-montmorillonite nanocomposites were investigated by Alexander et al. [149]. It was shown that Young's modulus increased significantly even at very low content of the filler while preserving high ultimate elongation and tensile stress. The shear and elongational flows of EVA-based nanocomposites were also studied in [153]. A stronger strain hardening was observed in nanocomposites when compared with the same effect in a pure EVA matrix. The impact of blending sequences on the microstructure and mechanical properties for ternary systems polypropylene/EVA/montmorillonite organoclay was discussed by Martins et al. [154]; they observed a relationship between the clay location and the morphology of ternary nanocomposites. A similar relationship was found between the morphology and mechanical properties of the studied systems. Moreover, electric insulation properties of EVA copolymer and EVA-layered silicate nanocomposites were studied by Gustavino et al. [155], where it was found that the presence of inorganic layered nanofillers improved the electric insulating properties.

EVA copolymer containing 28 wt. % of vinyl acetate and two different types of nano clays were used to modify a base asphalt of penetration grade 50/70, thus preparing EVA/asphalt nanocomposites. After a preliminary study of the binary asphalt/clay and polymer/clay blends, the ternary blends were prepared by adding the clay and polymer to the asphalt, either separately or in the form of a premixed master batch. The obtained PMANs were found to have intercalated features in both cases. However, the results showed that the nature of the clay and the mixing procedure significantly affected the clay dispersion and the blend morphology. This chapter describes the thermo-mechanical, morphological and crystalline behavior of the prepared samples.

3.2 MATERIALS AND METHODS

The base asphalt (BA) was 50/70 Pen grade conventional asphalt from vacuum distillation, with ring and ball softening point (RB) = 49 °C and penetration = 63 dmm. The polymer modifier was Greenflex HN70®, ethylene vinyl acetate copolymer with melt flow index 6 (190 °C/10 min), containing 28% of vinyl acetate with a shore A hardness = 75. Two different kinds of nano clays were utilized for the nano composite preparation. The first was Cloisite 20A®, (subsequently

referred to as 20A) from Southern Clay Products, USA. 20A is an organoclay prepared from a sodium montmorillonite having a cation exchange capacity of 0.926 meq g^{-1} by treatment with 0.95 meq g^{-1} of Me2(HT)2NH4Cl (dimethyldihydrogenated-tallow ammonium chloride). Hydrogenated tallow is a blend of saturated n-alkyl groups with an approximate composition of C18 at 65%, C16 at 30% and C14 at 5%. The organic content of 20A was 38.5 wt.% as determined by thermogravimetric analysis (TGA). The second nanoclay was Dellite 43B® (subsequently referred to as 43B), a clay derived from naturally occurring montmorillonite, especially purified and modified by dimethy dibenzyl hydrogenated talloammonium, from Laviosa Chimica Mineraria, S.p.A., Livorno, Italy.

Two sets of blends were prepared for each clay: (1) EVA/clay (2) BA/EVA/clay. In all cases the weight ratio EVA/clay was set to 60/40. The EVA/clay blends were prepared by melt compounding in a Brabender Plasticorder static mixer of 50 mL capacity, preheated to 190 °C (20A) or 120 °C (43B). The rotor speed was maintained at 30 rpm for about 2.5 min and then it was increased gradually (in 30 s increments) to 60 rpm. The organoclay was added into the molten polymer matrix before increasing the rotor speed. The overall blending time was 13 min. The applied torque and blend temperature were recorded during the whole compounding period. At the end, the molten products were extracted from the mixer and cooled naturally in the atmosphere. The blends were then made into sheets using a Carver Laboratory Press, Model C, Fred. S. Carver Inc., USA, at a temperature of 120 °C. After cooling the sheets for 3 h, they were cut into uniform chips.

A typical procedure for asphalt modification was as follows: aluminium cans of approximately 500 mL were filled with 250–260 g of asphalt and put in a thermoelectric heater. When the asphalt temperature reached 180 °C, a high shear mixer was dipped into the can and set to about 4000 rpm. The polymer and clay (or the polymer/clay nanocomposite) were added gradually (5 g per minute), while keeping the temperature within the range of 190 ± 1 °C during the addition and the subsequent 1.0 h of mixing. Finally, the obtained PMA was split into appropriate amounts to prepare samples for the characterization. The samples were stored in a freezer at – 20 °C. After preparation, the PMAs were characterized by the classical ring and ball softening point procedure (ASTM D36-76)) and by fluorescence microscopy (UNI prEN 13632).

Wide angle X-ray diffraction (WAXD) measurements were made in reflection mode with a Siemens D500 Krystalloflex 810 apparatus X-ray, with a wavelength of 0.1542 nm at a scan rate of 2.0° min^{-1}. The clay was analyzed as a powder; and, the EVA/clay composites were analyzed as disks of 2 mm thickness and 20 mm diameter prepared by compression molding of the melt-compounded materials. The BA/clay and BA/EVA/clay samples were obtained directly from the mixing can and poured into small cylindrical moulds (10 mm diameter, 1 mm height), externally shaped to be directly allocated in the instrument.

Calorimetric analysis was carried out with a DSC Q100 differential scanning calorimeter from TA Instruments equipped with a modulated temperature set-up

and a liquid nitrogen cooling system. Ultra pure nitrogen was used to purge the cell. Standard aluminum pans were used for all the experiments. The sample mass was in the range of 7–11 mg. The modulated DSC (MDSC) method for all asphalt samples was as follows: fast heating up to 150 °C, isothermal for 5 min, cooling (10 °C/min) to – 60 °C followed by a slower (2–4 °C/min) cooling to – 120 °C, data were collected during heating with a rate of 4 °C/min and an amplitude of ± 3 °C every 40 s, until the sample reached 150 °C. The MDSC data was used to determine the glass transition temperature, as well as the compatibility of the amorphous domain (through the derivative of reversing heat capacity). Standard differential scanning calorimetry (DSC) was performed upon cooling from 150 °C to – 120 °C at 2°C/min for all samples. This test provided the onset temperature of crystallization and the enthalpy of crystallization.

Dynamic oscillatory measurements were performed (isothermal conditions) in small amplitude oscillatory shear flow, by using a TA ARES LS2-M rheometer, which operates under strain control. The geometries were the plate–plate (diameters 10, 25 and 50 mm) and torsion bar (with linear dimensions of 37*12.5*2.7 mm) depending on the operating temperatures [156], which varied from – 20 to + 70 °C. The frequency was varied from 0.1 to 100 rad/s, depending on the temperature.

Asphalt samples were prepared by pouring the molten material into small cans in order to avoid frequent reheating and then loaded into the rheometer. This procedure assures that the morphology formed during the mixing stage is preserved until the rheological measurement is carried out. Preliminary strain sweep tests were performed in order to ensure that all experimental conditions remained in the linear domain. Master curves of the dynamic material functions (storage *G'* and loss *G"* moduli, as well as the loss tangent tan δ) were built by applying the time–temperature superposition principle (Tr = 0 °C) [157] with the help of the commercial software IRIS. The reference temperature of 0 °C was chosen because it was about in the middle of the temperature interval of the individual testing temperatures. No anomalous behavior of these material functions was observed, the horizontal (a_T) shifting factors were easily fitted to the WLF form [50] and the applicability of the time–temperature superposition principle was verified for all the studied materials by constructing the van Gurp–Palmen [158] plots of the phase angle versus the magnitude of the complex modulus. Rheological properties of the materials discussed in this contribution are further described in [159] where the verification of rheological simplicity for all the studied materials can be found.

3.3 INTERNAL STRUCTURE AND LINEAR VISCOSITY

As noted in the previous section, a first set of binary blends was prepared and characterized by X-ray analysis, in order to find out if, and what type of nanocomposites were formed when blending EVA and the two clays. Then, the ternary BA/EVA/clay mixtures were prepared by using a 60/40 (w/w) EVA/clay ratio and a content of 3% or 6% of polymer with respect to the total amount. Moreover, for each composition two ternary mixtures were prepared. The first one

corresponded to physical mixing (PM) obtained by adding the polymer and clay separately to the asphalt during the modification, while the second one was obtained by adding the EVA/clay (60/40) nanocomposites as a master batch (MB). The total list of prepared asphalt mixtures is reported in Table 3.1, together with their respective softening points. The PMAs obtained with base asphalt and EVA is referred to as PMA3 and PMA6 depending on the polymer content. The PMANs are denoted as ‘‘polymer content/clay type/preparation method”. As an example, 3/20A/MB is the ternary blend with 3 % EVA and cloisite 20 A from the master batch.

Table 3.1 EVA asphalt nanocomposites (EVAN) details

Mixture	EVA (wt. %)	20A (wt. %)	43B (wt. %)	Prep. Method	$T_{R\&B}$ (°C)
BA					49
PMA3	3	-	-	-	53
3/20A/PM	3	2	-	PM	55
3/20A/MB	3	2	-	MB	57.5
3/43B/PM	3	-	2	PM	54
3/43B/MB	3	-	2	MB	55
PMA6	6	-	-	-	59
6/20A/PM	6	4	-	PM	61.5
6/20A/MB	6	4	-	MB	65.5
6/43B/PM	6	-	4	PM	59.5
6/43B/MB	6	-	4	MB	64

The softening point changed depending on the quantity of added polymer, and also on the type of nanoclay and preparation method. The addition of only EVA resulted in the increase of the ‘‘ring and ball” temperature which was almost linear (4.5 °C for 3% and 10 °C for 6%) with the polymer content. In the presence of clay and physical mixing, there was a similar trend, but the ring and ball temperature increased a little more than in samples without clay. Analogously, the trend in EVA content remained qualitatively similar in the case of the MB mixtures, but a further increase in $T_{R\&B}$ was registered. This was true for both 20A and 43B, but cloisite seemed to have a slightly higher effect on the final performance. Therefore, the clay addition determined an increase in $T_{R\&B}$, which was clearly correlated with the addition method and this was a first indication that the PM and MB mixtures did have a different structure, at least with respect to the clay dispersion. We can suppose that (i) in the case of MB the clay platelet remained confined in the polymeric phase whilst in PM there was stronger interaction with the asphaltphase, (ii) cloisite could be dispersed better than dellite.

A further confirmation that the type of clay and the method of addition affected the structure of the mixtures was obtained from the morphological analysis (Fig. 3.1).

In all cases the mixtures with only 3% weight of added polymer were homogeneous, whilst significant differences were observed at higher polymer content. The binary mixture BA/EVA showed a two-phase morphology, with well defined dark and white-grey areas. The dark zones corresponded to the asphalt-rich phase whilst the grey part was the polymer-rich phase, swelled by asphalt. In fact, this is a classical image consistent with the low compatibility between asphalt and polymer. More precisely, the polymer shows affinity with only some of the asphalt components and operates as a ‘‘local” solvent extraction agent where the most fluorescent components of asphalt (mainly the saturates and aromatics, which are less polar than resins and asphaltenes) migrated to the polymer phase, thus generating this two-color image. In the case of the 3/20A/PM mixture, the morphology appears to be qualitatively similar to that of the binary mixture, but the dimensions of the pattern are completely different. Moreover, the contrast between the dark and grey areas appears to be lower than in the binary mixture. This means that the clay enhances the asphalt/polymer compatibility. The reason for this is probably the high polarity of the clay, which allows also the polar asphalt molecules to swell the polymer-rich phase. For the same reason, a better dispersion of the polymer was obtained in all the ternary mixtures, with clear difference between the morphology of the PM and MB samples. The most important difference that can be noted is the homogeneous aspect of the 6/20A/MB mixture. This result seems to suggest that in the MB mixture the clay has a better compatibilizing effect, than in PM. The reason could be the higher clay dispersion that can lead to a greater clay surface available for the interaction with asphalt molecules. Therefore, both the softening point and the morphological analysis suggest that cloisite leads to a better dispersion of EVA in the base asphalt.

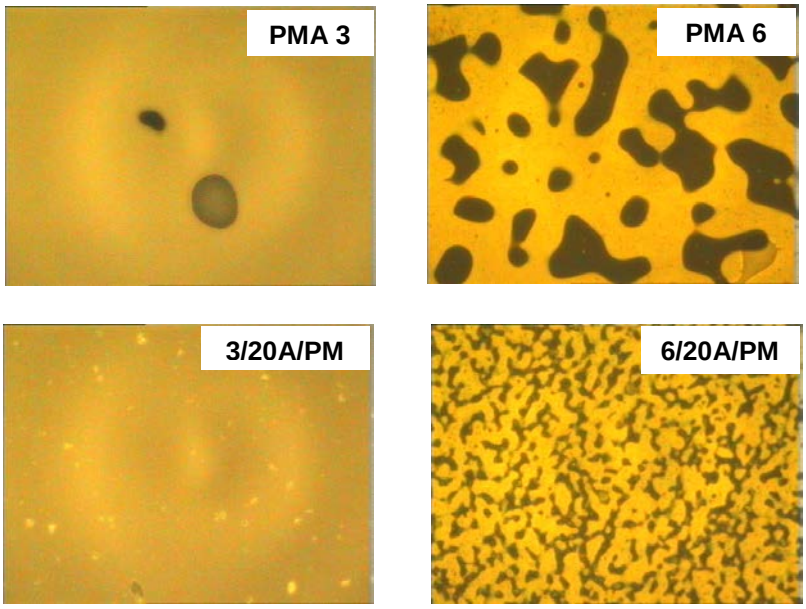

Figure 3.1 *Fluorescence microscopy of EVAN mixtures*

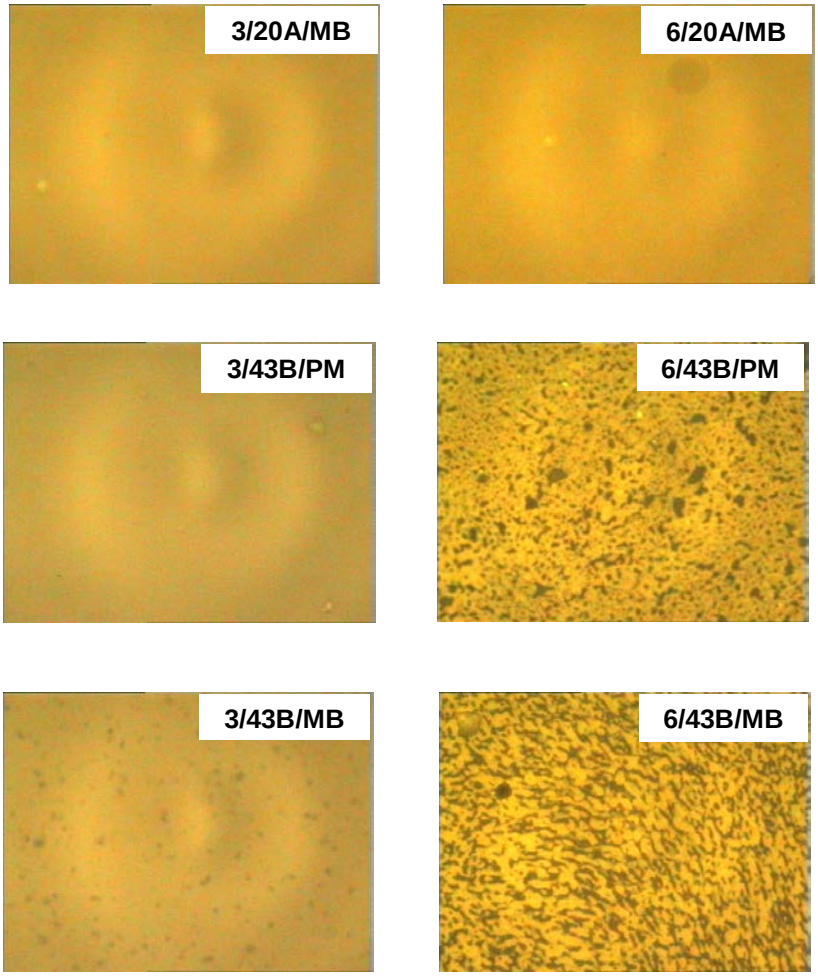

Figure 3.1 *Fluoroscence microscopy of produced mixtures (continued)*

In the EVA/43B 60/40 XRD pattern (trace d) the original peak of 43B at about 4.8° was still present, but a new peak trace was observed at lower angle indicating that, in this case, we obtained only a partially intercalated hybrid, where the intercalation was not complete and some tactoids still remain unchanged. This could be due to the high clay content but Li and Ha [163] found similar results preparing an EVA-based nanocomposite using 3 wt. % of cloisite 10A, which was organomodified with the same ammonium cation as 43B. Similarly to Olabisi et al. [164], we also observed that the basal peak of the clay in the hybrid had a shoulder at higher angles. This probably means that part of the original tactoids that were not intercalated collapsed, perhaps due to degradation of the organo-modifier. With regard to the binary EVA/clay mixes, we can conclude that EVA/20A MB has more homogeneous clay dispersion when compared with EVA/43B MB.

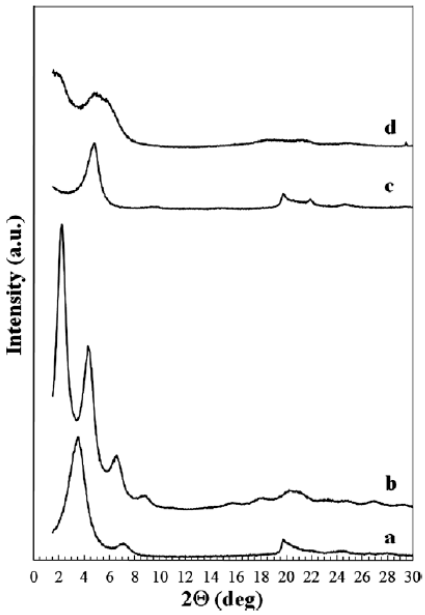

Figure 3.2 *XRD patterns of: (a) 20A (b) 20A/MB (c) 43B (d) 43B/MB*

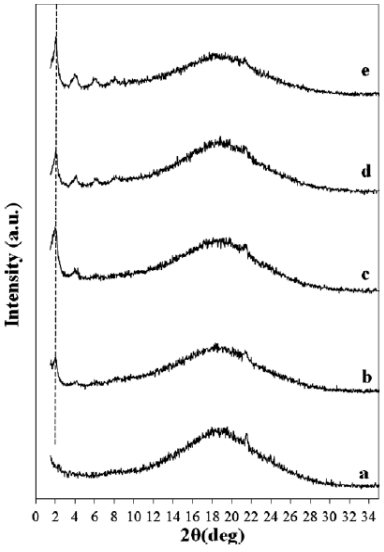

Figure 3.3 *XRD patterns of: (a) BA (b) 3/20A/PM (c) 6/20A/PM (d) 3/20A/MB (e) 6/20A/MB*

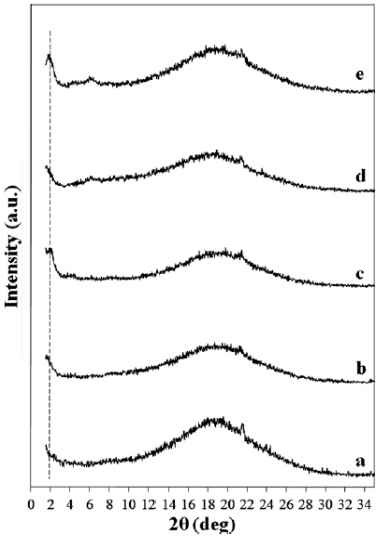

Figure 3.4 XRD *patterns of: (a) BA (b) 3/43B/PM (c) 6/43B/PM (d) 3/43B/MB (e) 6/43B/MB*

In Fig.3.3 the XRD patterns of BA/EVA/20A ternary mixtures prepared by PM (traces b and c) or by MB (traces d and e) are reported. The XRD analysis was performed on several different samples and it is important to underline that while for the mixtures prepared using the MB technique the data were consistent, when the mixtures were prepared by PM the intensity of the clay peak was highly scattered. This indicates that we obtained a more homogeneous dispersion of the clay using the master batch procedure than by adding the polymer and clay separately to the asphalt. For all the mixtures the basal spacing of the clay was shifted to the left with respect to the original position (2h = 2.1°). With the interlayer spacing of about 4.1 nm, the results were quite similar to those obtained for the EVA/20A binary blend. For the mixtures prepared by master batches d_{002} and d_{003} peaks were also clearly defined as in the polymer nanocomposites. This probably means that the affinity of EVA and 20A is so high that the polymer chains remain in the gallery during the mixing with asphalt. Therefore, the highly polar clay probably acts as surfactant for the polymer in the asphalt matrix. In the physical mixtures, the tactoids have the same interlayer spacing but the higher orders are not clearly visible and the intercalated structure is not highly coherent. It is reasonable to assume that, by adding clay and EVA separately to the asphalt, the polymer chains were less efficient in intercalating the clay galleries because they compete with asphalt components and part of the polymer probably did not interact with the clay. In the physical mixtures the surfactant action of the clay is therefore reduced and we can expect fewer homogeneous tactoids.

In Figure 3.4 the XRD patterns of BA/EVA/43B ternary mixtures prepared by PM (traces b and c) or by MB (traces d and e) are reported. For all the blends the original basal peak of the clay disappeared and was shifted to a lower angle, thereby indicating that asphalt can intercalate all the organosilicate galleries. The clay intercalation process of EVA/43B master batch was therefore completed by the asphalt components. Nevertheless, the d and e traces still showed a weak peak at higher angle (about 6°) corresponding to the collapsed tactoids formed during the EVA/43B MB preparation. For the same reasons as in BA/EVA/20A mixtures, we expect that the samples prepared by master batches should be more homogeneous with respect to those prepared by physical mixing. However the surfactant effect of 43B should be lower than that of 20A because this clay has less affinity for EVA and part of the polymer did not intercalate the clay.

MTDSC is capable of separating the overlapping thermal events via the decomposition of the total heat flow into the reversing and non-reversing components. Important information can be obtained from the derivative of the reversing heat capacity, dCp/dT, in the glass transition domain. By using this function one can study the multicomponent systems and their miscibility [164-166]. In a two component system of miscible blends, the function dCp/dT exhibited a single clear and symmetric peak. In physical mixtures this peak was broader, showing a shoulder or even another peak, depending on the difference between the glass transition temperature (T_g) of individual components. In the case of our systems, the situation was quite complex because asphalt itself, due to its colloidal structure and multicomponent nature, had an asymmetric peak with the maximum

positioned at the glass transition temperature (Fig. 3.5). Nevertheless, it is interesting to observe how this peak changed in shape when base asphalt was mixed with EVA (6% by weight) and clay. When BA was modified by EVA alone, the shoulder almost disappeared, thus indicating that the polymer altered the internal structure of BA, and this can be associated with the already mentioned selective swelling of EVA by some of the asphalt components. In Figs. 3.6 and 3.7, the graphs of dCp/dT are shown for systems with 6% EVA and the two clays. It can be seen that in the case of PM the shoulder is still visible and shifted to higher temperatures, while the curves for MB are similar to that of the binary asphalt/EVA mix. This seems to indicate that when polymer and clay are added separately there are different interactions between asphalt molecules and polymer. In PM samples, the asphalt had a weaker interaction with the polymer and maintained part of its original structure, while if the clay is dispersed (MB samples) in the polymer the latter remained able to absorb the asphalt molecules responsible for the shoulder. In systems with a low concentration of EVA (3% by weight) the effect of clays as well as the methods of preparation, on the shape of dCp/dT, was almost negligible.

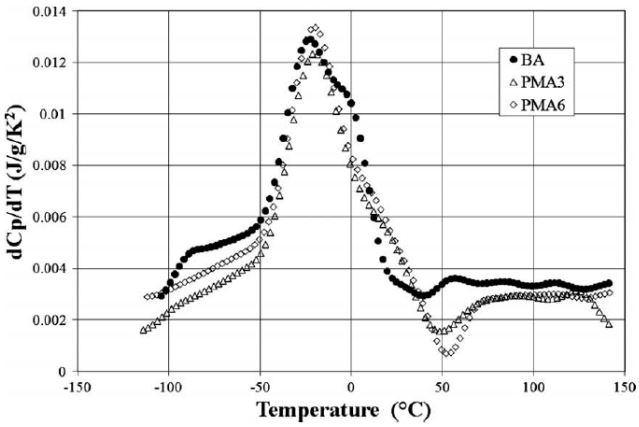

Figure 3.5 *Derivative of the reversing heat capacity for BA, PMA3 and PMA6*

With regard to the linear viscoelastic properties of the prepared samples, Fig. 3.8 shows the master curves of tan δ as a function of the reduced frequency for all the PM mixtures. Two groups of curves can be easily identified: the first group is formed by the materials with 3% content of EVA and the second one by the materials with 6% of EVA. In Fig. 3.9, the same material functions of the MB systems are shown.

The presence of nanoclay can be identified in both figures only at reduced frequencies ($\omega = a_T \tilde{\omega}$) less than 0.001 rad/s. The differences between the studied systems are more clearly seen on the graph of the modified loss tangent function, tan c (δ) = (J" – 1/ $\omega\eta_0$)/J' (eqn. 3.1), where J" is the loss compliance and η_0 is the zero-shear viscosity). This function represents the ratio of: (energy dissipated per cycle minus the energy dissipated due to the Newtonian flow) and (the energy stored and recovered per cycle). In all PMAN, the function tan c (δ) is a peak

function that approaches zero at low, and high frequencies (corresponding to high and low temperatures). At low ω the graph of tan c (δ) is more steep than at high ω where one can observe a rather long ‘‘tail”. In 6% PMAN systems the maximum values of tan c (δ) were smaller than in 3% PMAN. This maximum was smallest for PMAN 6/20A/MB (Fig. 3.10).

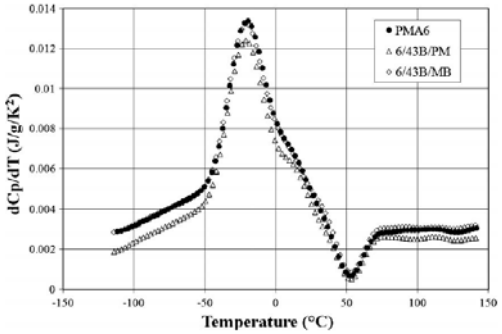

Figure 3.6 *Derivative of the reversing heat capactiy for PMA6, 6/43B/PM and 6/43B/MB*

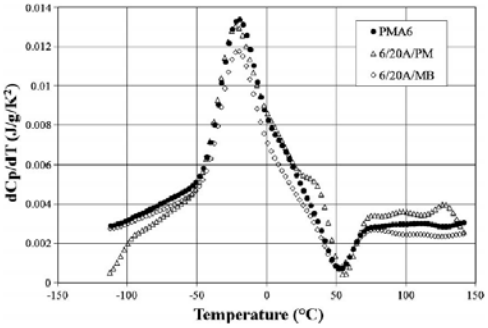

Figure 3.7 *Derivative of the reversing heat capactiy for PMA6, 6/20A/PM and 6/20A/MB*

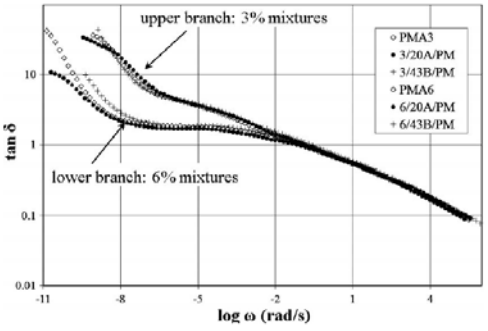

Figure 3.8 *Master curves of tan δ for PMA3, PMA6 and mixture prepared by PM*

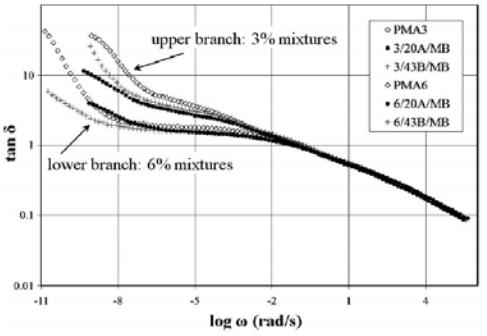

Figure 3.9 *Master curves of tan δ for PMA3, PMA6 and mixture prepared by MB*

The systems prepared by MB show a behavior quite different from those prepared by PM. In Fig. 3.10 (MB) the function tan c (δ) shows a wide flat ‘‘peak” for systems with either clay. Such behavior was not observed in other PMAN systems studied in this contribution. From Fig. 3.10 one can see that the system with clay 43B (melt blending method) started the Newtonian flow at much lower ω than the system with clay 20A (MB). In both of these materials the ratio of energy dissipated to the energy stored (assuming that the Newtonian flow is mainly carried by the base asphalt) in the clay–polymer matrix is only weakly dependent on the reduced frequency and this is true on a relatively large interval of ω (almost three orders of magnitude). Only for $\omega < 10^{-7}$ rad/s the flow begins in systems with clay 20A. The

similar situation is observed for the system with clay 43B however, roughly at reduced frequencies less than 10^{-8} rad/s.

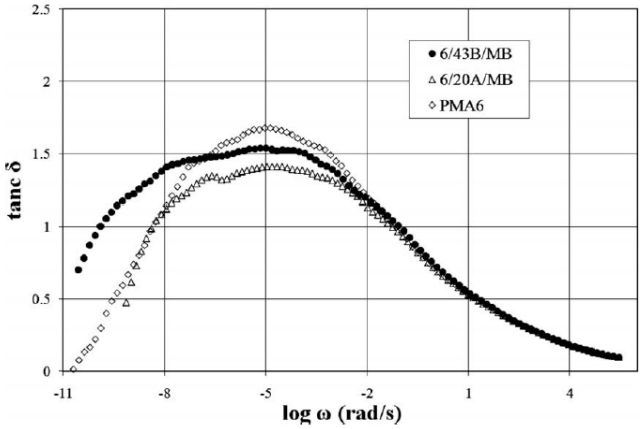

Figure 3.10 *Master curves of tan (c) δ for PMA3, PMA6 and mixture prepared by MB*

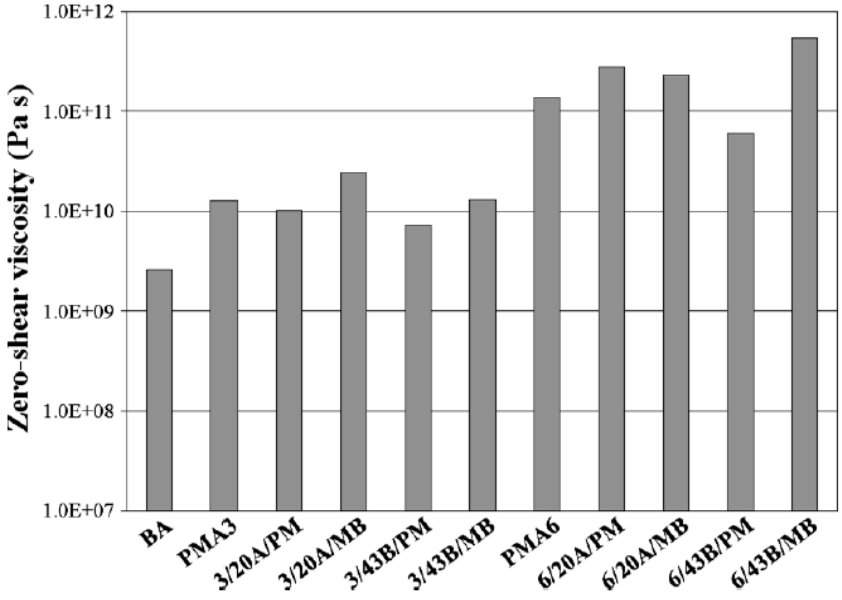

Figure 3.11 *Estimates of Zero shear viscosities at 0 °C, for all the studied systems*

Thus the estimated zero-shear viscosity of 6/43B/MB at 0 °C was the highest of all the studied materials (Fig. 3.11). This might mean less exfoliation, i.e. larger solid-like domains. In materials with clay 20A (the same method of preparation, MB),

the zero-shear viscosity is smaller and that might be due to better dispersion in this system. Generally, in modified systems, the zero-shear viscosity and the steady state compliance increased when compared with the values of these parameters in the base asphalt, as expected. From a practical point of view, it means that modified systems became more stiff and more elastic, which might have a positive impact on low temperature cracking and high temperature rutting of pavements with such binders [167]. As an example, the discrete relaxation spectrum of 6/20A/MB is given in Fig. 3.12. From this figure and also from Fig. 3.9, it can be can seen that the performed dynamic testing covers the beginning of the terminal zone however, to cover the whole terminal zone unreasonably high temperatures (rarely reached in pavements) would have to be used. Thus the values of the zero-shear viscosity, given in Fig. 3.11 have to be taken only as estimates.

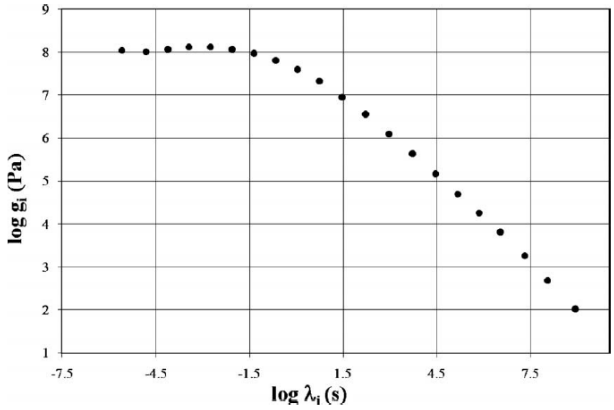

Figure 3.12 *Discrete relaxation spectrum of 6/20A/MB*

3.4 CONCLUSIONS

The effect of clay addition as a third component in polymer-modified asphalts was investigated in a system composed of base asphalt, EVA copolymer and either an organomodified cloisite or dellite clays. The properties of the modified binders obtained with and without clay were compared. The ternary blends were prepared either by the separate additions of clay and polymer to the asphalt or by addition of premixed polymer/clay intercalated nanocomposites. A simple morphological analysis showed that at high polymer concentrations the presence of the clay favors the dispersion of the polymer in the asphalt matrix. However, the two clays do not have the same effect and, moreover, also the method of clay addition is important. In particular, cloisite 20A, when premixed with EVA allowed obtain a completely homogeneous asphalt/polymer mixture at high polymer concentration. Thus the clay seems to have a compatibilizing effect in the asphalt/polymer interactions and cloisite is more efficient than dellite. A possible explanation of this effect can be attempted via the X-ray diffraction, which gave two main indications. The first one is that in the polymer/clay master batches, both clays have an

intercalated structure, but cloisite appears to have a higher affinity with the polymer. In fact, cloisite is completely intercalated by the EVA chains; whilst with dellite a partially intercalated hybrid, containing unchanged tactoids, was obtained. The second indication is that some differences can be seen between the mixtures with analogous composition, but prepared by melt blending or physical mixing. Considering their chemical structure, it is easy to predict that clays have a higher affinity for asphalt than for the polymer. Therefore, in physical mixing the clays are mainly intercalated by the asphalt molecules. On the contrary, in the case of MB, the pre-formed interactions between clay and polymer seem to survive the phase of mixing with asphalt. This is true for cloisite, but also for dellite, where the partial intercalation obtained with EVA is completed by the asphalt components. A qualitative confirmation of these findings is visible also in the MDSC traces where only in physical mixes the derivative of the reversing heat capacity shows a structure similar to that of the PMA. Therefore, even if the clay is more compatible with asphalt than with polymer, once polymer/clay interactions are established, they are not altered by the asphalt molecules added subsequently. Moreover, the polymer/clay master batch, thanks to the clay, has a higher polarity than the polymer alone and this enhances the compatibility with asphalt. The clay acts as a surfactant that increases the interactions between the incompatible phases; the higher is the clay/polymer affinity, the higher is this effect. That is why the homogeneity in morphology increases going from asphalt/polymer to asphalt/polymer/dellite, to asphalt/polymer/cloisite. The observed differences in the internal structure and polymer/clay dispersion, of course influence the rheology, which basically gave results coherent with the previous considerations. Moreover, the low values of the loss tangent function, in the studied system, indicate the better engineering properties of the material (higher elasticity, greater recovery i.e. smaller accumulated deformation during the repetitive loading etc.). Linear viscoelastic properties of the system were studied in this contribution and a deeper understanding of such complex systems can be achieved by studying also their nonlinear rheology. Preliminary investigations of nonlinear behavior of systems discussed here are reported in [158].

3.5 DYNAMIC MATERIAL FUNCTIONS AND STRUCTURAL CHARACTERISTICS

3.5.1 Introduction

Polymer modified asphalt nanocomposites (PMAN) obtained from the ternary systems of bitumen/polymer/clay, represent a new generation of modifiers for paving bituminous binders. Such materials have to be thoroughly investigated before their prospective introduction into the paving industry. The incorporation of layered silicates into polymer matrices is not a new topic [168, 169]. The renewed interest in polymer-layered silicate nanocomposites dates back to 1985 when the Toyota research After loading a small amount of layered silicate loaded into Nylon-6 resulted in significant improvement of thermomechanical properties [121]. The next important step was the observation that it is possible to melt-mix polymers with layered silicates without the use of organic solvents [169]. After sufficient mobility of polymer chains is reached, the chains can diffuse into the silicate clay

galleries thus producing a new polymer-silicate structure. To achieve the miscibility of layered silicates with a large number of polymers a normally hydrophilic silicate surface has to be converted to an organophilic one. This can be achieved by ion-exchange reactions with cationic surfactants [126, 170, 171]. Obviously one cannot obtain a nanocomposites by simple mixing of polymer and silicate (or generally any inorganic material). In such systems, the interaction of organic and inorganic components is weak and thus reflected in poor mechanical properties. When particle agglomeration occurs these systems might have further reduced strength [123]. Depending on the strength of interfacial interaction between the polymer matrix and the layered silicate, two types of nanocomposites can be obtained: (a) intercalated structures where a single (or more) polymer chain is inserted between silicate layers; (b) exfoliated (delaminated) structures, where the clay layers are separated and individually dispersed in the continuum matrix [123, 173-175]. Intercalation results in well ordered multilayer structures of alternating polymeric and silicate layers with a separation distance less than 20–30 A ° [123, 173]. In delaminated structures the polymer separates the silicate platelets by 80–100A° or more [123, 173]. The exfoliation maximizes the polymer-clay interactions and thus should yield the most significant changes in the physical properties of such systems. It is difficult to achieve complete exfoliation of clays and most of the polymer nanocomposites will have intercalated or mixed (intercalated-exfoliated) nanostructures [174]. There are only a few studies of ternary systems bitumen/ polymer/clay, that is, bitumens modified by polymer-layered silicate nanocomposites. SBS premixed with kaolinite and organobentonite, respectively, were used as modifiers of conventional bitumen in [176, 177]. SBS premixed with kaolinite was used as modifier of bitumen in [178]. Preparation and properties of asphalt modified by montmorillonite organoclay were studied in [179]. Rheological properties of the bitumen/SBS/Cloisite20A system were studied in [117]. It was shown that intercalation and the glass transition domain were not affected by the mixing procedures. On the other hand, important differences were observed in the rheological behavior of these ternary systems. The two systems, bitumen/Cloisite15A and bitumen/nanofil15 were studied in [119]. The authors claimed that the bitumen used was able to intercalate and partially exfoliate the organoclays. It was also concluded that the elasticity (storage modulus *G'*) of the modified bitumen was higher than in the virgin bitumen, while the loss modulus (*G"*) was much lower in the modified binder than in the virgin binder.

3.5.2 Experimental

Materials and preparation methods are discussed in detail in section 3.2 of this Chapter, the change is nomenclature is indicated in Table 3.2

All the materials were subjected to the following rheological tests:

(a) Small amplitude oscillations in a TA-ARES LS2-M rheometer (strain control mode);
(b) Stress growth after initiation of a constant shear rate (start-up experiment);
(c) Repeated creep and recovery (sometimes referred to as the dynamic creep) in a CVOR 200-Malvern rheometer (stress control mode).

Table 3.2 Composition and preparation method of the EVAN mixtures.

Label used in 3.3	Present Labeling	EVA (wt %)	CL (wt %)	DL (wt %)	Method
BA	B	0	0	0	-
PMA3	3M	3	0	0	-
PMA6	6M	6	0	0	-
3/43B/PM	3M2DP	3	0	2	PM
3/43B/MB	3M2DB	3	0	2	MB
3/20A/PM	3M2CP	3	2	0	PM
3/20A/MB	3M2CB	3	2	0	MB
6/43B/PM	6M4DP	6	0	4	PM
6/43B/MB	6M4DB	6	0	4	MB
6/20A/PM	6M4CP	6	4	0	PM
6/20A/MB	6M4CB	6	4	0	MB

Tests (a) were performed in the parallel plate geometry (plates of diameter 10, 25, and 50 mm) and in the torsion bar geometry, depending on the temperatures used. Isothermal oscillations (frequency ω̃ ranging from 0.1 to 100 rad/s) at temperatures from – 20 to 70 °C were performed and the master curves of dynamic material functions (*G", G",* tan *δ*) were constructed in the software platform IRIS [156, 180]. The time temperature shifting was possible for all the studied systems however, a vertical shifting factor had to be applied. Tests (b) were done in cone and plate geometry (diameter 25mm and cone angle 0.1 rad) at fixed temperature T = 60 °C and shear rates varying from 0.5 to 5 s^{-1}. The repeated creep and recovery tests were performed in plate-plate geometry (25 mm diameter) and T = 40 °C. One hundred cycles of 1 s creep and 9 s recovery were studied with the applied shear stress of 100 Pa. Both tests (a) and (c) were performed in the linear viscoelastic domain. The strains in test (b) were high enough to reach the nonlinear behavior of some of the systems studied.

The full characterization of the chemistry and morphology of the prepared mixes is given in [179]. Briefly, the morphological analysis showed that at high polymer concentrations the presence of the clay favored the dispersion of polymer in the asphalt matrix. However, both the type of clay and the method of clay addition affected the final properties. In particular, CL had a significant compatibilizing effect on the asphalt/polymer interactions. This was explained by the X-ray diffraction, which showed that: (1) CL, with respect to DL, had a higher affinity with the polymer; (2) in PM the clays were mainly intercalated by the asphalt molecules, while in MB the preformed interactions between clay and polymer survived the process of mixing with asphalt. The two clays acted as compatibilizers that increased the interactions between asphalt and polymer. The higher the clay/polymer affinity, the stronger was this effect. Therefore, the homogeneity in morphology increased from asphalt/polymer to asphalt/ polymer/dellite, and then to asphalt/polymer/cloisite.

3.5.3 Results and Discussions

The addition of clay did not reveal dramatic changes in the behavior of the master curves of storage and loss moduli of the studied modified bitumens. Based on the linear viscoelastic behavior of *G'* and *G"* all systems resembled amorphous polymeric systems of low molecular weight [156, 181]. Generally, the values of both dynamic moduli, in modified systems, were higher than in the base bitumen. As the master curves of the dynamic material functions (reference temperature Tr = 0°C) cover the temperature interval – 20/70°C, the ''master'' loss moduli displayed a strong (absolute maximum at high reduced frequencies ($\omega = a_T\tilde{\omega}$).

On the other hand, none of the master storage moduli, *G'*, showed the plateau modulus, G^0_N. Only an inflection point can be identified on master curves of *G'*. To distinguish the studied systems one has to use some more exotic linear viscoelastic plot. The modified loss tangent function [$tan\ c\ (\delta) = (J'' - 1/\omega\eta_0)/J'$] where $\eta 0$ is the zero-shear viscosity] was successfully used to achieve this goal [117]. Another possibility is to use the so called Van Gurp–Palmen plot [157]. A Van Gurp–Palmen (vGP plot) is the plot of the phase angle versus the magnitude of the complex modulus |G*| and it was originally proposed as a tool for the verification of the time superposition principle [157]. This plot is also known under the name Black diagram [182]. The method of van Gurp and Palmen was used for the identification of polydispersity and long chain branching in polymer melts [183]. Figure 1 is a vGP-plot for systems BA, PMA3, and PMA6. It is clear that the absence of the pronounced plateau modulus yields a smooth vGP-plot for each of these systems and similarly no characteristic minimum can be observed for either of the studied systems.

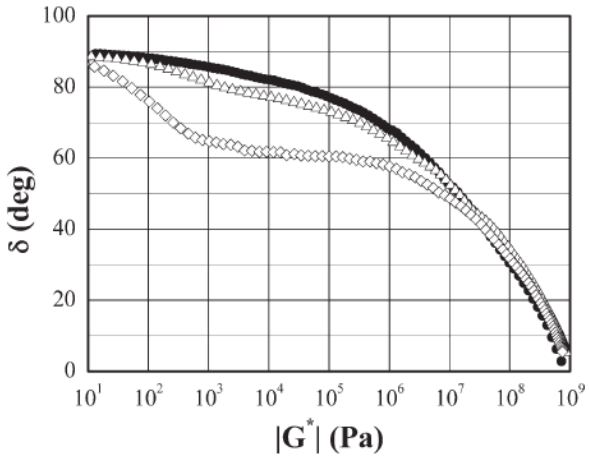

Figure 3.13 *The Van Gurp-Palmen plots, Tr = 0 °C, ● BA, ▲PMA3, ◊ PMA6*

Similar vGP-plots can be constructed for the rest of the studied systems (base bitumen modified by EVA organoclay nanocomposites). The main difference apparent from such plots is the clear split between materials with 3 and 6% wt EVA.

A better chance to illuminate the differences in the composition or/and the method of preparation of the studied materials would have the derivative of the phase angle w.r.t. the reduced frequency ω. Figure 3.13 shows $d\delta / d\omega$ for the base bitumen (BA) and its modifications PMA3 and PMA6. The rates of change of the phase angle were negative in all three systems, that is, the phase angle is monotonically decreasing from π/2 to 0 with increasing ω. The magnitude of the rate of change of δ is much smaller in Ba than in PMA3 and PMA6. The characteristic peak in BA is positioned roughly between ω ~ 0.01 and 1 rad/s. This peak splits into a wave form in PMA3 and then changed into a symmetric peak in the PMA6 system. A shoulder at ω < 100 rad/s is basically preserved in all three systems.

The domain ω < 0.01 rad/s is populated with several changes in the systems PMA3 and PMA6. A small shoulder at $\omega < 10^{-5}$rad/s (visible only in ''magnification'') in base bitumen BA disappeared in PMA3 and exists in much weaker form in PMA6 as a part of a broad peak centered at $\omega \sim 10^{-5}$rad/s. The system PMA3 shows a principal maximum at the same frequency. Left of this maximum the clear minima, in both 3M and 6M, are seen. The minimum in 6M (at $\omega \sim 10^{-9}$rad/s) is of much larger magnitude than that in 3M ($\omega \sim 10^{-7}$rad/s). Systems containing the clay DL and prepared by both methods (PM and MB) are depicted in Figure 3.14(a). The first noticeable effect is the split into systems containing two different concentrations of EVA copolymer. Generally, the rates of changes of the phase angle are ''slower'' over a large part of the portrayed ω-domain, in the systems with 6 wt % concentration of EVA.

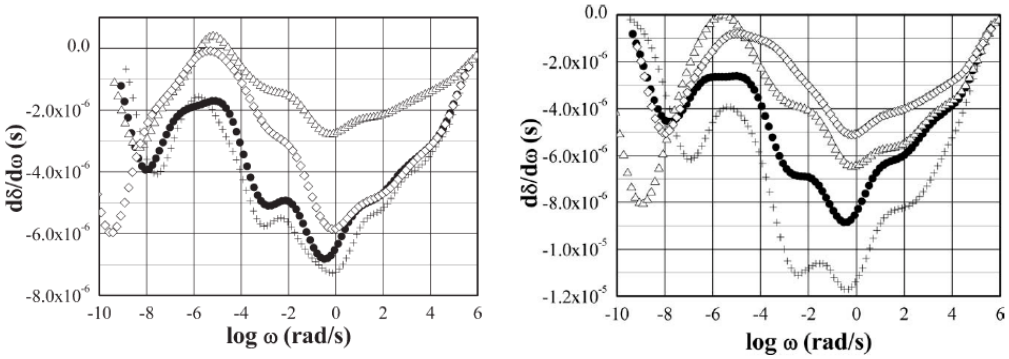

Figure 3.14 *Derivative of phase angle, Tr = 0 °C, (a) + 3M2DP ● 3M2DB, ▲6M4DP, ◊ 6M4DB and (b) + 3M2CP ● 3M2CB, ▲6M4CP, ◊ 6M4CB*

The shapes of $d\delta / d\omega$ for systems 3M2DP and 3M2DB are remarkably similar except the flat principal maximum peak in 3M2DB (positioned at $\omega \sim 10^{-5}$rad/s). The central ''wavy'' part of 3M is still visible in 3M2DP and 3M2DB but with the minimum peak at ω ~ 1 rad/s, and of larger magnitude than in 3M system. The minimum peak of 6M (at $\omega \sim 10^{-9}$rad/s) is now reflected by the system 6M4DB however, with smaller magnitude. The system 6M4DP shows a minimum peak

coinciding with the minimum peak of 3M2DB. The principal maxima peaks of 6M4DP and 6M4DB are quite similar. Both are slightly shifted to the right of the principal maximum peak of 3M and positioned at about the same reduced frequency $\omega \sim 10^{-5}$rad/s as is the maximum peak of 6M system. The methods of preparation (systems with clay DL) had a greater impact on the systems with 6% wt of EVA copolymer than on systems with 3% wt EVA, as can be seen over a large part of the ω domain.

Figure 3.14(b) is similar to Figure 3.14(a), but shows the systems with clay CL. The split into two groups, determined by the concentration of EVA, is again apparent. The previously mentioned ''wavy'' character of the principal minimum peak is now preserved only in the system 3M2CP.

Remarkable is the flat maximum peak of the system 3M2CB centered at $\omega \sim 10^{-5}$rad/s. This peak is quite broad but not as flat as in the system 6M4CB. The minimum peak at $\omega \sim 10^{-9}$rad/s now appears in system 6M4CP and the minimum peak at $\omega \sim 10^{-8}$rad/s is almost identical in systems 3M2CB and 6M4CP. The latter of these systems also has the ''strongest'' maximum of all the systems portrayed in Figure 4. From both Figures 3 and 4, one can see the impact of the method of preparation (of nanocomposites) on the modified bitumens. It seems to be possible to conclude that the information hidden in the phase angle and particularly in its derivative w.r.t. the reduced frequency ω is quite rich and Figures 3.13 and 3.14 show the structural changes in the studied modified systems.

3.5.3.1 Start-up of steady shear

One of the crucial tests of any theory of viscoelastic behavior of materials is a simple stress growth experiment [156, 184-187]. In this test, in polymeric systems, the stresses can reach quite high values before settling to their asymptotic values and the ubiquitous stress-overshoot is observed. Multiple overshoots of the shear stress were observed and discussed [184, 187, 188]. Stress overshoots in organoclay nanocomposites were studied [137, 189-190] and related to the structure of nanocomposites. We have studied the above described systems in transient shear flows (start-up of steady shear) with several shear rates at constant temperature T = 60 °C. Similarly, as in dynamic shear experiments, materials with 3% and 6 wt % EVA formed two distinct groups. This can be seen in Figures 3.15(a) and (b). In these figures, the shear stress (τ) normalized by its asymptotic value (τ_a) is plotted versus the strain (γ) for the tests with shear rate , $\dot{\gamma} = 4\ s^{-1}$. Much smaller overshoots are observed for the modified bitumens with 3% wt EVA (data for 3M2DP and 3M are almost identical) than for the ones modified by 6% wt EVA. Comparing the magnitudes of τ/τ_a (from the highest to the smallest) the sequence of the tested materials is: 3M2CB, 3M2DB, 3M2CP, 3M2DP, 3M—for systems with 3% wt EVA.

Similarly the sequence for 6%wt EVA materials ($\dot{\gamma} = 4s^{-1}$) was: 6M4CB, 6M4CP, 6M4DB, 6M4DP, 6M. Because the 6%wt EVA systems are more clearly distinguishable we are presenting their transient properties in the following figures:

Figures 3.16(a) and (b) show the stress growth function η^+ in systems 6M4CP and 6M4CB, respectively.

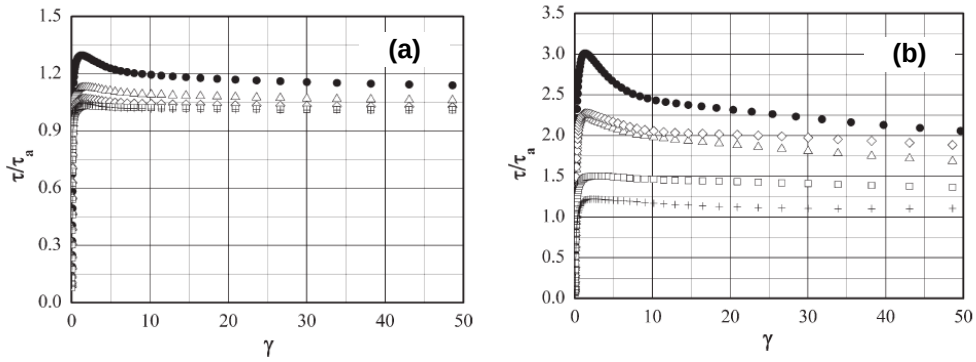

Figure 3.15 *Normalized stress as a function of strain, T = 60°C, $\dot{\gamma}$ = 4 s^{-1}. (a) 3M2CB, ▲ 3M2DB, ◊ 3M2CP, □ 3M2CP, + 3M, (last two samples are almost indistinguishable) (b) 3M2CB, ▲ 6M4DB, ◊ 6M4CP, □ 6M4CP, + 6M*

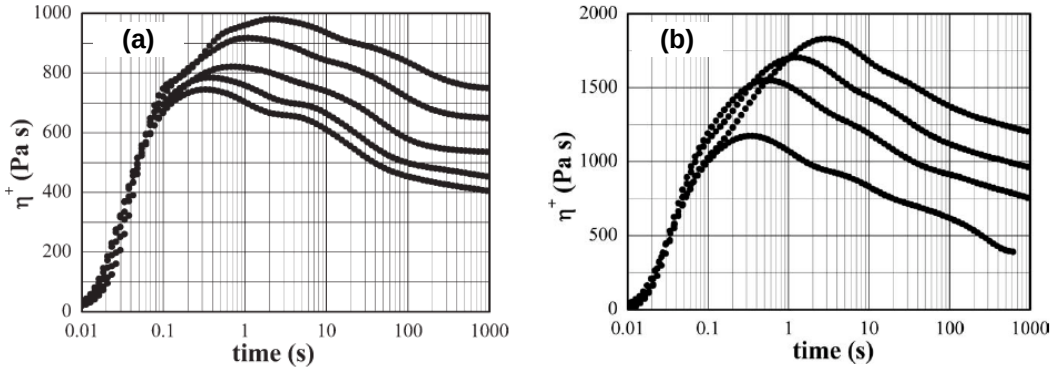

Figure 3.16 *Stress growth function, T = 60°C, $\dot{\gamma}$ = 0.5, 1, 2, 4, 5 s^{-1}. (a) Modified bitumen 6M4CP. (b) Modified bitumen 6M4CB*

Both systems show typical primary maxima of η^+ and their positions move toward shorter times with increasing applied shear rate. In system 6M4CB the shear rate $\dot{\gamma}$ = 5 s^{-1} produced unreliable results and this shear rate is not included in Figure 8. Aside from the principal maxima there are weak secondary maxima of η^+, these are more visible at higher shear rates in system 6M4CP. This system approaches the asymptotic steady state value for lower shear rates (0.5, 1, 2 s^{-1}) after 1000s. The values of η^+ are much higher in system 6M4CB and the stress growth function, η^+, is still decreasing after 1000s. The systems with 6 wt. % EVA and clay DL are portrayed in Figures 3.17 (a) and (b). The sample 6M4DP, Figure 3.17(a), is reaching the steady state values of η^+ after 1000s and is also showing weak secondary maxima for the tests at higher values of the shear rate. The values of η^+ were smaller in this system when compared with the system 6M4DB.

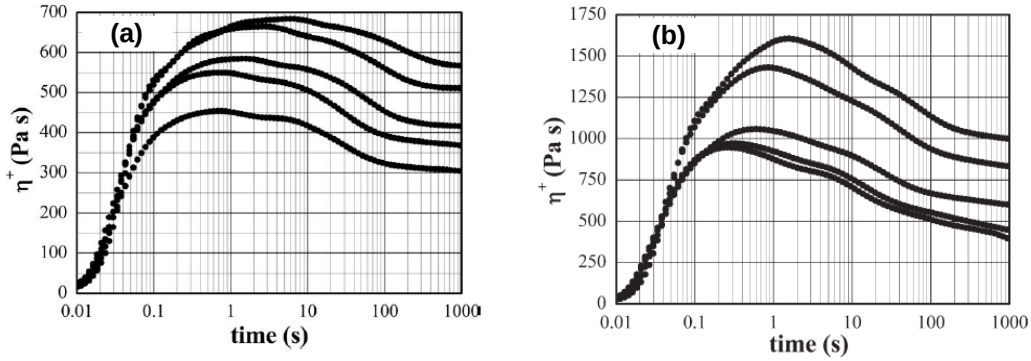

Figure 3.17 *Stress growth function, T = 60°C, $\dot{\gamma}$ = 0.5, 1, 2, 4, 5 s^{-1}. (a) Modified bitumen 6M4DP. (b) Modified bitumen 6M4DB.*

The latter system seems to approach the steady state after 1000s for $\dot{\gamma}$ = 0.5, 1, 2 s^{-1}. The tests at higher shear rates ($\dot{\gamma}$ = 4 and 5 s^{-1}) show η+ still decreasing at t ¼ 1000 s. When the transient data are plotted as the shear stress versus the strain, the principal maximum (overshoots of τ) appeared roughly at the same value of the strain c, see Figure 3.18 where the system 6M4CB is portrayed (γ_{max} ~ 1.4).

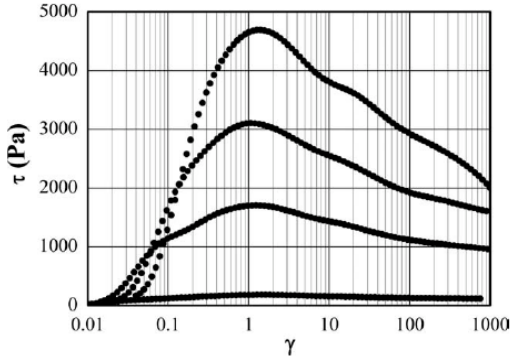

Figure 3.18 *Stress as a function of Strain, T = 60°C, $\dot{\gamma}$ = 4, 2, 1, 0.5 s^{-1}. Modified bitumen 6M4CB*

The magnitude of the overshoot was increasing with the increasing shear rate in all the systems studied. Generally, the stresses generated in the tested modified bitumens were much higher in systems containing the clay CL when the nanocomposites were prepared by the MB method. The discussed transient shear flow was performed up to very high strains, that is, the nonlinear region was reached very quickly and as shown, at least for the systems with 6% wt EVA, one

can easily recognize the materials with different clays and prepared by the two discussed methods of preparation.

The magnitude of the overshoot was increasing with the increasing shear rate in all the systems studied. Generally, the stresses generated in the tested modified bitumens were much higher in systems containing the clay CL when the nanocomposites were prepared by the MB method. The discussed transient shear flow was performed up to very high strains, that is, the nonlinear region was reached very quickly and as shown, at least for the systems with 6% wt EVA, one can easily recognize the materials with different clays and prepared by the two discussed methods of preparation.

3.5.3.2 Repeated creep and recovery

Experiments employing the repetitive loading and unloading are frequently used in the testing of engineering materials [156, 191, 192]. This type of testing is also applied to samples of paving mix and recently also to the bituminous binders of such mixes [195-197]. All the systems studied in this contribution were subjected to one hundred cycles of shear creep (duration of 1 s) and recovery (9 s of duration) [196, 197]. The applied stress was 100 Pa, the testing temperature was 40 °C and the accumulated compliance $J_{acc}(t)$ was monitored during the experiment. The relatively low level of stress was chosen in order to keep the strain small (linear viscoelastic domain) at least during the first 10–20 cycles. Of course with the increasing number of cycles the strain is increasing and the final accumulated strain can reach high values (depending on the temperature of the test). It is believed that such accumulated strain, in bituminous binders, is responsible for rutting, a very common distress mode in bituminous paving. At higher temperatures the recovery (during the 9s of recovery in one cycle) is usually very small and elastic properties of the tested bitumen are strongly suppressed. At T = 40°C, the studied systems, with the exception of the base bitumen B, displayed recovery (viscoelastic behavior) in individual cycles. On the other hand, at this temperature, one can expect the onset of rutting in pavements with this bituminous binder.

The plots of accumulated compliances for the systems B, 3M, and 6M are shown in Figure 3.19. As expected, the highest values of $J_{acc}(t)$ were attained in the base bitumen and the lowest ones were obtained in 6M. The values of J_{acc} in 3M were between those found in systems B and 6M. The plots for other systems are similar in appearance to those in Figure 3.19, thus, the individual systems can be graded by the values of J_{acc} attained after 100 cycles of creep and recovery. From high to low values of J_{acc}, the sequence of the 3% wt EVA systems is: 3M2DP, 3M, 3M2CP, 3M2DB, and 3M2CB. The accumulated strain is high in systems with both clays prepared by the PM method. The systems modified by melt blended nanocomposites (DL or CL clays) had a smaller accumulated compliance (i.e., also the strain) compared to the base bitumen modified by 3% wt EVA only. The system 3M2CB was best ‘‘performing’’ of all 3% wt EVA materials.

In 6% wt EVA systems the situation was similar. The best ''performing'' systems were again the materials prepared by MB method with little difference between the two used clays (DL or CL). In samples prepared by PM the clay CL ''performed'' better (smaller J_{acc}) than clay DL (Table 3.3).
The accumulated compliance function $J_{acc}(t)$ can be described with the help of small number of Voigt elements [179, 195, 196], i.e. assuming that the shear compliance function $J(t)$ has the form,

$$J(t) = J_g + \sum_{i=1}^{N} J_i\left(1 - e^{-\frac{t}{\Lambda_i}}\right) + t/\eta_0$$

where N is the number of modes, J_g is the glassy compliance, $\{\Lambda_i, J_i\}$ is the retardation spectrum and η_0 is the zero shear viscosity.

The fit of $J_{acc}(t)$ for 6M4CB is shown in Figure 3.20, where N = 3. One can see that after first five cycles the compliance function (eqn. 3.2) describes the accumulated compliance $J_{acc}(t)$ quite well even with a minimum of retardation modes. The base bitumen (B) represents the other ''end'' of the tested materials. This material (at T = 40°C) had almost no recovery in individual cycles and thus the viscous approximation of (eqn. 3.1) is satisfactory for the description of the repeated creep and recovery test, that is,

$$J(t) = J_e^0 + t/\eta_0 \qquad (3.3)$$

was suitable for the description of J_{acc} in the base bitumen. Je 0, in (3.3) is the steady state compliance. The fit of J_{acc}, for the base bitumen B is given in Figure 3.21.

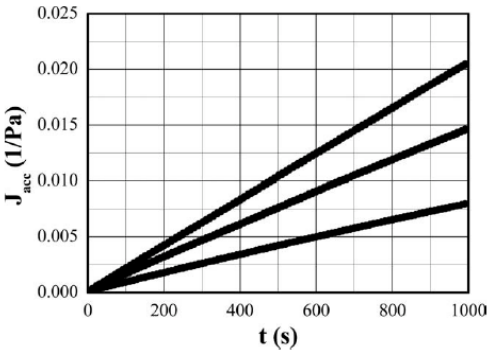

Figure 3.19 *Accumulated Creep, Stress as a function of Strain, Tr = 40 °C, Systems B, 3M, 6M*

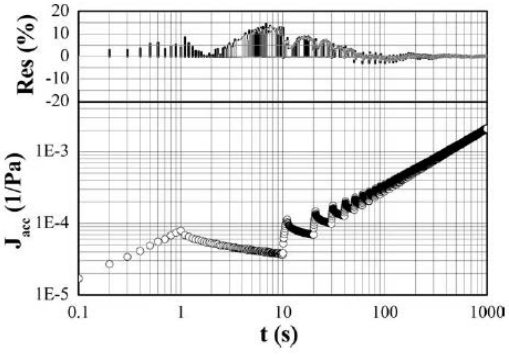

Figure 3.20 *Accumulated compliance in 6M4CB, T = 40 °C, (fit to eqn. 3.2, for clarity, the goodness of the fit is identified by the residuals of the fit*

Table 3.3 Accumulated compliance at t =1000s, τ = 100 Pa.

System	J_{acc}(1000), [1/Pa]
B	0.0205
3M	0.0146
6M	0.00795
3M2DP	0.0188
3M2CP	0.0159
3M2DB	0.0139
3M2CB	0.00711
6M4DP	0.00725
6M4CP	0.00301
6M4DB	0.00205
6M4CB	0.00203

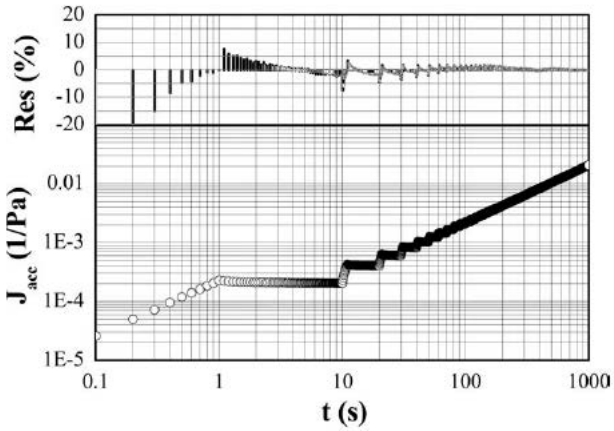

Figure 3.21 *Accumulated compliance in 6M4CB, T = 40 °C, (fit to eqn. 3.3, for clarity, the goodness of the fit is identified by the residuals of the fit)*

3.5.4 Conclusions

From the behavior of the phase angle in the linear viscoelastic domain, it follows that the concentration of EVA copolymer had a strong impact on the rheological properties of the ternary systems B/EVA/clay. The physical method of mixing polymer and clay and subsequent modification of the base bitumen by this mixture

produced modified bitumen with a structure that is not so different from the structure of the bitumen modified just by the EVA copolymer. On the other hand, the MB of polymer and clay with subsequent modification of the base bitumen by such nanocomposites produced modified bitumens with structures different from that of B/EVA modified bitumen. The experiments in which large strains were used were able to distinguish the individual modified bitumens very easily. Different morphologies of modified bitumens could be identified when the two methods of processing were used (PM or MB). The stress overshoots were attributed to a rupture of the network structure and to particle orientation [189, 190]. In our ternary systems (PMAN), the magnitudes of overshoots and the times where they were observed were strongly dependent on the applied shear rates. The stresses and the overshoots were highest in bitumens modified by clay CL and prepared by the MB method. Similarly, the stresses and overshoots in ternary systems with clay DL were higher when the MB method was used however, with much smaller magnitudes in comparison to the systems with clay CL. Thus, one can assume that the network and exfoliation were strongest in modified bitumen 6M4CB followed by the system 6M4CP. The analogous sequence was followed by systems with clay DL. Similar conclusions can be drawn from the comparison of accumulated creep compliances in the repeated creep and recovery tests. Ternary systems prepared by MB displayed the smallest Jacc. The PM of EVA and clay CL produced modified bitumens with much lower values of the accumulated compliance than the same method using clay DL. These conclusions are supported by the results of wide angle X-ray diffraction discussed in [179] and [198], where it was shown that in PM systems, B/EVA/CL, the intercalated structure was not as coherent as in MB systems. In systems with clay DL, the MB again produced more homogeneous systems than those prepared by PM, however, the surfactant effect of clay DL was not as strong as that of clay CL because DL has weaker affinity for EVA, and thus, part of the polymer did not intercalate this clay.

Chapter 4

4.1 INTRODUCTION

Polymers are the widely accepted material for modifying asphalt for pavement and other applications. Airport pavement has entirely different service condition when compared to highway pavement. Kerosene (classified as Jet Fuel A1) spills on aprons and taxiways during fuelling operations, aircraft sitting in queue softens the asphalt pavements in airports. This weakens the asphalt leads to raveling which causes permanent deformation or failure. This occurs due to the high solubility of asphalts in conventional hydrocarbon fuels. Generally, asphalt pavement at airports, filling stations and industrial houses were treated with fuel-resistant coal-tar pitch. But, coal-tar sealers which is used to prevent pavements from fuel damage fails in short period due to difference in thermal co-efficient of coal tar which causes alligator cracking. Once cracking initiates, fuel easily penetrates and damages the pavement. Apart from this, tar-derived products are carcinogenic due to the presence of polycyclic aromatic compounds [198]. To address this issue resin-based coatings were employed [199-201]. These materials failed due to the thermal and fatigue cracking witnessed by airport pavements. In addition to this, they were not environment friendly and involve expensive techniques for preparation. To overcome this technological issue, it is preferable to develop pavement materials with fuel resistance characteristics. Few such materials were reported in the literature [202-205].

Polymers increase the durability of pavements by increasing the high temperature stiffness and reducing the low temperature stiffness. In case of special applications like airport pavements, the demands are not met by polymer alone. Still there is a demand for a durable and environment friendly pavement material in this type of special application. Materials world has witnessed the innovative

materials developed from polymer nanocomposites with the invention of nanoclays in 1985. The realization of advantages of nanoclays in polymers attracted several research areas in which asphalt technology is also encompassed. In 1997, Edit et. al patented the first thermoplastic elastomer-asphalt nanocomposite [206]. Later, kaolinite/styrene-butadiene-styrene(SBS)/asphalt compound reported [175]. Ghile [116] discuss the effects of nanoclay modification on the rheological and performance properties. Yu [207-209] and co-workers [215] have reported several properties of asphalt modified with montmorillonite. For the first time, Polacco [117] reported that the method of incorporation of nanoclay in the asphalt or preparation of asphalt/polymer/nanoclay has significant impact in the final properties of this ternary blends. The addition of nanoclay along with polymer gives rise to a new class of materials called polymer modified asphalt nanocomposites (PMAN) with higher softening point, improved flow properties than those obtained with polymer modification alone. In line with this research [117] Polacco and co-workers have developed PMAN based on ethylene vinyl acetate and nanoclays [158, 179]. As new avenues with nanoclays have opened up in asphalt technology, several research papers are included in this area [211, 212] and it is very difficult to include all of them.

Based on the earlier research work [117, 158, 179], various polymers such as SBS, EVA and ethylene methacrylate (EMA) were selected as polymer modifier along with a nanoclay and studied with asphalt obtained from two different sources. Two different methods such as: physical mixing which facilitate the direct interaction of clay and polymer with asphalt and nanocomposite addition, where polymer and nanoclay is melt blended in an internal mixer and the obtained polymer nanocomposite is introduced to asphalt. In the second method, the nano structure developed is confined within the polymer matrix and the effect of nanocomposite is studied. A detailed discussion about the internal structure, linear viscosity and its rheological validation for qualifying as pavement material have been made in Chapter 3. As the main objective of this study is about the fuel resistance, kerosene immersion tests developed [198, 212] in our laboratory carried out amidst the regular test for polymer modified asphalt. In this paper the preliminary results obtained from ring and ball test, microscopy and solubility is reported.

4.2. MATERIALS

Conventional vacuum distillated asphalt from two different sources with a pen grade 50/70 indicated as L and R were used. Styrene butadiene styrene (SBS), trade name Kraton™ D 1102, CS available as porous pellets dusted with silica is a triblock copolymer with mid-block as butadiene contains 29.5 wt. % bound styrene from Shell Chemical Co., ethylene methacrylate (EMA), trade name Elvaloy™ 1125 AC with 25 % methacrylate from Dupont and ethylene vinyl acetate (EVA), trade name Greenflex HN70™ with 28 wt. % vinyl acetate content from Polimeri Europa were the polymers used. Nanoclay used in this study is Cloisite 20 A (CL) from Southern Clay Products, USA. Kerosene (classified as Jet Fuel A1) as obtained from Air Force station was used as fuel for determining the fuel resistance.

4.3 METHODS

In line with our earlier studies [117, 158, 179], two different methods were followed to introduce nano clay into asphalt. In the first method, physical mixing, polymer and nanoclay was mixed manually and introduced into asphalt. This method facilitates the direct interaction of clay and asphalt. Nanocomposite mixing is the second method adopted to incorporate nanoclay into the asphalt. In this method, polymer and nanoclay is blended in an internal mixer at suitable processing temperature. The obtained nanocomposite is molded into sheets and cutted into uniform chips. Then the nanocomposite is added to asphalt.

Around 250 g of asphalt is taken in an aluminium can and heated for an hour at 180 °C. Then it is transferred to an electrical heater and the temperature is maintained. During this time, a high speed Silverson L4R mixer is introduced. Once the asphalt reaches 180 °C, then polymer/asphalt physical mix or polymer nanocomposite is introduced with equal increments. The rotor is speed is maintained at 4500 ± 500 rpm and the temperature is maintained at 180 ± 2 °C. The mixing time is 45 minutes followed by degassing for 5 minutes to eliminate the entrapped air during mixing. After completion of mixing, samples were isolated for ring and ball test, microscopy and solubility. The nomenclature of all the blends is provided in Table 4.1.

Table 4.1 Nomenclature of Blends

Blending details	Blends with Livorno base asphalt (L)	Blends with Ravenna base asphalt (R)
Base asphalt	L	R
Base asphalt with clay	LCL	RCL
SBS	LSBS	RSBS
SBS/clay physical mix	LSBP	RSBP
SBS/clay melt blend	LSBM	RSBM
EMA	LEMA	REMA
EMA/clay physical mix	LEMP	REMP
EMA/clay melt blend	LEMM	REMM
EVA	LEVA	REVA
EVA/clay physical mix	LEVP	REVP
EVA/clay melt blend	LEVM	REVM

4.4 CHARACTERIZATION

Softening point obtained from ring and ball temperature ($T_{R\&B}$, ºC) method as per ASTM D 36-76 was used to determine the softening point. For morphological analysis, asphalt samples were isolated from the cans after mixing and poured into cylindrical mold of diameter 1cm and height 2 cm. In order to preserve the instantaneous morphology the molds were pre-heated to mixing

temperature so that asphalt is not quenched when it comes in contact with the metal part of the mold. After the mold is filled it is kept for 2 minutes at 180 ºC, to ease the flow and to prevent the chances of vacuum which may have generated during filling. Then it is cooled to room temperature. Till morphology is analyzed the samples along with the cylindrical molds are preserved under 0 ºC. Then the samples are cryo-fractured and morphology is recorded using a fluorescence microscope (Leica DM LB).

Solubility test was done to determine the fuel resistance. Kerosene is used as the fuel. Samples for solubility is prepared by pouring hot asphalt immediately after mixing in a cylindrical mold (diameter 25.4 mm and height 10 mm) that is pre-heated at 180 ºC. After pouring the mold along with the sample is kept in an oven maintained at 180 ºC for 2 minutes, to achieve uniform filling. Then it is cooled to room temperature. Before starting the experiment, the sample is kept in freezer at 0 ºC to facilitate the removal of sample from the mold.

(a) Samples and cylinder used for preparing samples

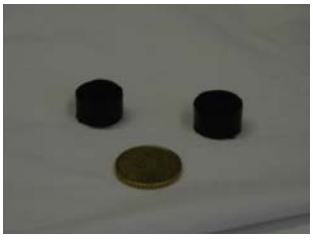

(b) Samples for fuel resistance through solubility

(c) Beakers with wire gauze before experiment

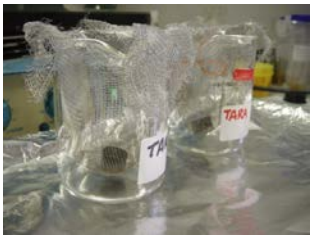

(d) Beakers with wire gauze and samples

(e) Beakers with kerosene and magnetic stirrer

(f) Solubility when the sample is introduced

***Figure 4.1** Schematic methodology adopted for solubility (continued)*

Then the sample is transferred to a metallic net of 0.5 mm mesh and weighed. Then, in a 400 ml beaker, half of the beaker (i.e., 200 ml) is filled accurately with kerosene. Then it is agitated with a magnetic stirrer around 50 rpm. The wire mesh with sample is immersed in the beaker. At an interval of 20 minutes difference in weight is calculated by removing the wire mesh from the beaker. Excess kerosene is wiped with filter paper during weighing. The schematic

methodology adopted for solubility test is shown in Figure 4a to 4i. This is based on the repeatability of results obtained with the earlier reports [198, 212].



(g) Removal of excess solvent from the sample during regular intervals of weighing

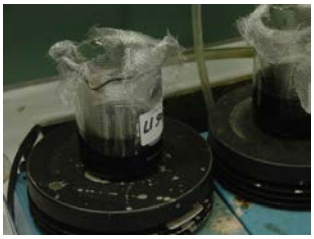

(h) Status at the end of the test (2 hour)

(i) Status of the sample at the end of the test (2 hour) [only insoluble sample shown]

***Figure 4.1** Schematic methodology adopted for solubility (continued)*

4.5 RESULTS AND DISCUSSION

Softening point (Table 4.2) of the base asphalt found to increase around 2 ºC, by the addition of clay. Out of the polymers used in this experiment, the addition of SBS showed the highest softening point up to 20 ºC irrespective of the base asphalt. As compared to the base asphalts, SBS with base asphalt L showed higher softening point of 2 ºC. When SBS/clay is introduced, further increase of 3 ºC in asphalt L and 2 ºC in asphalt R was observed. Further increase of softening point up to 5 ºC and 3 ºC was noticed with asphalt L and R respectively, when SBS nanocomposite is added. In all the SBS based binary blends and SBS based PMANs the blends with base asphalt L showed higher softening point. In case of EMA an increase of 15 ºC was noticed when it is added alone. The addition of EMA/clay was not found to have much impact in the softening point of as 2 ºC for asphalt L and 1 ºC for asphalt R was noticed. Surprisingly, EMA nanocomposite has reduced the softening point to 3 ºC then the binary blends with EMA. This may be due to the fact that EMA might have crosslinked/partially degraded during melt-blending with clay that might have reduced the possible reaction/inter-connection with the asphaltene irrespective of the presence of nanoclay. The softening point of blends and PMAN with EVA is similar to SBS based blends, but only 10 ºC increase was observed with the addition of EVA. Interestingly, asphalt R based

EVA/clay ternary blend and EVA PMAN showed 5 ºC rise in softening point as compared to its counter-part with asphalt L.

Table 4.2 Softening point ($T_{R\&B}$, ºC) data

Blend code	$T_{r\&b}$, ºC	Blend code	$T_{r\&b}$, ºC
L	49.0	R	48.0
LCL	52.3	RCL	52.3
LSBS	72.7	RSBS	68.9
LSBP	75.1	RSBP	71.4
LSBM	80.8	RSBM	75.3
LEMA	77.5	REMA	74.0
LEMP	76.8	REMP	76.2
LEMM	72.6	REMM	71.1
LEVA	60.5	REVA	62.0
LEVP	61.1	REVP	66.9
LEVM	70.2	REVM	76.3

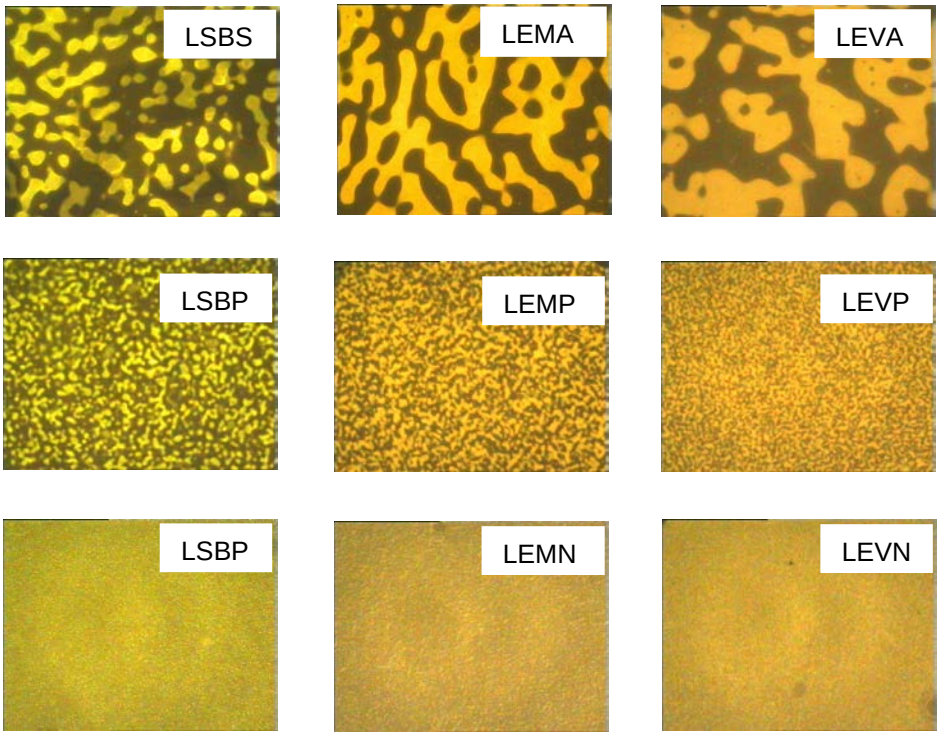

Figure 4.2 *Fluorescence microscopy of PMAN obtained from base asphalt L*

Softening point data clearly shows that compatibility of polymer, polymer/nanoclay combination and its nanocomposite nature/structure with the base asphalt plays a vital role in enhancing the softening point of the base asphalt.

It could be seen clearly that ethylene based polymers (figure 4.2, LEMP and LEVP) found to swell to a larger extent as compared to SBS which is confirmed from the higher dimension of the dispersed domains. The introduction of nanoclay directly to the asphalt has altered the phase morphology completely that could be observed from figures 4.2, LSBP, LEMP and LEVP. In case of LSBP (figure 4.2), an interwined, rather unstable phase is observed which is neither dominated by SBS nor by asphalt. The initiation of phase reversion from asphaltic phase to polymer is noticed with LEMP (figure 4.2). Here, the asphaltic domains are completely surrounded by EMA/CL combination. In turn LEVP (figure 4.2) features with a continuous polymeric phase with a fine dispersion of asphalt components featured as dark/black droplets. The affinity of EVA with asphalt L is found to be more in presence of nano clay when compared with EMA which is observed from the dimension of dispersed asphalt droplets (figure 4.2 LEMP and LEVP). Figure 4.2, LSBM, LEMM and LEVP, shows the morphology of PMANs prepared by introducing the polymer/clay nanocomposite obtained by melt blending to asphalt. The phase morphology of all the above systems infers that the melt-blending of polymer/nanoclay has led to increase in surface area of the corresponding polymer. Also the equi-phase morphology (where polymer and asphalt is uniformly dispersed and distributed) confirms that nanoclay (CL) is acting as surfactant that facilitated the asphalt components to form inter-connected network which is line with the earlier studies [158]. At the same time, it could be clearly observed from LEMP (figure 4.2) and LEMM (figure 4.2), phase inversion initiated with the introduction of nano clay is not dominated by polymeric phase as the case with EVA PMANs (figure 4.2, LEVP and LEVM). Rather, fine dispersion of asphaltic phase featuring with dark/black is observed. This factor may be due to the presence of partial crosslink arises during the melt blending of EMA and clay. All the morphological features lie in agreement with the softening point changes provided in table 4.2.

Figure 4.3 provides the morphology of asphalt blends and nanocomposites with base asphalt R. It could be noticed that, polymers added in asphalt R is found to swell to lesser extent (figure 4.3, RSBS, REMA and REVA) as compared with asphalt L (figure 4.2, LSBS, LEMA and LEVA). The dimension of the light or yellow/green region confirms this observation (figure 4.3, RSBS, REMA and REVA) with asphalt as continuous phase and polymer as dispered phase. In case of EMA (figure 4.3, REMA) and EMA (figure 4.3, REVA), we could notice large size continuously dispersed domains of polymer that infers lesser interaction with the asphaltene components.

With the addition of nanoclay, initiation of phase inversion observed with EMA (figure 4.3, REMP) and EVA (figure 4.3, REVP) except SBS (figure 4.3, RSBP). It is similar to the interwined or unstable phase of asphalt and polymer co-exisiting

with the asphalt L (figure 4.3). This co-continuous morphology becomes polymer rich continuous phase as the polymer nanocomposite is introduced (figure 4.3, RSBM, REMM, REVM). Due to the fact that nano clay is acting as surfactant asphaltene components found dispersed with the addition of polymer nanocomposite (figure 4.3, RSBM, REMM, REVM) when compared with the PMAN with physical mixing (figure 4.3, RSBP, REMP, REVP). The morphological feature infers that the asphalt R is having lesser compatibility with the polymers used in this study and with clay. In spite of the coarse dispersion of asphaltenes in EVA PMAN (figure 4.3, REVM), found to have higher softening point as compared to its asphalt L counter-part (figure 4.2, LEVM). This fact clearly states that excessive swelling of polymer will cease the effect of polymer in the asphalt [22] which is evidenced from the morphology (figure 4.2, LEVP and figure 4.3, REVP) and softening point values of EVA based binary/ternary blends (table 4.2).

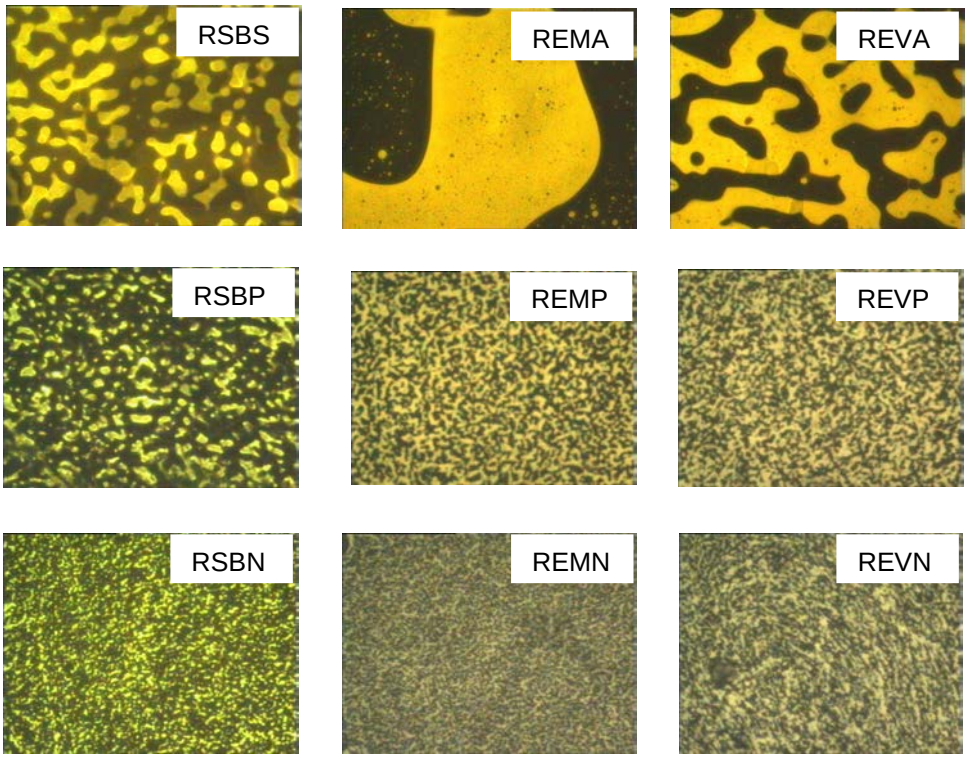

Figure 4.3 *Fluorescence microscopy of PMAN obtained from based asphalt R*

Fuel resistance as obtained by immersing the binary blends and PMANs in kerosene is shown in figure 4.4 and 4.5 for the base asphalts L and R respectively. The addition of nanoclay found to increase the solubility of both the asphalts (figure 4.4 and 4.5) when compared with the solubility of base asphalts L and R. The introduction of nanoclay has different effect in the solubility or the fuel resistance of the binary blends and PMANs.

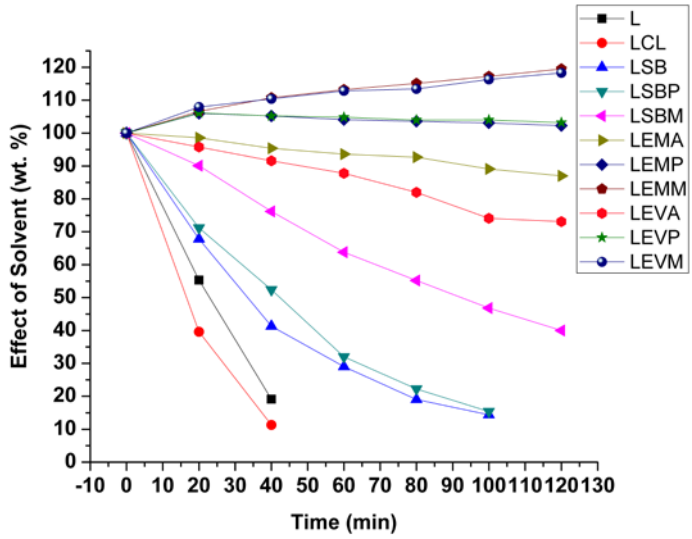

Figure 4.4 *Fuel resistance of mixes with base asphalt L*

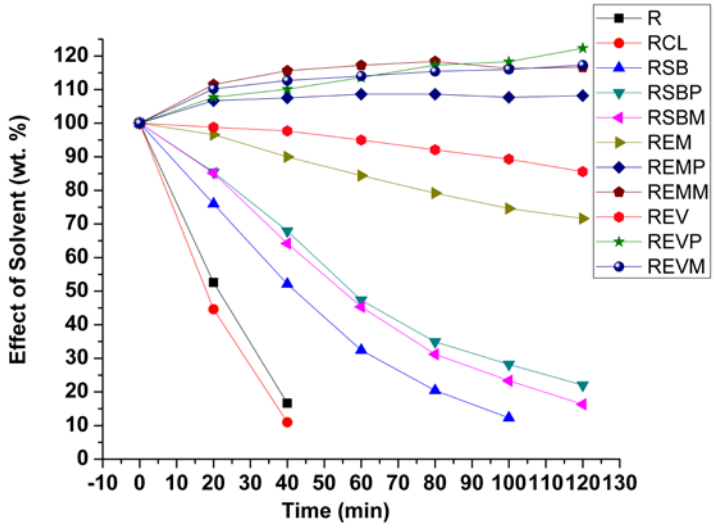

Figure 4.5 *Fuel resistance of mixes with base asphalt R*

In case of SBS, asphalt containing SBS alone found to solubilize/dissolve completely after 100 minutes (figure 4.4 and 4.5). The solubility of SBS and SBS/clay with asphalt L does not vary significantly. After 100 minutes both samples (LSBS and LSBP) found to be soluble completely (figure 4.4). In turn SBS nanocomposite, showed better resistance to kerosene and 40 % of the sample was remaining after 120 minutes. In turn asphalt R based SBS blends

showed a different trend (figure 4.5). Both the PMANs (RSBP and RSBM) found to withstand upto 120 minutes and around 20 % of the sample recovered after test.

EMA and EVA based binary/blend found to show excellent fuel resistance when compared with SBS. The fuel resistance of EMA alone is higher in asphalt L with a reduction of just 13 % from its original mass and EVA retains 85.6 % of its original weight in asphalt R. Irrespective of physical mixing or nanocomposite melt blending methods, PMANs with EMA and EVA exhibit remarkable fuel resistance. For physical mixes, the samples swelled with increase in time and up to 2 % swelling was noticed. Interestingly, for nanocomposite blends at the end of the test almost the sample swelled up to 18 %.

4.6 CONCLUSION

Various polymer modified asphalt nanocomposites (PMAN) obtained from different preparation techniques resulted in novel pavement materials with higher softening point and enhanced fuel resistance. Among all the polymers used in this study EMA and EVA showed exceptional fuel resistance. The phase morphology clearly shows that exceptional swelling will not yield better softening point.

Chapter 5

5.1 INTRODUCTION

Flame resistance or fire retardant property is one of the major research areas in asphalt since four decades. Earlier fire retardant asphalt base cover or shingles for roofing application along with other thermoplastic material [213], eco-friendly material [214], and similar compositions using halogenated catalyst [215] were developed. The incorporation of flame retardant initiated with ammonium sulfate [216, 217], followed by colemanite along with SBS [218], and further developed with other flame retardant and its combinations [219]. Though several literatures report the flammability properties of asphalt [220-222], till date there is no clear data on the flammability properties of asphalt when it is modified with polymer and polymer nanocomposite. This chapter discusses the flammability of asphalts, polymer modified asphalts and polymer modified asphalt nanocomposites as obtained through limiting oxygen index (LOI) measurements developed at University of Pisa.

5.2 EXPERIMENTAL

Ethylene vinyl acetate (EVA) with 28 wt. % vinyl acetate content (Greenflex HN70, EVA) from Polymeri Europa, Styrene-butadiene-styrene, linear (Kraton D-1102, LSBS) with 28 % polystyrene from Kraton Polymers are the polymers used in this study. Cloisite 20A® (CL), from Southern Clay Products, USA, an organoclay prepared from a sodium montmorillonite having a cation exchange capacity of 0.926 meq·g^{-1} by treatment with dimethyldihydrogenated-tallow ammonium chloride is the nano clay employed. Vacuum distilled asphalt with 50/70 pen grade as available was employed for preparing the binary blends with polymer and PMAN. Neat asphalt is indicated with A. Binary blends of asphalt are indicated as EA for EVA modified asphalt and LA for LSBS modified asphalt. Ternary blends of

polymer/nanoclay and asphalt, i.e., PMAN from EVA and LSBS are indicated as EVAN and LSAN respectively. The blends were prepared as described in the previous chapters. Polymer nano composites were prepared by adding polymer and nanoclay in the ratio 60:40 wt. % using a Brabender Plasticorder at temperatures 190 °C and 140 °C for EVA and LSBS respectively. For morphology, hot asphalt mix is poured into a cylindrical mold preheated to 180 °C. Detail preparation and sampling methods are available in the earlier chapters. Morphology is studied using Fluorescence microscope and flammability property is measured using Dynisco Plastics limiting oxygen index (LOI) Analyzer. Disc shape samples were prepared by pouring hot asphalt in a ring of 25.6 mm outer diameter with height 10 mm. Prior to the filling of asphalt, the ring is coated with silicone gel to avoid sticking and to facilitate easy removal. After making the asphalt/PMA/PMAN disc, it is placed in a brass cylinder of diameter 25.4 mm and height 30 mm. Then the cylinder is placed in the LOI gas vent and the sample is placed. To prevent falling of molten asphalt while burning, aluminum foil was placed beneath the cylinder. LOI measurements carried out based on ASTM D 2863-97 by developing new experimental set-up (Figure 5.1a to 5.1h).

Figure 5.1 *Schematic representations for LOI test carried out, (a) LOI equipment without the facility for asphalt, (b) LOI equipment with the facility for asphalt testing*

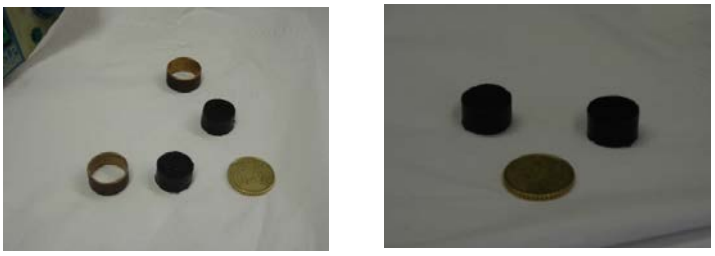

Figure 5.1 *Samples for LOI test carried out, (c) Samples and cylinder used for making samples, (d) Samples after removed from the cylinder*

Figure 5.1 *Samples for LOI test carried out (e) Sample after positioning (f) Set up to collect the molten asphalt during testing*

Figure 5.1 *Samples for LOI test carried out (g) Sample before ignition (h) Status during testing*

5.2.1 Strategies for Flammability test

Period or extent of burning	- 60 s
Gas velocity	- 3.2 cm/s
Flame projection	- 16 ± 4
Flame contact time	- 15 s

5.3 RESULTS AND DISCUSSIONS

Table 5.1 provides the flammability of asphalt, its binary and ternary blends. In general, neat asphalt was found to have better fire retardant property. But the introduction of polymers and polymer nano composite found to be quiet interesting. From the literature it was noticed that EVA and LSBS have low oxygen index values of 17-20 [221] and 19 [225] respectively. So naturally this may reduce the oxygen index value or increase the flammability of the asphalt which is evidenced

Table 5.1 Oxygen Index of Asphalt and its binary/ternary blends (PMAN)

Sl. No.	Component	LOI (%)
1.	A	39.01
2.	EA	36.59
3.	EVAN	38.65
4.	LA	36.78
5.	LSAN	28.12

in Table 5.1. In case of PMAN's, EVAN found to improve the fire retardancy to a considerable extent (table 5.1) but less than the oxygen index value of A. At the same time, LSAN found to decrease the fire retardant property of asphalt much lower than its original value. To understand this features, morphology (x200 magnification) of the blends obtained using fluorescence microscope.

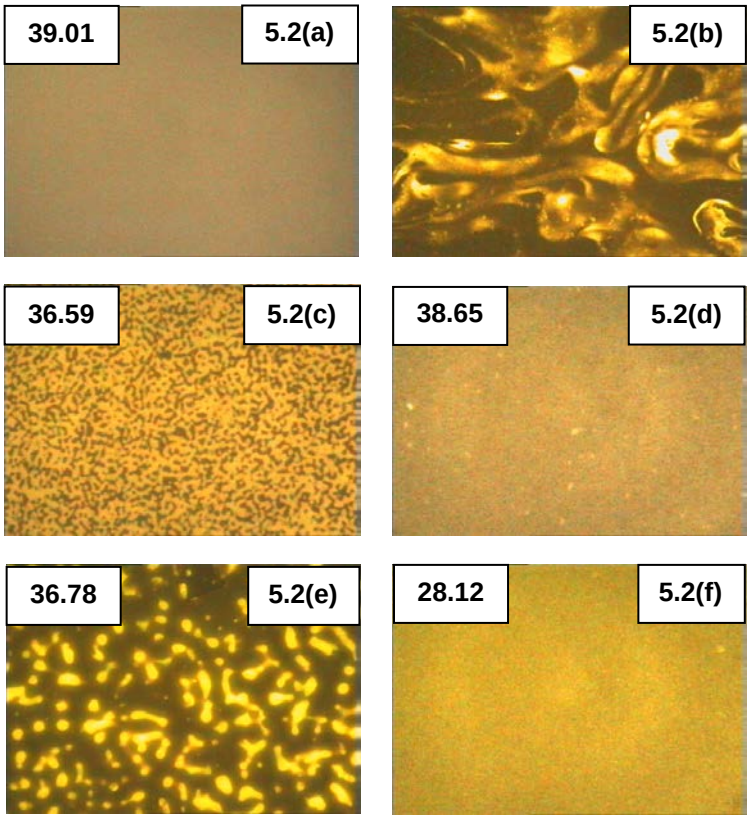

Figure 5.2 *Morphology of mixes obtained for flammability studies (a) Base asphalt (b) Mixing phase of asphalt (c) EVA modified asphalt (d) EVA asphalt nanocomposite (e) LSBS modified asphalt (f) LSBS asphalt nanocomposite*

Figure 5.2(a) to 5.2(f) shows the morphology of all the blends. The morphology of neat asphalt and the inter-connected, interactive phase during blending is shown in figures 5.1 (a) and (b). Neat asphalt features with a single uniform pale region representing characteristic fluorescence by asphaltene. A typical record of morphology of mixing phase is shown in Figure 5.2 (b). Figures 5.2 (c) and (e) provides the morphology with EVA and LSBS respectively. It could be clearly noticed that in case of EVA [figure 5.2(c)] the dispersion of EVA in the asphalt has resulted in phase inversion, i.e., the continuous phase of asphalt has been replaced by EVA phase which is due to the dispersion of EVA which is having good compatibility with asphalt. Through the formation of this continuous phase EVA responds the flammability, which resulted in lower value. But in the case of LSBS [figure 5.2(d)], the continuous phase of asphalt is retained and the LSBS is swelled in the asphalt moiety, due to lesser compatibility. In spite of the presence of LSBS the response arises from the asphalt continuous phase [figure 5.2(d)], where a slight increase in the oxygen index value is observed as compared to EA.

PMAN [figure 5.2 (d) and (f)] features with a highly dispersed single phase irrespective of EVA and LSBS. The presence of nano clay in case of EVAN [figure 5.2 (d)] has increased the fire retardancy when compared with EVA alone [figure 5.2(c)]. At the same time, the oxygen index is lesser than the base asphalt [Table 1, figure 5.2(a)]. This could be due to the change of preparation method as compared to earlier method [158], where a lesser dispersion was noticed. On the contrary, it is interesting to note that LSAN needs very less oxygen concentration to get ignited, which is very lower than the neat asphalt (Table 5.1).

LSBS alone [Figure 5.2(e)] could not found to be much compatible with the asphalt, but in presence of nano clay, which acts as a compatiblizer enhances the dispersion of LSBS in the asphalt and a single continuous phase of LSBS results [Figure 5.2(f)], where LSBS might be responding to the flame due this uniform phase, which considerably reduces the oxygen index value.

5.4 CONCLUSION

From the preliminary investigations, it could be observed that asphalt itself is having considerable flame resistance. EVA and LSBS having low oxygen index values tend to reduce the oxygen index of asphalt. At the same time, PMAN with EVA found to have better oxygen index as compared to EVA alone. At the same time, LSAN does not impart fire retardancy to asphalt.

Chapter 6

6.1 INTRODUCTION

Superpave performance grading (PG) is based on the idea that an HMA asphalt binder's properties should be related to the conditions under which it is used.

For asphalt binders, this involves expected climatic conditions as well as aging considerations. Therefore, the PG system uses a common battery of tests (as the older penetration and viscosity grading systems do) but specifies that a particular asphalt binder must pass these tests at specific temperatures that are dependant upon the specific climatic conditions in the area of use. Therefore, a binder used in the Sonoran Desert of California/Arizona/Mexico would have different properties than one used in the Alaskan tundra. This concept is not new – selection of penetration or viscosity graded asphalt binders follows the same logic – but the relationships between asphalt binder properties and conditions of use are more complete and more precise with the Superpave PG system. Information on how to select a PG asphalt binder for a specific condition is contained in Superpave mix design method. Table 6.1 shows how the Superpave PG system addresses specific penetration, AC and AR grading system general limitations.

Superpave performance grading is reported using two numbers – the first being the average seven-day maximum pavement temperature (°C) and the second being the minimum pavement design temperature likely to be experienced (°C). Thus, a PG 58-22 is intended for use where the average seven-day maximum pavement temperature is 58°C and the expected minimum pavement temperature is -22°C. Notice that these numbers are pavement temperatures and not air temperatures (these pavement temperatures are estimated from air temperatures using an algorithm contained in the [LTPP Bind] program). As a general rule-of-

thumb, PG binders that differ in the high and low temperature specification by 90°C or more generally require some sort of modification.

Table 6.1 Prior limitations vs. superpave testing and specification features

Limitations of Penetration, AC and AR Grading Systems	**Superpave Binder Testing and Specification Features that Address Prior Limitations**
Penetration and ductility tests are empirical and not directly related to HMA pavement performance.	The physical properties measured are directly related to field performance by engineering principles.
Tests are conducted at one standard temperature without regard to the climate in which the asphalt binder will be used.	Test criteria remain constant, however, the temperature at which the criteria must be met changes in consideration of the binder grade selected for the prevalent climatic conditions.
The range of pavement temperatures at any one site is not adequately covered. For example, there is no test method for asphalt binder stiffness at low temperatures to control thermal cracking.	The entire range of pavement temperatures experienced at a particular site is covered.
Test methods only consider short-term asphalt binder aging (thin film oven test) although long-term aging is a significant factor in fatigue cracking and low temperature cracking.	Three critical binder ages are simulated and tested: 1. Original asphalt binder prior to mixing with aggregate. 2. Aged asphalt binder after HMA production and construction. 3. Long-term aged binder.
Asphalt binders can have significantly different characteristics within the same grading category.	Grading is more precise and there is less overlap between grades.
Modified asphalt binders are not suited for these grading systems.	Tests and specifications are intended for asphalt "binders" to include both modified and unmodified asphalt cements.

6.2 GRADE SELECTION

To specify a performance graded asphalt binder, one needs to determine the temperature extremes under which the pavement must perform. A grade is

determined by indicating the high and low temperatures for performance. As an example, we expect PG 64-22 to perform at a high temperature of 64°C and a low temperature of -22°C. The grading system uses increments of 6°C for the high and low temperature designation. The Performance-Graded Binder specification in Item 300 uses high temperatures of 58, 64, 70, 76, and 82 and low temperatures of -16, -22, -8, and -34. The high temperature designation represents the 7-day average high pavement temperature. The low temperature designation represents a single occurrence low pavement temperature.

Any location is subject to mild summers and hot summers, and mild winters and cold winters. This means that at each location, the climate is a statistical distribution. There is an average 7-day high average pavement temperature and average low pavement temperature and associated standard deviations to account for yearly variations. The SHRP researchers recognized this and integrated this into the PG selection process. To be able to select a binder for any location, one needs to know the climate distribution and choose an acceptable risk factor of exceeding the design temperatures. The climate of the location, risk or reliability factors, and the standard grade temperatures will determine the actual PG binder to choose.

The specifier can choose to alter the climate grade by using the additional factors of traffic and loading. If there is slower moving traffic, the rutting potential is higher and the high temperature portion of the binder grade can be “bumped” up one grade (i.e. 64 to 70). If there is standing traffic, the rutting potential is even more, and the high temperature grade can be “bumped” up two levels over the standard climate-based grade (i.e. 64 to 76). In all these modifications, the low temperature grade remains the same. At TxDOT, we have additional criteria for bumping the high grade. This includes mixture type such as SMA and PFC.

6.3 THE DISTRESSES AND TESTS

If the pavement lasts long enough, the life of the binder and pavement is very predictable. Binders arrive at the hot mix plant, are aged during the mixing process, and after placement begin a long-term aging process in the road. If the binder is not stiff enough when the pavement is first placed, the mix is susceptible to rutting. If mixtures do not rut, the binder generally get harder and harder (stiffer and stiffer) in the pavement with time and the pavement eventually cracks. Cracking occurs because the binder gets too stiff and cracks when the road contracts at low temperatures or they may fail in fatigue. The effect is the same; the binder is too stiff to handle the stresses applied to it.

Knowing this typical pavement life cycle, the Superpave specification tests for resistance to rutting early in the pavement life and fatigue and thermal cracking resistance later in the pavement life.

The equipment used in the specification is several types of ovens (for aging procedures), a dynamic shear rheometer, a bending beam rheometer and a direct

tension tester. Asphalt binders are tested in a manner that simulates the stage in pavement life in which various distresses occur. These stages are: unaged, simulated aging through the hot mix plant, and simulated long-term aging in the roadway.

Unaged asphalts as-received (tank) are started as a material with a minimum amount of stiffness. Highly fluid materials that age severely through a hot mix plant are avoided. We measure binder stiffness with the Dynamic Shear Rheometer.

The Rolling-Thin-Film-Oven (RTFO) simulates the binder aging which occurs through the hot mix plant. This is to guard against rutting. As asphalts age in the pavement, they get harder and harder (stiffer and stiffer). If the binder is stiff enough to avoid rutting when placed, it will most likely not rut later in life.

The Pressure Aging Vessel uses RTFO aged binder to simulate long-term aging. This conditioning simulates approximately 5 to 8 years aging in the pavement. This is the time in the pavement's life where we are concerned about fatigue and thermal cracking. The Dynamic Shear Rheometer measures stiffness to indicate the binder's fatigue resistance and the Bending Beam Rheometer measures its resistance to thermal cracking. The direct tension test is used under some circumstances to indicate that even though a binder is otherwise too stiff at low temperatures, it is resistant to low temperature cracking if is capable of enduring at least 1% strain at low temperatures.

6.4 TESTING FOR COMPLIANCE

There are two mechanisms for determining the PG binder grade: Classification and Verification.

When the PG grade is unknown, Classification is done. This involves a trial and error process, performing the tests at various PG temperatures to bracket the specification temperatures at which the material passes and fails to meet the specification requirements.

When PG grade in available or informed, Verification is conducted. In this process, the test temperatures are known and tests are carried out at specified temperatures only, with either a passing or failing result. The elapsed time for complete testing will be 1.5 to 2.5 days. Most of TxDOT's binder testing falls into this category.

The high temperature portion of the PG binder by testing the RTFO residue with the Dynamic Shear Rheometer is verified. As the temperature is known, only one DSR test is sufficient. The time schedule for this testing will be: Sample preparation - approximately 1 hr (oven heating to 135C and stirring approximately 5 minutes with mechanical stirring device if needed); RTFO aging - 85 minutes; and DSR testing - 30 minutes. This results in a total elapsed time of approximately 3 hours. Person-hour requirements are approximately 1 hour.

The table below is the standard summary table presented in the AASHTO MP 1 specification for performance graded asphalt binder.

The following items may help to decipher this table:

- The top several rows (all the rows above the "original binder" row) are used to designate the desired PG grade. For instance, if the average 7-day maximum pavement design temperature is greater than 52°C but less than 58°C then you should use the "< 58" column. The temperatures directly under the "< 58" cell are selected based on the minimum pavement design temperature in °C.
- No matter what the desired PG binder specification, the same tests are run. The PG specification (e.g., PG 58-22) just determines the temperature at which the tests are run.
- Tests are run on the original binder (no simulated aging), RTFO residue (simulated short-term aging) and PAV residue (simulated long-term aging) in order to fully characterize the asphalt binder throughout its life. Notice that often the same test is run on different simulated binder ages. For instance, the dynamic shear test is run on all three simulated binder ages.

Table 6.2 Performance Graded Asphalt Binder Specifications (Source: AASHTO, 2001)

Performance Grade	PG 46			PG 52							PG 58					PG 64					
	34	40	46	10	16	22	28	34	40	46	16	22	28	34	40	10	16	22	28	34	40
Average 7- day Maximum Pavement Design Temperature, °C[a]	< 46			< 52							< 58					< 64					
Minimum Pavement Design Temperature, °C[a]	-34	-40	-46	-10	-16	-22	-28	-34	-40	-46	-16	-22	-28	-34	-40	-10	-16	-22	-28	-34	-40
ORIGINAL BINDER																					
Flash Point Temp, T 48, Minimum (°C)	230																				
Viscosity, ASTM D 4402:[b] Maximum, 3 Pa's, Test Temp, °C	135																				
Dynamic Shear, TP 5:[c] G*/sinδ, Minimum, 1.00 kPa Test Temp @ 10 rad/s, °C	46			52							58					64					
ROLLING THIN FILM OVEN RESIDUE (T 240)																					
Mass Loss, Maximum, percent	1.00																				
Dynamic Shear, TP 5: G*/sinδ, Minimum, 2.20 kPa Test Temp @ 10 rad/s, °C	46			52							58					64					
PRESSURE AGING VESSEL RESIDUE (PP 1)																					
PAV Aging Temperature, °C[d]	90			90							100					100					
Dynamic Shear, TP 5: G*/sinδ, Maximum, 5000 kPa Test Temp @ 10 rad/s, °C	10	7	4	25	22	19	16	13	10	7	25	22	19	16	13	31	28	25	22	19	16
Physical Hardening[e]	Report																				
Creep Stiffness, TP 1 Determine the critical cracking temperature as described in PP 42	-24	-30	-36	0	-6	-12	-18	-24	-30	-36	-6	-12	-18	-24	-30	0	-6	-12	-18	-24	-30
Direct Tension, TP 3 Determine the critical cracking temperature as described in PP 42	-24	-30	-36	0	-6	-12	-18	-24	-30	-36	-6	-12	-18	-24	-30	0	-6	-12	-18	-24	-30

[a] Pavement temperatures are estimated from air temperatures using an algorithm contained in the LTPP Bind program, may be provided by the specifying agency, or by following the procedures as outlined in MP 2 and PP 28.

[b] This requirement may be waived at the discretion of the specifying agency if the supplier warrants that the asphalt binder can be adequately pumped and mixed at temperatures that meet all applicable safety standards.

[c] For quality control of unmodified asphalt binder production, measurement of the viscosity of the original asphalt binder may be used to supplement dynamic shear measurements of G*/sinδ at test temperatures where the asphalt is a Newtonian fluid.

[d] The PAV aging temperature is based on simulated climatic conditions and is one of three temperatures 90°C, 90°C or 110°C. The PAV aging temperature is 100°C for PG 58- and above, except in desert climates, where it is 110°C.

[e] Physical hardening -- TP 1 is performed on a set of asphalt beams according to Section 12, except the conditioning time is extended to 24 hours ± 10 minutes at 10°C above the minimum performance temperature. The 24-hour stiffness and *m*-value are reported for information purposes only.

[f] G*/sinδ = high temperature stiffness and G*/sinδ = intermediate temperature stiffness

Table 6.2 Performance Graded Asphalt Binder Specifications (Source: AASHTO, 2001) (continued)

Performance Grade	PG 70						PG 76					PG 82				
	10	16	22	28	34	40	10	16	22	28	34	10	16	22	28	34
Average 7-day Maximum Pavement Design Temperature, °C[a]	< 70						< 76					< 82				
Minimum Pavement Design Temperature, °C[a]	-10	-16	-22	-28	-34	-40	-10	-16	-22	-28	-34	-10	-16	-22	-28	-34
ORIGINAL BINDER																
Flash Point Temp, T 48, Minimum (°C)	230															
Viscosity, ASTM D 4402:[b] Maximum, 3 Pa*s, Test Temp, °C	135															
Dynamic Shear, TP 5:[c] G*/sinδ[f], Minimum, 1.00 kPa Test Temp @ 10 rad/s, °C	70						76					82				
ROLLING THIN FILM OVEN RESIDUE (T 240)																
Mass Loss, Maximum, percent	1.00															
Dynamic Shear, TP 5: G*/sinδ[f], Minimum, 2.20 kPa Test Temp @ 10 rad/s, °C	70						76					82				
PRESSURE AGING VESSEL RESIDUE (PP 1)																
PAV Aging Temperature, °C[d]	100 (110)						100 (110)					100 (110)				
Dynamic Shear, TP 5: G*sinδ[f], Maximum, 5000 kPa Test Temp @ 10 rad/s, °C	34	31	28	25	22	19	37	34	31	28	25	40	37	34	31	28
Physical Hardening[e]	Report															
Creep Stiffness, TP 1 Determine the critical cracking temperature as described in PP 42	0	-6	-12	-18	-24	-30	0	-6	-12	-18	-24	0	-6	-12	-18	-24
Direct Tension, TP 3 Determine the critical cracking temperature as described in PP 42	0	-6	-12	-18	-24	-30	0	-6	-12	-18	-24	0	-6	-12	-18	-24

The tests run on the binder are listed in the left-hand column. They are not necessarily listed by their common names but the applicable AASHTO test procedure is listed. For instance, "Flash Point Temp. T 48, Minimum (^{o}C)" means that the flash point is measured according to AASHTO T 48 and that the value in the adjacent column represents the minimum allowable in degrees Centigrade.

A unique feature of Superpave specification, apart from other specifications, is based on the fact that the specified criteria the asphalt has to meet remain constant, but the temperatures at which the criteria must be achieved are different (performance grading system). Therefore regardless of the region or climate the asphalt road is constructed the good performance of pavements should be assured [226]. As mentioned previously, the Superpave tests measure physical properties that can be directly related to field performance and also the used test temperatures are temperatures the asphalt pavement can encounter during its service. Table 6.2 shows the current binder grades in AASHTO (American Association of State Highway and Transportation Officials) M 320-05 specification.

Table 6.3 Superpave Binder Grades

High Temperature Grades (°C)	Low Temperature Grades (°C)
PG 46	-34, -40, -46
PG 52	-10, -16, -22, -28, -34, -40, -46
PG 58	-16, -22, -28, -34, -40
PG 64	-10, -16, -22, -28, -34, -40
PG 70	-10, -16, -22, -28, -34, -40
PG 76	-10, -16, -22, -28, -34
PG 82	-10, -16, -22, -28, -34

The main motif of the Superpave specification is testing of asphalt binders at conditions which simulate the three critical stages during their life [226]. The tests performed on original asphalts represent the first stage of transport, storage and handling. To ensure that the asphalt binders can be pumped and handled at the hot-mixing facility the specification contains a maximum viscosity requirement 3 Pa.s which must be achieved at 135°C for all grades [227]. To address the safety concerns the flashpoint test [228] determines the temperature the asphalt can be safely heated to in the presence of an open flame. The minimum temperature e required for all grades is 230°C.

The second stage represents hot-mixing of asphalt binder with aggregates in mix production plant and road construction phase. To achieve that, the asphalt binder (eight sample bottles of 35 grams each) is aged in a rolling thin film oven test (RTFO or RTFOT, [229]) for 85 minutes at 163 °C. During this process fresh asphalt surface is continuously exposed to heat and air flow (Figure 6.1).

Another purpose of this method is to determine the mass quantity of volatile compounds lost from the asphalt during this process. The mass of lost volatiles can indicate the extent of aging which can occur in asphalt material during the hot-mixing process or during the road construction phase.

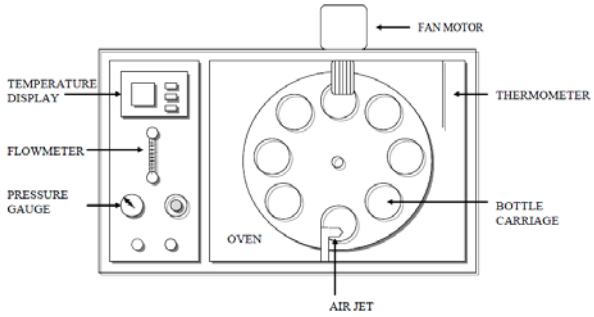

Figure 6.1 *Schematic diagram of Rolling Thin Film Oven*

The asphalt pavement accumulates small but permanent deformations after each traffic load eventually forming a depression in a wheel path. In Superpave specification the factor G^* / sinδ is a measure of rutting resistance of asphalt binder. It is determined by the dynamic shear rheometer (DSR, see Figure 6-2) and must be the minimum of 1 kPa for the original asphalt binder and 2.20 kPa for RTFOT aged asphalt binder. Therefore high values of G^* (magnitude of the complex modulus) and low values of δ (phase angle) are desirable for a good rutting resistance. The parameter is currently under the review because it was shown that it does not reflect correctly the properties of polymer modified binders [232, 233].

Another pavement distress, fatigue cracking, generally occurs at low to moderate temperatures when the stress from traffic load exceeds the tensile strength of the asphalt pavement. The characteristic feature of fatigue cracking is its progressiveness when the cracks join and lead to even more cracks. The measure of fatigue cracking resistance in Superpave specification is defined as G^* sinδ . In order to ensure good fatigue cracking resistance of asphalt pavement Superpave specification defines a maximum value of 5000 kPa for G^* sinδ factor in RTFOT and PAV aged asphalt samples.

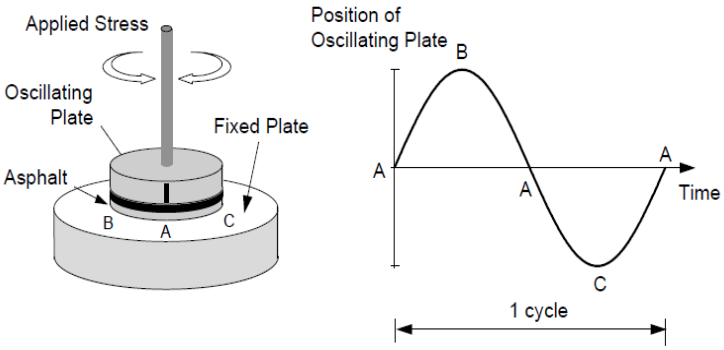

Figure 6.2 *Schematic diagram of Dynamic Shear Rheometer*

In this case low values of both *G** and δ are considered desirable in terms of fatigue cracking resistance. Thermal cracking occurs predominantly at low temperatures therefore term low temperature cracking is more often used. Low-temperature cracking is caused by adverse ambient conditions rather than by traffic loads.

At low temperatures the asphalt binder has tendency to shrink which leads to build-up of tensile stresses. Low-temperature cracks occur when the stresses exceed the tensile strength of the asphalt pavement. The bending beam rheometer (BBR, see Figure 6.3) is used to determine the low-temperature properties of asphalt binders. During the test the BBR applies a creep load to an asphalt beam and measures the creep stiffness (resistance to the load). The higher is the creep stiffness the higher is the probability of binder to crack at low temperatures. Therefore a maximum limit of 300 MPa for creep stiffness after 60 seconds of loading for RTFOT and PAV aged asphalt samples has been defined by Superpave specification [226]. To reasonably shorten the test time the so-called "time-temperature superposition (TTS) principle" is used. The test which otherwise would need to be ran for two hours at temperature 10°C lower can be performed at temperature about 10°C higher in 60 seconds due to the TTS principle [226]. The rate at which the asphalt binder changes its stiffness with time is defined through the so-called m-value parameter (a slope of the stiffness vs. time curve [226]). A minimum m-value of 0.300 after 60 seconds of loading is required by the Superpave binder specification.

A high m-value is desirable since it indicates lower stiffness (smaller tensile stresses) and therefore lower chance for low temperature cracking. If the m-value is higher than 0.300 and creep stiffness is in a range between 300 and 600 MPa another test, the direct tension test (DTT, see Figure 6-4) is used to determine whether the sample meets the Superpave criteria.

The purpose of Super pave (Superior Performing Asphalt Paving) test could be consolidated in the following table 6.4 and figure 6.5.

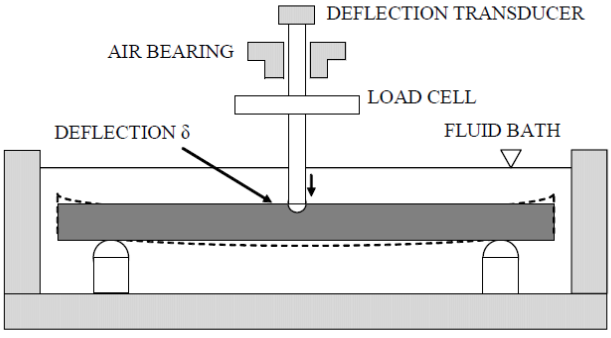

Figure 6.3 *Schematic diagram of the Bending Beam Rheometer (BBR) With the Sample Deflection at the Centre Point.*

Figure 6.4 *Direct Tension Test (DTT)*

Table 6.4 Purpose of Superpave tests

Superpave Binder Test	Purpose	Failure addressed
Dynamic Shear Rheometer (DSR)	Measure properties at high and intermediate temperatures	Rutting
Rotational Viscometer (RV)	Measure properties at high Temperatures	High temperature workability
Bending Beam Rheometer (BBR) Direct Tension Tester (DTT)	Measure properties at low temperatures	Cracking, Tensile failure
Rolling Thin Film Oven (RTFO) Pressure Aging Vessel (PAV)	Simulate hardening (durability) Characteristics	Cracking, Ageing behaviour

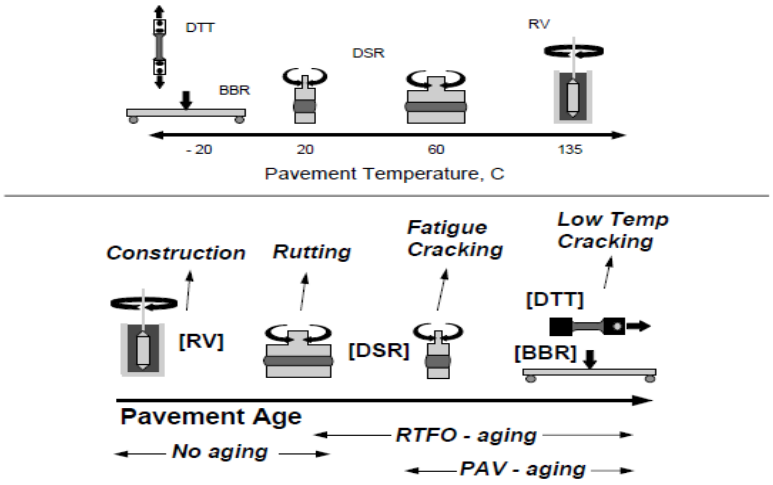

Figure 6.5 *Schematic diagram of Superpave tests, its purpose and properties addressed*

Table 6.7 Super pave Grading of Base Asphalt and PMAN

Original binder properties	SBAN		EVAN		BA	
Penetration @ 25°C, 100g, 5s [dmm]	40		70		40	
Viscosity @ 135°C [mPa.s]	22045		36555		301.4	
Dynamic Shear [G*/sin δ] [min 1.0 kPa] [kPa]	1.94		0.9	1.55	0.74	1.56
Temp [°C]	88.0		82.0	76.0	64.0	58.0
Pass / Fail Temp [°C]	96.5			80.9		61.6
Properties after RTFOT / TFOT						
RTFOT Mass Loss [%]	-0.06		-0.07		-0.35	
Dynamic Shear [G*/sin δ] [min 2.20 kPa] [kPa]	1.59	2.56	2.03	3.21	1.41	3.19
Temp [°C]	88.0	82.0	82.0	76.0	64.0	58.0
Pass / Fail Temp [°C]	83.9		81		60.7	
Multi-Stress Creep and Recovery, $R_{0.1}$ [kPa]	76.46		56.11		3.77	
Multi-Stress Creep and Recovery, $R_{3.2}$ [kPa]	3.63		1.61		0.69	
Multi-Stress Creep and Recovery, R_{diff} [%]	95.3		97.1		81.6	
Temp [°C]	82.0		82.0		58.0	
Non Recoverable Compliance, $J_{nr0.1}$ [%]	0.0		0.02		0.03	
Non Recoverable Compliance, $J_{nr0.1}$ [kPa^{-1}]	0.44		1.55		2.84	
Non Recoverable Compliance, $J_{nr3.2}$ [%]	0.05		0.08		0.03	
Non Recoverable Compliance, $J_{nr3.2}$ [kPa^{-1}]	5.48		8.1		3.15	
Non Recoverable Compliance $J_{nr\ diff}$ [%]	1148.6		424.2		11.1	
Final Accumulated Strain, [%]	1.752		2.591		1.008	
Properties after PAV						
PAV Aging Temperature [°C]	100		100		100	
Dynamic Shear [G* sin δ] [max 5000 kPa] [kPa]	5950	4127	6190	4319	5821	3972
Temp [°C]	22	25.0	19.0	22.0	22.0	25.0
Pass / Fail Temp [°C]	23.4		20.8		23.2	
Creep stiffness [S-max. 300 MPa] @ 60s	244	213	302	267	305	227
m-value [min. 0.300] @ 60 s	0.297	0.306	0.300	0.324	0.307	0.310
Temperature, [°C]	-15.0	-14.0	-16.0	-15.0	-15.0	-14.0
Performance Grade						
Superpave PG Grade	PG 82-22		PG 76-22		PG 58-22	
True Superpave Grade	PG 82-24		PG 80-25		PG 60-24	

6.5 MATERIALS

Ethylene vinyl acetate (EVA) with 28 wt. % vinyl acetate content (Greenflex HN70, EVA) from Polymeri Europa, Styrene-butadiene-styrene, linear (Kraton D-1102, LSBS) with 28 % polystyrene from Kraton Polymers are the polymers used in this study. Cloisite 20A® (CL), from Southern Clay Products, USA, an organoclay prepared from a sodium montmorillonite having a cation exchange capacity of 0.926 meq·g^{-1} by treatment with dimethyldihydrogenated-tallow ammonium chloride is the nano clay employed. Vacuum distilled asphalt with 50/70 pen grade as available was employed for preparing the ternary blends of polymer/nanoclay/asphalt (PMAN) is indicated as BA. PMAN were obtained by the melt blending of SBS and EVA with nanoclay designated as SBAN and EVAN respectively.

6.6 RESULTS AND DISCUSSION

Table 6.7 provides the detailed information about the Super pave performance grading of base asphalt, PMAN based on linear SBS and EVA. Of the three mixes EVAN shows very high penetration values, indicating the softness at room temperature which is far from the penetration values of BA and SBAN (table 6.7). Both the PMAN (table 6.7) found to possess very high viscosity, as compared BA, that may pose challenge during transport, storage and handling. To resist rutting binder must be stiff and elastic and to resist fatigue cracking a binder needs to be flexible and elastic. DSR measures the viscous and elastic behavior, by measuring the response of the asphalt to the applied force. By measuring *G** and *δ,* complete picture about the behavior of asphalt at pavement service temperature is arrived. *G**/*Sin δ*, rutting factor, represents the high temperature viscous component of overall binder stiffness. From the table 6.7, it is observed that rutting factor of EVAN is closer to BA, which is lower than the rutting factor of SBAN. A reverse trend was observed with the *G**/*Sin δ* values after RTFOT, i.e., *G**/*Sin δ* values are higher for BA and EVAN when compared to SBAN. Fatigue cracking as obtained from the *G**/*Sin δ* values found to be within the specification. Binders resistance to load as obtained from Creep stiffness (table 6.7) is higher for EVAN when compared with SBAN. A higher *m-value* indicates better low temperature cracking resistance. Based on the Superpave tests the performance grade of EVA asphalt nanocomposite is PG 80-25 and SBS asphalt nanocomposite is PG 82-24.

6.7 CONCLUSION

Polymer modified asphalt nanocomposite (PMAN) obtained from EVA (EVAN) and SBS (SBAN) after detailed investigation on thermal, morphological, structural and rheological front, found to emerge as new class of pavement material which is validated with Superpave tests. Challenging aspects are the cost of these materials due to nano clay and high viscosity.

Further Scope of Work

Polymer modified asphalt nanocomposites (PMAN) based on polymers like ethylene vinyl acetate (EVA) and styrene butadiene styrene (SBS) have been prepared and characterized with various techniques. From the validation of these new class of materials through Superpave tests, the performance grade of EVA asphalt nanocomposite (EVAN) is PG 80-25 and SBS asphalt nanocomposite (SBAN) is PG 82-24. These new class of materials features with better thermal resistance, structural stability, better flow properties as compared to the existing materials. Additionally these materials posses enhanced fuel resistance, which could address the airport filling station pavements and industrial pavements. A new method to obtain the flammability of asphalt, polymer modified asphalt and PMAN will help to study the fire resistance of these materials.

Within the scope of the work, this thesis outlines the preparation, characterization and validation of PMAN. As this new class materials need to be taken to field trial, further studies in this area would be:

- Storage stability and ageing studies.
- Effect of crystallinity, phase compatibility and overall chemistry on physical hardening should be studied.
- Effect of Jet Fuel on the rheology of PMAN.
- Hot Mix Asphalts (Asphalt concrete) should studied with PMAN and properties to be established.
- Flammability studies with various flame retardants with and without nanoclay.

References

1. History of Bitumen, *Nature*, Vol. 135 no. 3420, 1935, pp. 845.
2. Concawe Product Dossier 92/104, **Bitumen and Bitumen Derivatives**, Brussels, Concawe, 1992.
3. **The Oxford English Dictionary**, Oxford University Press, Oxford, 1989.
4. Standard terminology relating to materials for roads and pavements, **Annual Book of ASTM Standards**, 4.03, American Society for Testing and Materials, Philadelphia, ASTM D 8-97 2000.
5. Eilers, H., "The colloidal structure of asphalt", *Journal of Physical Chemistry*, Vol. 53, no. 8, 1948, pp. 1197-1211.
6. Read, J., Whiteoak, D., **The Shell Bitumen Handbook**, 5th edition, © Shell UK Oil Products Limited, 2003.
7. Murali Krishnan, J., Rajagopal, K.R., "Review of the uses and modeling of Bitumen from ancient to modern times", *Applied Mechanic Reviews,* Vol. 56, no. 2, 2003, pp. 150-214.
8. Williams, M.M., Sanskrit-English Dictionary: Etymologically and Philologically arranged with special reference to cognate Indo-European languages, Munshiram Manoharlal Publications Pvt., Ltd., 1999.
9. Forbes, R.J., "The nomenclature of bitumen, petroleum, tar and allied products in antiquity", *Mnemosyne – A Journal of Classical Studies,* Third Series, Vol. 4, Fasc. 1, 1936, pp. 67-77.
10. Forbes, R.J., **Bitumen and Petroleum in Antiquity,** in: Brill, E.J. (Ed), **Studies in Ancient Technologies,** Vol. 1, 2nd Edn., 1964, pp. 11-23.
11. Bikadii, Z., "Bitumen – A History", *Saudi Aramco World,* Vol. 35, no. 6, 1984, pp. 2-9.
12. Boëda, E., Connan, J., Dessort, D., Muhesen, S., Mercier, N., Valladas, H., Tisnérat, N., "Bitumen as hafting material on middle palaelithic artefacts", *Nature,* 380, 1996, pp. 336-338
13. Boëda, E., Connan, J., Muhesen, S., Bitumen as hafting material on middle palaeolithic artifacts from the El Kowm Basin, Syria, in: Akazawa, T., Aoki, K., Bar-Yosef, O. (Eds)., Neandertals and Modern Humans in Western Asia, Eds:, Plenum Press, Newyork and London, 1998.
14. Zimmer, H., **The Art of Indian Asia, its Mythology and Transformations**, Completed and Edited by Campbell J. Princeton University Press, New York, 1960.
15. Majumdar, R.C.,, Raychaudhari, H.C., Datta, K., **An Advanced History of India**, Macmilllan, London, 1963.
16. Basham, A.L., The Wonder that was India: A Survey of the History and

Culture of the Indian Sub-continent Before the coming of the Muslims, Taplinger Publications, New York, 1968.

17. Marshall, J., Mohenjadaro and Indus Civilization: Being an Official Account of Archaelogical Exacavations carried out by the Government of India between the years 1922 and 1923, 3 Volumes, Indological Book House, Delhi, 1973.
18. Yen, T.F., **The realms and definitions of Asphalts**, in: Yen, T.F, Chilingarina, G.V., (Eds)., **Asphalts and Asphaltenes**, Vol. 2, Elsevier, Netherlands, 2000.
19. Abraham, H., **Asphalts and Allied Substances**, Vol. 1, 6th edition. Van Nostrand, Princeton, New Jersey, 1960.
20. Connan, J., "Use and trade of bitumen in antiquity and pre-history: Molecular archaeology reveals secrets of civilizations. *Philosphical Transactions of Royal Society, B., Biological Sciences,* Vol. 354, no. 1379, 1999, pp. 33-50.
21. Asbeck, W.F.V., **Bitumen in Hydraulic Engineering**, Vol. 2, Elsevier, Amsterdam, 1964.
22. Schonian, E., The Shell Bitumen Hydraulic Engineering Handbook, Shell Bitumen, UK, 1999.
23. Clark, F.M., Insulating Materials for Design and Engineering Practice, Wiley, New York, 1962.
24. Densley, J., "Ageing mechanisms and diagnostics for power cables – An overview, *IEEE Electrical Insulation Magazine,* Vol. 17, no. 1, 2001, pp.14-22.
25. Mc Dermid, W., "Dielectric absorption characteristics of generator stator insulation" in: Proceedings of IEEE International Symposium on Electrical Insulation, Anaheim CA, 2000, pp. 516-519.
26. Wilkinson, M., "Material progress in cable accessories up to 33 kV", *Power Engineering Journal,* Vol. 8, no. 2, 1994, pp. 89-91.
27. Timperelye, J.E., Micahlec, J.R., "Estimating the remaining service life of asphalt-mica stator insulation", *IEEE Transactions on Energy Conversion*, Vol. 9, no. 4, 1994, pp. 686-694.
28. Mathes, K.N, "A brief history of development in electrical insulation", in: Proceedings of IEEE 20th Electrical Electronics Insulation Conference, Boston, Oct 07-10, 1991, pp.147-150.
29. Mac Donald, D.S., Weatherley, J.W., Hollick, D.J., "A modern joining system for medium voltage distribution cables", in: Proceedings of 3rd IEEE International Conference on Power Cables and Accessories 10kV – 500 kV, London, UK, Nov 23-25, 1993, pp. 82-86.
30. Speight, J.G., **The Chemistry and Technology of Petroleum**, Marcel Dekker Inc., New York, 1999.
31. Petersen, J.C., "Chemical Composition of Asphalt as related to Asphalt Durability: State of the Art", *Transportation Research Record*, No. 999,

1984, pp. 13-40.

32. Chatergoon, L., Whiting, R., Smith, C., “Use of elemental and functional group analysis for monitoring compositional changes occurring on air blowing and accelerated weathering of a natural asphalt”, *Analyst*, Vol. 118, no. 7, 1993, pp. 947-950.
33. Robertson, R.E., “Chemical properties of asphalts and their relationship to pavement performance”, in: Strategic Highway Research Program, National Research Council, Washinton, 1991.
34. Moschopedis, S.E., Speight, J.G., “Effect of air blowing on properties and consitituion of a natural bitumen”, *Journal of Material Science*, Vol. 12, no. 5, 1977, pp. 990-998.
35. Miknis, F.P., Pauli, A.T., Michon, L.C., Netzel, D.A., “NMR imaging studies of asphaltene precipitation in asphalts”, *Fuel*, Vol. 77, no. 5, 1998, pp. 399-405.
36. Morgan, P., Mulder, A., **The Shell Bitumen Industrial Handbook**, Design and Print Partnership Ltd, Surrey, UK, Shell Bitumen, 1995.
37. Pollack, S.S., Yen, T.F., “Structural studies of asphaltics by x-ray small angle scattering”, *Analytical Chemistry*, Vol. 42, no. 6, 1970, pp. 623-629.
38. Chilingarian, G.V., Yen, T.F., (Eds.)., in: **Bitumens, Asphalts and Tar Sands, Developments in Petroleum Science 7**, Elsevier Scientific Publ, Amsterdam 1978.
39. Yen, T.F., Chilingarian, G.V. (Eds.), in: **Asphaltenes and Asphalt – 1**, Developments in Petroleum Science 40A, Elsevier, Amsterdam, 1994.
40. Yen, T.F., Chilingarian G.V. (Eds.), in: **Asphaltenes and Asphalt - 2**, Developments in Petroleum Science 40B, Elsevier, Amsterdam 2000.
41. Nellensteyn, F.J., “Analysis of asphaltic bitumen-tar mixtures”, in: Proceedings of 1st World Petroleum Congress, London, UK, Paper No. 210, July 18-24,1933, pp. 1-3.
42. Pfeiffer, J.Ph., Saal, R.N.J., “Asphaltic bitumen as colloid system”, *Journal of Physical Chemistry*, Vol. 44, no. 2, 1940, 139-149.
43. Andersen, S.I., Jensen, J.O., Speight, J.G., “X-Ray diffraction of sub-fractions of petroleum asphaltenes”, *Energy and Fuels*, Vol. 19, no. 6, 2005, pp. 2371 – 2371.
44. Christopher, J., Sarpal, A.S., Kapur, G.S., Krishna, A., Tyagi, B.R., Jain, M.C., Jain, S.K., Bhatnagar, A.K., “Chemical structure of bitumen-derived asphaltenes by nuclear magnetic resonance spectroscopy and x-ray diffractometry”, *Fuel* , Vol. 75, no. 8, 1996, pp. 999- 1008.
45. Diamond, R., “X-Ray diffraction data for large aromatic molecules”, *Acta Crystallographica*, Vol. 10, no. 5, 1957, pp. 359 – 364.
46. Ebert, L.B., Scanlon, J.C., Mills, D.R., “X-Ray diffraction of N-paraffins and stacked aromatic molecules – insight into asphaltene structure”, *Petroleum Science and Technology*, Vol. 2, no. 3, 1984, pp. 257-286.

47. Dickinson, E.M., “Structural comparison of petroleum fractions using proton and 13C n.m.r. spectroscopy”, *Fuel*, Vol. 59, no. 5, 1980, pp. 290 – 294.
48. Gillet, S., Rubini, P., Delpuech, J.J., Escalier, J.C., Valentin, P., “Quantitative Carbon-13 and proton nuclear magnetic resonance spectroscopy of crude oil and petroleum products-I. Some rules for obtaining a set of reliable structural parameters”, *Fuel*, Vol. 60, no. 3, 1981, pp. 221 – 225.
49. Hasan, M., Ali, M.F., Arab, M., “Structural characterization of Saudi Arabian extra light and light crudes by 1H and 13C N.M.R. spectroscopy”, *Fuel*, Vol. 68, no. 6, 1989, pp. 801 – 803.
50. Hasan, M., Ali, M.F., Bukhari, A., “Structural characterization of Saudi Arabian heavy crude oil by N.M.R. spectroscopy”, *Fuel*, Vol. 62, no. 5, 1983, pp. 518 – 523.
51. Jemison, H.B., Burr, B.L., Davison, R.R., Bullin, J.A., Glover, C.J., “Application and use of the ATR, FT-IR method to asphalt aging studies”, *Fuel Science and Technology*, Vol. 10, no. 2, 1992, pp. 795 – 808.
52. Lamontagne, J., Dumas, P., Mouillet, V., Kister, J., “Comparison by fourier transform infrared (FTIR) spectroscopy of different ageing techniques: application to road bitumens”, *Fuel*, Vol. 80, no. 4, 2001, pp. 483 – 488.
53. Permanyer, A., Douifi, L., Lahcini, A., Lamontagne, J., Kister, J., “FTIR and SUVF spectroscopy applied to reservoir compartmentalization: a comparative study with gas chromatography fingerprints results”, *Fuel*, Vol. 81, no. 7, 2002, pp. 861 – 866.
54. Pieri, N., Planche, J.P., Kister, J., “Chemical characterization of road paving bitumen using FTIR and UV synchronous fluorescence”, *Analysis*, Vol. 24, no. 4, 1996, pp. 113 –122.
55. Yen, T.F., Erdman, G.J., Pollack, S.S., “Investigation of the structure of petroleum asphaltenes by x-ray diffraction”, *Analytical Chemistry*, Vol. 33, no. 11, 1961, pp. 1587 – 1594.
56. Decroocq, D., Thomas, M., Fixari, B., le Perchec, P., Bogois, M., Lena, L., des Couriers, T., Rossarie, J., “Improving heat treatment processes for residues by optimizing the transformation of resins and asphaltenes”, *Revue De Institut Français du Pétrole*, Vol. 47, no. 1, 1992, pp. 103 – 131.
57. Moschopedis, S.E., Fryer, J.F., Speight, J.G., “Investigation of asphaltene molecular weights”, *Fuel*, Vol. 55, no. 3, 1976, pp. 227 – 232.
58. Acevedo, S., Gutierrez, LB, Negrin G, Pereira, J.C., “Molecular weight of petroleum asphaltenes: a comparison between mass spectrometry and vapor pressure osmometry”, *Energy Fuels*, Vol. 19, no. 4, 2005, pp. 1548-1560.
59. Peramanu, S., Pruden, B.B., “Molecular weight and specific gravity distributions for Athabasca and Cold Lake bitumens and their saturate, aromatic, resin and asphaltene fractions”, *Industrial & Engineering Chemistry Research*, Vol. 38, no. 8, 1999, pp. 3121-3130.

60. Dwiggins, C.W., “A small angle X-Ray scattering study of the colloidal nature of petroleum”, *Journal of Physical Chemistry*, Vol. 69, no. 10, 1965, pp. 3500-3506.
61. Ravey, J.C., Ducouret, G., Espinat, D., “Asphaltene macrostructure by small angle neutron Scattering”, *Fuel*, Vol. 67, no. 11, 1988, pp. 1560-1567.
62. Pollack, S.S., Yen, T.F., “Structural studies of asphaltics by X-Ray small angle scattering”, *Analytical Chemistry*, Vol. 42, no. 6, 1970, pp. 623-629.
63. Baginska, K., Gawel, I., “Effect of origin and technology on the chemical composition and colloidal stability of bitumen”, *Fuel Processing Technology*, Vol. 85, no. 13, 2004, pp. 1453-1462.
64. Dickie, J.P., Haller, M.N., Yen, T.F., “Electron microscopic investigations on the nature of petroleum asphaltics”. *Journal of Colloid and Interface Science*, Vol. 29, no. 3, 1969, pp. 475-484.
65. Camacho-Bragado, G.A., Santiago, P., Marin-Almazo, M., Espinosa, M., Romero, E.T., Murgich, J., Rodriquez Lugo, V., Lozada-Cassou, M., Jose-Yamacan, M., “Fullerenic structures derived from oil asphaltenes”, Carbon Vol. 40, no. 15, 2002, pp. 2761-2766.
66. Loeber, L., Sutton, O., Morel, J., Valleton, J., Muller, G.J., “New direct observations of asphalts and asphalt binders by scanning electron microscopy and atomic force microscopy”, *Journal of Microscopy*, Vol. 182, no. 1, 1996, pp. 32 – 39.
67. Little, D.N., Letton, A., Prapnnachari, S., Kim, Y.R., “Rheological and rheo-optical characterization of asphalt cement and evaluation of relaxation properties”, *Transportation Research Record*, No. 1436, 1994, pp. 71-82.
68. Masson, J.-F., Leblond, V., Margeson, J., “Bitumen morphologies by phase detection microscopy”, *Journal of Microscopy*, Vol. 227, no.1, 2006, pp. 17-29.
69. Masson, J.-F., Leblond, V., Margeson, J., Bundalo-Perc, S., “Low temperature bitumen stiffness and viscous paraffinic nano and micro-domains by cryogenic AFM and PDM”, *Journal of Microscopy*, Vol. 227, no. 3, 2007, pp. 191-202.
70. DE Moraes, M.B., Pereira, R.B., Simao, R.A., Leite, L.F., “High temperatue AFM study of CAP 30/45 pen grade bitumen”, *Journal of Microscopy*, Vol. 239, no. 1, 2010, pp. 46-53.
71. Garrick, N.W., Wood, L.E., Relationship between HP-GPC data and the rheological properties of asphalts. *Transportation Research Record*, No. 1096, 1986, pp. 35-41.
72. **The Asphalt Handbook**, manual series no. 4., Asphalt Institute, 1965.
73. Deme, I., “Processing of sand-asphalt-sulphur mixes”, *Journal of Association of Asphalt Paving Technologists*, Vol. 43, 1974, pp. *465-482.*
74. Fromm, H.J., Kennepohl, G.J., “Sulphur asphaltic concrete on three Ontario test roads”, *Journal of Association of Asphalt Paving Technologists*, Vol. 48, 1979, pp. 135-162.

75. Denning, J.H., Carswell, J., “Improvements in rolled asphalt surfacings by the addition of organic polymers”, *Transport and Road Research Lab Report*, LR 989, Department of Environment, Department of Transport. 1981.1988
76. Jain, P.K., Sengupta, J.B., “Studies on mitigation of moisture damage in bituminous pavements”, Vol. 14, no. 1, 2007, pp. 48-54.
77. King, G.N., Muncy, H.W., Prudhome, J.B., Polymer modification: binder’s effect of mix properties”, *Journal of Association of Asphalt Paving Technologists*, Vol. 55, 1986, pp. 591-540.
78. Button, J.W., Little, D.N., Kim, Y., Ahmed, J., “Mechanistic evaluation of selected additives”, *Journal of Association of Asphalt Paving Technologists*, Vol. 56, 1987, pp. 62-90.
79. Omeis, J., Mueller, M., Pennewiss, F., “Alky (meth)acrylate-maleic anhydride modified bitumen (to Roehm GmbH, Chemische Fabrik, Darmstadt, DE)”, *U.S. Pat. No. 5,266,615*, 1993, pp. 13.
80. Jian-Shiuh Chen, P.E., Min-Chih, L., Ming-Shen, S., “Asphalt modified by styrene-butadiene-styrene triblock copolymer: morphology and model”, *Journal of Materials in Civil Engineering*, Vol. 14, no. 3, 2002, pp. 224-229.
81. Abdellatif, A.-K., Brahim, B., Bousmina, M., “Polymer blends for enhanced asphalt binders”, *Polymer Engineering and Science*, Vol. 36, no. 12, 1996, 1724-1733.
82. Morrison, G.R., Van Der Stel, R., Hesp, S.A.M., “Modification of asphalt binders and asphalt concrete mixes with crumb and chemically devulcanized rubbers”, *Transportation Research Record,* No. 1515, 1995, pp.56-63.
83. Vargas, M., Chávez, A., Herrers, R., Manero, O., “Asphalt modified by partially hydrogenated SBS triblock copolymers”, *Rubber Chemistry and Technology*, Vol. 78, no. 8, 2005, 620-643.
84. Ali,, M.F. Siddiqui, M.N., “Changes in asphalt chemistry and durability during oxidation and polymer modification”, *Petroleum Science and Technology*, Vol. 19, no. 9&10, 1995, pp. 1229-1249.
85. Chaala, A., Roy, C., Ait-Kadi, A., “Rheological properties of bitumen modified with pyrolytic carbon black”, *Fuel*, Vol. 75, no. 13, 1996, pp. 1575-1583.
86. Herrington, P.R., Wu, Y., Forbes, M.C., “Rheological modification of bitumen with maleic anhydride and dicarboxylic acids”, *Fuel*, Vol. 78, no. 1, 1999, pp. 101-110.
87. Pokonova, Yu.V., Mitrofanova, L.M., “Modification of asphalts with phosphazenes”, Chemistry and Technology of Fuels and Oils, Vol. 41, no. 4, 2005, pp. 315-318.
88. Shin-Che, H., Rayond, E.R., Jan, F.B., Claine Petersen, J., “Impact of lime modification of asphalt and freeze-thaw cycling on asphalt-aggregate interaction and moisture resistance to moisture damage”, *Journal of Materials in Civil Engineering*, Vol. 17, no. 6, 2005, pp. 711-718.

89. Ray, J., “History and development of modified bitumen”, Proceedings of *c.* Eight Conference on Roofing Technology, Gaithersburg, USA, April 16-17, 1987, pp. 81-84.
90. Isaccson, U., Lu, X., “Testing and appraisal of polymer modified road bitumens – state of art”, *Materials Structures*, Vol. 28, no. 3, 1995, pp. 139-159.
91. Iqbal, M.H., “Influence of polymer type and structure on polymer modification”, *M.S., Thesis*, King Fahd University of Petroleum and Minerals, Dharan 31261, Saudi Arabia, Chapter 2, Page No. 9, 2004, pp. 1-156.
92. Yue, H., Roger, N.B., Oliver, H., “A review of the use of solid waste materials in asphalt pavements”, *Resources Conservation and Recycling,* Vol. 52, no. 1, 2007, pp. 58-73.
93. Thayer, C.H., “Asphalt composition containing polyethylene (to Sun Oil Company, Philadelphia, U.S.A.), U.S. Pat. No. 2,871,212, 1959, pp. 1-2.
94. Morrison, G.R., Lee, J.K., Hesp, S.M.H., “Chlorinated polyolefins for asphalt binder modification”, *Journal of Applied Polymer Science*, Vol. 54, no. 2, 1994, pp. 231-240.
95. Adelman, R.L., “Asphalt-ethylene/vinyl acetate copolymer compositions (to E.I. du pont de Nemours and Company, U.S.A.)”, U.S. Pat. No. 3,442,841, 1969, pp. 1-3.
96. Ramsay, R.D., “Modification of asphalt with ethylene vinyl acetate copolymers to improve properties (to Philips Petroleum Company, U.S.A.)”, U.S. Pat. No. 3,869,417, 1975, pp.1-6.
97. Blanco, R., Rodrigues, R., Garcia-Garduno, M., Castano, V.M., “Morphology and tensile properties of styrene-butadiene copolymer reinforced asphalt”, *Journal of Applied Polymer Science*, Vol. 56, no. 1, 1995, pp. 57-64.
98. Blanco, R., Rodrigues, R., Garcia-Garduno, M., Castano, V.M., “Rheological properties of styrene-butadiene copolymer reinforced asphalt”, *Journal of Applied Polymer Science*, Vol. 61, no. 9, 1996, pp. 1493-1501.
99. B. Brule, “Polymer modified cement used in road construction”, *Transportation Research Record: Journal of the Transportation Research Board*, Vol. 1535, no. , 199, pp. 48-53.
100. Bahia, H.U., Hislop, W.P., Zhai, H., Rangel, A., “Classification of asphalt binders into simple and complex binders’, *Journal of the Association of the Asphalt Paving Technologists*, Vol. 67, 1998, pp. 1-41.
101. Polacco, G., Berlincioni, S., Biondi, D., Stastna, J., Zanzotto, L., “Asphalt modification with different polyethylene based polymers”, *European Polymer Journal*, Vol. 41, no. 12, 2005, pp. 2831-2844.
102. Smith, L.M., “Some viscous and elastic properties of rubberized bitumens”, *Journal of Applied Chemistry*, Vol. 10, no.7, 1960, pp. 269- 305.
103. Thomson, P.D., “The use of natural rubber in road surfacing’, *The Natural Rubber Producers Association Technical Bulletin*, No. 9, 1964, pp. 1-26.

104. Mullins, L., “Natural rubber in asphalt pavements”, © Malaysian Rubber Producers Research Association, *Rubber Development Supplement*, No. *7*, 1971, pp. 1-17.
105. Fernando, M.J., Nadarajah, M., “Use of natural rubber latex in road construction”, *Journal of Rubber Research Institute of Malaysia*, Vol. 22, no. ,5 1969, pp. 430-440.
106. Nrachai, T., Direk, L., Chayatan, P., “The modification of asphalt with NR latex”, in: Proceedings of the 6th International Conference on Eastern Asia Society for Transportation Studies (EAST), Bangkok, Thailand, Sep, 21-23, 2005, pp. 679-694.
107. Lesueur, D., Gerard, J.F., Claudy, P., Letoffe, J.M., Martin, D., Planche, J.P., “Polymer modified asphalts as viscoelastic emulsion”, *Journal of Rheology*, Vol. 42, no. 5, 1998, pp. 1059-1074.
108. Xiaohu, L., Ulf, I., “Artificial aging of polymer modified bitumens”, *Journal of Applied Polymer Science*, Vol. 76, no. 12, 2000, pp. 1811-1824.
109. Vargas, M., Manero, O., “Rheological characterization of the gel point in polymer-modified asphalts”, *Journal of Applied Polymer Science*, Vol. 119, no. 4, 2011, pp. 620-643.
110. Mikols, W.J., “Stabilized bituminous blends (to Shell Oil Company, U.S.A.,)”, U.S. Pat. No. 4,490,493, 1984, pp. 1-4.
111. Polacco, G., Statsna, J., Biondi, D., Antonelli, F., Vlachovicova, Z., Zanzotto, L., “Rheology of asphalts modified with glycidylmethacrylate functionalized polymers”, Journal of Colloid and Interface, Vol. 280, no. 2, 2004, pp. 366-37.
112. Murphy, M., O’ Mahony, M., Lycett, C., Jamieson, I., “Recycled polymers for use as bitumen modifiers”, *Journal of Materials in Civil Engineering*, Vol. 13, no. , 2001, pp. 306-314.
113. Jun L, Yuxia Z, Yuzhen Z., “The research of GMA-g-LDPE modified Qinhuandago bitumen”, *Construction and Building Materials*, Vol. 22, no. 6, 2008, pp. 1067-1073.
114. SBS Polymer Supply Outlook, Henry Ramogosa, ICI Performance Products, Ron Corun, Nustar Asphalt Refining & Robert Berkeley, Exe. Director, Source: www.modifiedasphalt.org
115. Clarance, Jr., M.E., Martin, L.G., Chester, W.E., George P., “Thermoplastic elastomer-asphalt nanocomposite composite (to Exxon Research and Engineering Company, U.S.A.)”, U.S. Pat. No. 5,652, 284, pp. 1-6, 1977.
116. Ghile, D.B., “Effect of nano clay modification on the rheology of bitumen and on performance of asphalt mixture”, *Ph D Thesis*, Delft University of Technology, Netherlands, 2006, pp. 1-151.
117. Polacco, G., Kříž, P., Fillippi, S., Stastna, J., Biondi, D., Zanzotto, L., “Rheological properties of asphalt/SBS/clay blends”, *European Polymer Journal*, Vol. 44, no. 11, 2008, pp. 3512-3521.
118. Sureshkumar, M.S., Biondi, D., Filipi, S., Polacco, G., in: Proceedings of the

International Conference on Nanotechnology and Advanced Materials (ICNAM-2009), University of Bahrain, Bahrain, May 4-7, 2009, pp. 138.

119. Jahromi, S.G., Khodaii, A., "Effects of nanoclay on rheological properties of bituminous binder", *Construction and Building Materials*, Vol. 23, no. 6, 2009, pp. 2984-2904.
120. Sureshkumar, M.S., Polacco, G., "Polymer Modified Asphalt Nanocomposite: Fuel Resistance", in: Proceedings of the International Conference on Advancement on Nanoscience and Nanotechnology (ICOANN-2010), Alagappa University, Karaikudi, India, NC-OP-07, Mar 01-05, 2010, pp. 42.
121. Ray, S.S., Okamoto, M., "Polymer/layered silicate nanocomposites: a review from preparation to processing", *Progress in Polymer Science*, Vol. 28, no. 11, 2003, pp. 1539-1641.
122. Gupta, R.K., Pasanovic-Zujo, V., Bhattacharya, S.N., "Shear and extensional rheology of EVA/layered silicate-nanocomposites", *Journal of Non-Newtonian Fluid* Mechanics, Vol. 128, no. 2-3, 2005, pp. 116-125.
123. Alexander, M., Dubois, P., "Polymer-layered silicate nanocomposites: preparation, properties and uses of a new class of materials", *Materials Science and Engineering: R: Reports*, Vol. 28, no. 1-2, 2000, pp. 1-63.
124. Krishnamoorti, R., Yurekli, K., "Rheology of polymer layered silicate nanocomposites", *Current Opinion in Colloid and Interface Science*, Vol. 6, no. 5-6, 2001, pp. 464-470.
125. Chung, J.W., Han, S.J., Kwak, S.Y., "Dynamic viscoelastic behavior and molecular mobility of acrylonitrile–butadiene copolymer nanocomposites with various organoclay loadings", *Composites Science and* Technology, Vol. 68, no. 6, 2008, pp. 1555-1561.
126. Krishnamoorti, R., Vaia, R.A., Giannelis, E.P., "Structure and dynamics of polymer-layered silicate nanocomposites", *Chemistry of Materials*, Vol. 8, no. 8, 1996, pp. 1728-1734.
127. Zhao, J., Morgan, A.B., Harris, J.D., "Rheological characterization of polystyrene–clay nanocomposites to compare the degree of exfoliation and dispersion", *Polymer*, Vol. 46, no. 20, 2005, pp. 8641-8660.
128. Galgali, G., Ramesh, C., Lele, A., "A rheological study on the kinetics of hybrid formation in polypropylene nanocomposites", *Macromolecules* Vol. 34, no. 4, 2001, pp. 852-858.
129. Krishnamoorti, R., Silva, A.S., **Rheological properties of polymer-layered silicate nanocomposites**. in: Pinnavaia, T.J., Beall. G.W. (Eds.), Polymer–clay nanocomposites, Wiley, 2000, pp. 315-343.
130. Ren, J., Silva, A.S., Krishnamoorti, R., "Linear viscoelasticity of disordered polystyrene–polyisoprene block copolymer based layered-silicate nanocomposites", *Macromolecules*, Vol. 33, no. 10, 2000, pp. 3739-3746.
131. Krishnamoorti, R., Ren, J., Silva, A.S., "Shear response of layered silicate nanocomposites", *Journal of Chemical Physics*, Vol. 114, no. 11, 2001, pp.

4968-4973.

132. Kojima, Y., Usuki, A., Kawasumi, M., Okada, A., Kurauchi, T., Kamigaito O., Kaji, K., “Novel preferred orientation in injection-molded nylon 6-clay hybrid”, *Journal of Polymer Science, Part B: Polymer Physics*, Vol. 33, no. 7, 1995, pp. 1039-1045.
133. Kojima Y, Usuki A, Kawasumi M, Okada A, Kurauchi T, Kamigaito O., Kaji, K., “Fine structure of nylon 6-clay hybrid”, *Journal of Polymer Science, Part B: Polymer Physics* , Vol. 32, no. 4, 1994, pp. 625-630.
134. Medelin-Rodriquez, F.J., Burger, C., Hsiao, B.S., Chu, B., Vaia, R.A., Phillips, S., “Time-resolved shear behavior of end-tetherd nylon 6-clay nanocomposites followed by non-isothermal crystallization”, *Polymer*, Vol. 42, no. 2, 2001, pp. 9015-9023.
135. Okamato, M., Nam, P.H., Maiti, P., Kotaka, T., Hasegawa, N., Usuki, A., “A house of cards structure in polypropylene/clay nanocomposites in elongational flow”, *Nano Letters*, Vol. 1, no. 6, 2001, pp. 295–298.
136. Schmidt, G., Nakatani, A.L., Butler, P.D., Karim, A., Han, C.C., “Shear orientation of viscoelastic polymer–clay solutions probed by flow birefringence and SANS”, *Macromolecules*, Vol. 33, no. 20, 2000, pp. 7219–7222.
137. Vermanta, J., Ceccia, S., Dolgovskij, M.K., Maffletone, P.L., Macosko, C.W., “Quantifying dispersion of layered nanocomposites via melt rheology”, *Journal of Rheology*, Vol. 51, no. 3, 2007, pp. 429–450.
138. Panda, M., Mazumdar, M., “Engineering properties of EVA modified paving mixes”, *Journal of Materials in Civil Engineering*, Vol. 11, no. 2, 1996, pp. 131–137.
139. Airey, G.D., “Rheological evaluation of EVA polymer modified bitumens”, *Construction and Building Materials*, Vol. 16, no. 8, 2002, pp. 473-487.
140. González, O., Muñoz, M.E., Santamaria, A., Garcìa-Morales, M., Navarro, F.J., Partal, P., “Rheology and stability of bitumen/EVA blends”, *European Polymer Journal*, Vol. 40, no. 10, 2004, pp. 2365-2372
141. Hussein, I.A., Iqbal, M.H., Al-Abdul-Wahab, H.I., “Influence of Mw of LDPE and vinyl acetate content of EVA on the rheology of polymer modified asphalts”, *Rheologica Acta*, Vol. 45, no. 1, 2005, pp. 92-104.
142. Garcìa-Morales, M., Partal, P., Navarro, F.J., Martìnez-Boza, F., Gallegos, C., González, O., González, N., Muñoz, M., “Viscous properties and microstructure of recycled EVA modified bitumen”, *Fuel*, Vol. 83, no. 1, 2003, pp. 31-38.
143. Garcìa-Morales, M., Partal, P., Navarro, F.J., Martìnez-Boza, F., Gallegos, C., “Linear visco-elasticity of recycled EVA modified bitumen”, *Energy Fuel*, Vol. 18, no. 2, 2004, pp. 357-364.
144. Garcìa-Morales, M., Partal, P., Navarro, F.J., Gallegos, C., “Effect of waste polymer addition on the rheology of modified bitumen”, *Fuel*, Vol. 85, no. 7, 2006, 936-943.

145. Garcìa-Morales, M., Partal, P., Navarro, F.J., Martìnez-Boza, F., Gallegos, C., “Process rheokinetics and micro-structure of recycled EVA/LDPE modified bitumen”, *Rheologica Acta*, Vol. 45, no. 4, 2006, pp. 513-524.

146. Garcìa-Morales, M., Partal, P., Navarro, F.J., Martìnez-Boza, F., Gallegos, C., “Processing, rheology and storage stability of recycled EVA/LDPE modified bitumen”, *Polymer Engineering and Science*, vol. 47, no. 2, 2007, pp. 181-191.

147. González, O., Muñoz, M.E., Santamaria, A., Garcìa-Morales, M., Navarro, F.J., Partal, P., “New routes for roads: using recycled greenhouse films”, *International Journal of Environmental Technology and Management*, Vol. 7, no. 2-7, 2007, pp. 218-227.

148. Alexander, M., Beyer, G., Henrist, C., Cloots, A., Ralmont, R., Jerome, R., Dubois, P., “Preparation and properties of layered silicate nanocomposites based on ethylene vinyl acetate copolymers”, *Macromolecular Rapid Communication*, Vol. 22, no. 8, 2001, pp. 643-646.

149. Zanetti, M., Camino, G., Thomann, R., Mulhaupt, R., “Synthesis and thermal behavior of layered silicate EVA nanocomposites”, *Polymer*, Vol. 42, no. 10, 2001, pp. 4501-4507.

150. Riva, A., Zanetti, M., Braglia, M., Camino, G., Falqui, L., “Thermal degradation and rheological behavior of EVA/montmorillonite nanocomposites”, *Polymer Degradation and Stability*, Vol. 77, no. 2, 2002, pp. 299-304.

151. Lee, M.H., Park, B.J., Vhoi, H.J., Gupta, R.K., Bhattachary, S.N., “Preparation and rheological characteristics of ethylene–vinyl acetate copolymer/organoclay nanocomposites”, *Journal of Macromolecular Science: Part B: Polymer Physics*, Vol. 46, no. 2, 2007, pp. 261-273.

152. La Mantia, F.P., Tzankova Dintcheva, N., “EVA copolymer-based nanocomposites: rheological behavior under shear and isothermal and non-isothermal elongational flow”, *Polymer Testing*, Vol. 25, no. 5, 2006, pp. 701-708.

153. Martins, C.G., Larocca, N.M., Paul, D.R., Pessan, L.A., “Nanocomposites formed from polypropylene/EVA blends”, *Polymer*, Vol. 50, no. 7, 2009, pp. 1743-1754.

154. Gustavino, F., Coletti, G., Dardano, A., Montanari, G.C., Deorsola, F., Di Lorenzo Del Casale, M., “Electrical treeing in EVA-layered silicate nanocomposites”, in: Proceedings of the Annual Report Conference on Electrical Insulation and Dielectric Phenomena, Missouri, U.S.A., Oct 15-18, 2006, pp. 294-297.

155. Polacco, G., Vacin, O.J., Biondi, D., Stastna, J., Zanzotto, L., “Dynamic master curves of polymer modified asphalt from three different geometries”, *Applied Rheology*, Vol. 13, no. 3, 2003, pp. 118-124.

156. Ferry, J.D., **Viscoelastic Properties of Polymers**. New York: Wiley; 1980.

157. Van Gurp M., Palmen, J., “Time–temperature superposition for polymeric

blends", *Rheological Bulletin*, Vol. 67, no. 1, 1998, pp. 5-8.

158. Sureshkumar, M.S., Stastna, J., Polacco, G., Filippi, S., Kazatchkov, I., Zanzotto, L., "Rheology of bitumen modified by EVA – organoclay nanocomposites", *Journal of Applied Polymer Science*, Vol. 118, no. 1, 2010, pp. 557-565.
159. Lili, C., Xiaoyan, M., Paul, D.R., "Morphology and properties of nanocomposites formed from ethylene–vinyl acetate copolymers and organoclays", *Polymer*, Vol. 48, no. 21, 2007, pp. 6325-6329.
160. Peeterbroeck, S., Alexandre, M., Jerome, R., Dubois, Ph., "Poly(ethylene-co-vinyl acetate)/clay nanocomposites: effect of clay nature and organic modifiers on morphology, mechanical and thermal properties", *Polymer Degradation and Stability*, Vol. 90, no. 2, 2005, pp. 288-294.
161. Mainil, M., Alexandre, M., Monteverde, F., Dubois, P., "Polyethylene organo-clay nanocomposites: the role of the interface chemistry on the extent of clay intercalation/exfoliation", *Journal of Nanoscience and Nanotechnology*, Vol. 6, no. 2, 2006, pp. 337-344.
162. Li, X., Ha, C.S., "Nanostructure of EVA/organoclay nanocomposites: effects of kinds of organoclays and grafting of maleic anhydride onto EVA", *Journal of Applied Polymer Science*, Vol. 87, no. 12, 2003, pp. 1901-1909.
163. Olabisi, O., Robeson, L., Shaw, M.T., **Polymer–Polymer Miscibility**, In: Polymer–Polymer Compatibility, Academic Press, New York, 1979.
164. Song, M., Hammiche, A., Pollock, H.M., Hourston, D.J., Reading, M., "Modulated differential scanning calorimetry: 4. Miscibility and glass transition behaviour in poly(methyl methacrylate) and poly(epichlorohydrin) blends", *Polymer*, Vol. 37, no. 25, 1996, pp. 5661-5665.
165. Song, M., Hammiche, A., Pollock, H.M., Hourston, D.J., Reading, M., "Modulated differential scanning calorimetry: 1. A study of the glass transition behaviour of blends of poly(methy methacrylate) and poly(styrene co-acrylonitrile)", *Polymer*, Vol. 36, no. 17, 1995, pp. 3313-3316.
166. Michalica, P., Kazatchkov, I.B., Stastna, J., Zanzotto, L., "Relationship between chemical and rheological properties of two asphalts of different origins", *Fuel*, Vol. 87, no. 15-16, 2008 pp. 3247-3253.
167. Cho, J.V., Paul, D.R., "Nylon-6 composites by melt blending", *Polymer*, Vol. 42, no. 3, 2001, pp. 1083-1094.
168. Uskov, I.A., **Filled Polymers III**. Polymerization of methyl methacrylate during dispersion of sodium betonite, *Vysokomol Soed*, Vol. 2, 1960, 926-930.
169. Vaia, R.A., Ishhi, H., Giannelis, E.P., "Synthesis and properties of two-dimensional nano structures by direct intercalation of polymer melts in layered silicates", *Chemistry of Materials*, Vol. 5, no. 12, 1993, pp. 1694-1696.
170. Blumstein, A., "Polymerization of adsorbed monolayers. II. Thermal degradation of the inserted polymer", *Journal of Polymer Science Part A:*

General Papers, Vol. 3, no. 7, 1965, pp. 2665-2672.

171. Ray, S.S., Bousima, M., "Biodegradable polymers and their layered silicate nanocomposites: in greening the 21st century materials world", *Progress in Material Science*, Vol. 50, no. 8, 2005, pp. 962-1079.
172. Giannelis, E. P., "Polymer layered silicate nanocomposites", *Advanced Materials*, Vol. 8, no. 1, 1996, pp. 29-35.
173. Chin, I.J., Thurn-Albrecht, T., Kim, H.C., Russell, T.P., Wang, J., "On exfoliation of montmorillonite in expoxy", *Polymer*, Vol. 42, no. 13, 2001, pp. 5947-5952.
174. Kim, C.M., Lee, D.H., Hoffman, B., Kressler, J., Stoppelman, G., "Influence of nano fillers on the deformation process in layered silicate/polyamide-12 nanocomposite", *Polymer*, Vol. 42, no. 3, 2001, pp. 1095-1100.
175. Ouyang, C., Wang, S., Zhang, Y., Zhang, Y., "Preparation and properties of styrene-butadiene-styrene copolymer/kaolinite clay compound and asphalt modified with the compound", *Polymer Degradation and Stability*, Vol. 87, no. 2, 2005, pp. 309-317.
176. Wang, Y.P., Liu, D.J., Wang, Y.P., Gao, J.M., "Preparation and properties of asphalt modified with SBS/organo betonite blends", *Polymer and Polymer Composites*, Vol. 14, no. 6, 2006, pp. 403-411.
177. Ouyang, C., Wang, S., Zhang, Y., "Thermo-rheological properties and storage stability of SEBS/kaolinite clay compound modified asphalts", *European Polymer Journal*, Vol. 42, no. 2, 2006, pp. 446-457.
178. Jianying, Y., Zheng, X., Wu, S., Liu, G., "Preparation and properties of montmorillonite modified asphalts", *Materials Science and Engineering A*, Vol. 447, no. 1-2, 2007, pp. 233-238.
179. Sureshkumar, M.S., Filippi, S., Polacco, G., Kazatchov, I., Stastna, J., Zanzotto, L., "Internal structure and linear viscosity of EVA/asphalt nanocomposites", *European Polymer Journal*, Vol. 46, no. 2, 2010, pp. 621-633.
180. Mours, M., Winter, H.H., **IRIS Handbook**, IRIS Development, Amherst, MA, 2004.
181. Stastna, J., Zanzotto, L., "Linear response of regular asphalts to external harmonic fields", *Journal of Rheology,* Vol. 43, no. 3,1999, pp. 719-734.
182. Trinkle, S., Walter, P., Friedrich, C., "Van-Gurp Palmen Plot II – classification of long chain branched polymers by their topology", *Rheologica Acta*, Vol. 41, no. 1-2, 2002, pp. 103-113.
183. Marastenau, M.O., Anderson, D. A., "Techniques for determining errors in asphalt binder rheological data", *Transportation Research Record* No. 1766, 1981, pp. 32-39.
184. Osaki, K., Inoue, T., Isomura, T., "Stress overshoot of polymer solutions at high rates of shear", *Journal of Polymer Science Part B: Polymer Physics*, Vol. 38, no. 14, 2000, pp. 1917-1925.

185. Osaki, K.; Inoue, T., Uematsu, T., “Stress overshoot of polymer solutions at high rates of shear: semidilute polystyrene solutions with and without chain entanglements”, *Journal of Polymer Science Part B: Polymer Physics*, Vol. 38, no. 24, 2000, pp. 3271-3276.

186. Inoue, T., Yamashita, Y., Watanabe, H., “Stress overshoot of entangled polymers in theta solvent”, *Macromolecules*, Vol. 37, no. 11, 2004, pp. 4317-4320.

187. Islam, M.T., *Rheologica Acta*, “Prediction of multiple overshoots in shear stress during fast flows of bi-disperse polymer melts”, Vol. 45, no. 6, 2006, pp. 1003-1008.

188. Osaki, K., Watanabe, H., Inoue, T., “Stress overshoot in shear flow of an entangled polymer with bimodal molecular weight distribution”, *Nihon Reoroji Gakaishi*, Vol. 27, no. 1, 1999, pp. 63-64.

189. Solomon, M.J., Almusallam, A.S., Seefedt, K.F., Somwangthanaroj, A., Vardan, P., “Rheology of polypropylene/clay hybrid materials”, *Macromolecules*, Vol. 34, no. 6, 2001, pp. 1864-1872.

190. Letwimolnun, W., Vergnes, B., Ausias, G., Carreau, P.J., “Viscosity overshoots of organoclay nanocomposites in transient flow”, Journal of Non-Newtonian Fluid Mechanics, Vol. 141, no. 2-3, 2007, pp. 167-179.

191. Payne, A.R., Kraus, G., **Reinforcement of Elastomers**, Interscience Publishers, New York, 1965.

192. Song, B., Chen, W., “Loading and unloading SHPB pulse shaping techniques for dynamic hysteretic loops”, *Experimental Mechanics*, Vol. 44, no. 3, 2004, pp. 622-627.

193. Lai, J.S., “Irrecoverable and recoverable nonlinear visco-elastic properties of asphalt concrete”, *Highway Research Record*, No. 468, 1973, pp. 73-88.

194. Bahia, H., Hanson, D.I., Zheng, M., Zhai, H., Khatri, M.A., Anderson, R.M., National Cooperative Highway Research Program, Report 459, Washington, DC, 2001.

195. Stastna, J., Zanzotto, L., Wasage, T.L.J., Polacco, G., Cantu, M., “Accumulated strain and shear compliance function in asphalt binders”, in: Proceedings of the International Conference on Advanced Characterization of Pavement and Soil Engineering Materials, Loizos, S., Ed. Taylor & Francis Group: Athens, June 20-22, 2007, Vol.1, pp. 303–315.

196. Polacco, G., Stastna, J., Zanzotto, L., “Accumulated strain in polymer modified asphalts”, *Rheologica* Acta, Vol. 47, no. 5-6, pp. 491-498.

197. Sureshkumar, M.S., Polacco, G., “Polymer modified asphalt nanocomposites (PMAN): preparation and charactierization”, in. Proceedings of the International Conference on Nanoscience and Nanotechnology (ICONN-2010), SRM University, Kattankulathur, India, Feb 24-26, 2010, pp. 40.

198. Giuliani, F., Merusi, F., Filippi, S., Biondi D., Finocchiaro, M.L., Polacco G., “Effects of polymer modification on fuel resistance of asphalt binders”, *Fuel*,

Vol. 88, no. 9, 2009, pp. 1539-1546.

199. Newman, K., Shoenberger, JE., “Polymer concrete micro-overlay for fuel and abrasion resistant surfacing: laboratory results and field demonstrations”, in: Proceedings of the 2002 Federal Aviation Administration Airport Technology Conference, Federal Aviation Administration, Atlantic City, New Jersey; May 5–8, 2002, pp. P-44.
200. Deneuvillers, C., Letaudin, F., “Environmentally friendly fuel resistant surfacing”, in: Proceedings of World Road Association (PIARC) Conference, Durban, South Africa, Oct 18–20, 2003.
201. Giuliani, F., Rastelli, S., “Test methods to evaluate fuel resistance of aprons asphalt pavements in airports and heliports”, in: Proceedings of the 2nd International Airports Conference: Planning, Infrastructure & Environment, Sao Paulo, Brazil, Aug 2-4, 2006.
202. Plug, C., Srivastava, A., De Bondt, A.H., “A durable jet fuel resistant pavement layer with the use of a polymer modified asphalt emulsion”, in: Proceedings of the 3rd International Symposium on asphalt emulsion technology, Washington DC, USA, October 28-31, 2004.
203. Thornton, J., “A bituminous binder and its manufacturing process, and a process for improving fuel resistance of such bituminous binder (to COLAS, France)”, EP 1 700 887 A1, 2006, pp. 1-16.
204. Planche, J.P., Chaverrot, P., Lapalu, L., Ponsardin, M., “Procede de preparation de compositions bitumen/polymere a resistance aux solvants petroliers amelioree, compositions ainsi obtenues et leur utilisation comme liant bituminuex”, Repubblique Française, Institut National de la Propriété Industrielle 2849047, 2002.
205. Scholten, E.J., Asphalt binders for porous pavements (to KRATON Polymers, USA), US 2009/0182074 A1, 2009, pp. 1-6.
206. Eidt, C.M. Jr., Gorbaty, M.L., Elspass, C.W., Peiffer, G., Thermoplastic elastomer-asphalt nanocomposite (to Exxon Research and Engineering Compnay), US Patent 5,652,284; 1997, pp. 1-6.
207. Yu, J.-Y., Wang, L., Zeng, X., Wu, S.-P., Li, B., Effect of montmorillonite on properties of SBS copolymer modified bitumen, *Polymer Engineering and* Science, Vol. 47, no. 9, 2007, pp.1289-1295.
208. Yu, J.-Y., Zeng, X., Wu, S.-P., Wang, L., Gang, L., “Preparation and properties of montmorillonite asphalts”, *Materials Science and Engineering A*, Vol. 447, no. 1-2, 2007, pp. 233-238.
209. Yu, J.-Y., Feng, P.-C., Zhang, H.-L., Wu, S.-P., “Effect of organo-montmorillonite on the aging properties of asphalt”, *Construction and Building Materials*, Vol. 23, no. 7, 2009, pp. 2636-2640.
210. Tao, Y.-Y., Yu. J.-Y., Li, B., Feng, P.-C., “Effect of different montmorillonite on rheological properties of bitumen/clay nanocomposites”, *Journal of South University of Technology*, Vol. 15, no. 1, 2008, pp. 172-175.
211. Kim, H., Yang, J.-F., Sekino, T., Lee, S.W., “Preparation and properties of

nanoclay/TPS/asphalt ternary binders", *Materials Science Forum*, Vol. 620-622, 2009, pp. 497-500.

212. Merusi, F., Nicoletti, A., Giuliani, F., Polacco, G., "Kerosene resistance of asphalt binders modified with crumb rubber: Solubiliy and rheological aspects", *Materials Structure,* Vol. 43, no. 9, 2010, pp. 1271-1281.
213. Schroeder, J.F., "Fire Resistant Asphalt Roofing", U.S. Patent 3,751,291 (to United States Gypsum Co., Chicago, U.S.A), 1-3, 1973.
214. Rashid, S.A., Bray, H.S., Boarini, E.J., "Fire Resistant Asphalt Roofing Shingles", U. S. Patent 4,082,885 (to United States Gypsum Co., Chicago, U.S.A), 1-5, 1978.
215. Graham, J., "Flame Resistant Asphaltic Compositions", U.S. Patent 4,512,806 (to Minnesota Mining and Manufacturing Company, St. Paul, U.S.A.), 1985, pp. 1-5.
216. Jolitz, R.J., Kirk, D.R., "Flame Retardant Asphalt Composition" U.S. Pat. No. 4,804,696 (to Tamko Asphalt Products, Joplin, U.S.A.), 1989, 1-3.
217. Jolitz, R.J., Kirk, D.R., "Flame Retardant Asphalt Composition", U.S. Pat. No. 5,102,463, (to Tamko Asphalt Products, Joplin, U.S.A.), 1-3, 1992.
218. Grube, L.L., Frankoksi, S.P., "Flame Retardant Bitumen" U.S. Patent 5,110,674 (to GAF Building Materials Corporation, New Jersey, U.S.A.), 1992, pp. 1-3.
219. Zimmerman, H., Plonese, D., Lilleston, R., Butera, M., Fire resistant asphalt roofing composition. U.S. Patent 5,326,797 (to GS Roofing Products Company Inc., Irving, U.S.A.), 1994, pp. 1-5.
220. Wagner, J.P., Mendez, C.L., Gidden, R.P., "Paving Asphalts: Environmental and Flammability Considerations", *Polymer-Plastics Technology and Engineering*, Vol. 34, no. 2, 1995, pp. 177-212.
221. Wang, L., He, X., Wilkie, C.A., "The Utility of Nanocomposites in Fire Retardancy", *Materials*, Vol. 3, no. 9, 2010, pp. 4580-4606.
222. Wu, S., Cong, P., Yu, J., Luo, X., Mo, L., "Experimental investigation of related properties of asphalt binders containing various flame retardants', *Fuel*, Vol. 85, no. 9, 2006, pp. 1298-1304.
223. Zhao, H., Li, H.-P., Liao, K.-J., "Study on Properties of Flame Retardant Asphalt for Tunnel", *Petroleum Science and Technology*, Vol. 28, no. 11, 2010, pp. 1096-1107.
224. Wu, S., Cong, P., Yu, J., Luo, X., Mo, L., "Experimental investigation of related properties of asphalt binders containing various flame retardants", *Fuel*, Vol. 85, no. 9, 2006, pp. 1298-1304.
225. http://www.azom.com/Details.asp?ArticleID=868
226. Asphalt Institute Superpave Series No. 1 (SP-1). **Performance Graded Asphalt Binder Specification and Testing**. Asphalt Institute, Lexington, Kentucky.
227. ASTM D 4402-84. Standard Method for Viscosity Determinations of Unfilled

Asphalts Using the Brookfield Thermosel Apparatus. In: Annual Book of ASTM Standards; 1987, 04.04, pp. 432-433.

228. ASHTO T 48-06. Flash and Fire Points by Cleveland Open Cup. In: Standard Specifications for Transportation Materials and Methods of Sampling and Testing; 2006, Part 2A: Tests T2-T215, pp. T48-5-T48-14.
229. ASTM Standard D 2872-97. Test method for effect of heat and air on moving film of asphalt (rolling thin - film oven test). In: Annual Book of ASTM Standards; 2004, 04.03, pp. 259-263.
230. AASHTO T 240-06. Effect of Heat and Air on a Moving Film of Asphalt (Rolling Thin Film Oven Test); 2006, Part 2B: Tests T 216-T 329, pp. T 240-1-T 240-10. 209.
231. ASTM Standard D 6521-03a. Practice for accelerated aging of asphalt binder using a pressurized aging vessel (PAV). In: Annual Book of ASTM Standards; 2004, 04.03, pp. 801-806.
232. D`Angelo, J., Dongre, R., “Superpave Binder Specifications and Their Performance Relationship to Modified Binders”, in: Proceedings of the Annual Meeting of Canadian Technical Asphalt Association, 2002, pp. 91-103.
233. Wasage, T.L.J., Cantu, M., Stastna, J., Polacco, G., Zanzotto, L., “Role of Viscosity in Dynamic Creep Tests in Conventional, Oxidized, and Polymer-Modified Asphalts”, *Transportation Research Record*, No. 1998, 2007, pp. 56-64.

Award Received

Silver Jubilee Celebration

INTERNATIONAL CONFERENCE ON ADVANCEMENT OF NANOSCIENCE AND NANOTECHNOLOGY (ICOANN - 2010)

March 1-3, 2010

Certificate of Participation

BEST PRESENTATION

This is to Certify that Dr./Mr./Ms. M. S. SURESHKUMAR, UNIVERSITY OF PISA, ITALY [NC-OP-07]

has ~~Participated~~ / Presented (Oral / ~~Poster~~) a Paper in the International Conference on Advancement of Nanoscience and Nanotechnology (ICOANN - 2010) Organized by the Department of Nanoscience and Technology, Alagappa University, Karaikudi - 630 003, India during March 1-3, 2010.

Prof. K. GURUNATHAN
CONVENER
ICOANN - 2010
MARCH 1 - 3, 2010
Department of NanoScience & Technology

Prof. R. JAYAVEL
Dr. R. JAYAVEL
DIRECTOR
CENTRE FOR NANOSCIENCE AND TECHNOLOGY
ANNA UNIVERSITY CHENNAI
CHENNAI-600 025, INDIA

Dr. R. ILANGOVAN
Organising Secretary
ICOANN - 2010
MARCH 1 - 3, 2010
Department of NanoScience & Technology

List of Publications

(2 + 1 + 5 + 6 = 14)

Journal (2)

1. **M.S. Sureshkumar**, J. Stastna, G. Polacco, S. Filippi, I. Kazatchov, L. Zanzotto, "*Rheological properties of Bitumen Modified by EVA-organo clay nanocomposites*", *Journal of Applied Polymer Science*, Vol. 118, No. 1, 557-565, 2010

2. **M.S. Sureshkumar**, S. Filippi, G. Polacco, I. Kazatchov, J. Stastna, L. Zanzotto, "*Internal Structure and Linear Viscoelastic Properties of EVA/Asphalt Nanocomposites*", European Polymer Journal, Vol. 46, No. 4, 621-633, 2010.

Book Chapter (1)

3. Giovanni Polacco*, Sara Filippi, Massimo Paci, **M.S. Sureshkumar**, Filippo Merusi and Felice Giuliani, Chapter 13: Fuel resistance of bituminous binders, In: Polymer Modified Bitumen: Preparation and Characterization, Edited by: Tony Mc Nally, © Woodhead Publishing Co., 2011.

Invited Lecture (5)

4. **M.S. Sureshkumar**, Polymer Modified Asphalt Nanocomposites: New Class of Pavement Materials, International Conference on Advanced Materials and its Applications (INCAMA-2011), Kalasalingam University, Krishnankoil, India, Mar 04-05, 2011.

5. **M.S. Sureshkumar**, Special Address on 'Polymer Asphalt Nanocomposites', First National Science Day Celeberation – 2011, Anna University of Technology, Madurai, India, Feb 28, 2011.

6. **M.S. Sureshkumar**, Polymer Modified Asphalt, National Seminar on Applications of Nanomaterials in Civil Engineering' K.L.N. College of Information Technology, Pottappalayam, Sivagangai, India, Mar 15, 2010.

7. **M.S. Sureshkumar,** Polymer Modified Asphalt Nanocomposites (PMAN): Rheological Properties, International Conference on Synthesis, Consolidation, Characterization and Modelling of Nanomaterials (ICON-2010), PSG College of Technology, Coimbatore, India, Mar 05-06, 2010.

8. **M.S. Sureshkumar,** "Polymer Modified Asphalt" National Seminar in 'Advanced Developments in Polymer Technology (APTECH'10), Ultra College of Engineering and Technology for Women, Madurai, India, Feb 19, 2010.

Conference (6)

9. Şevket GÜMÜŞTEKİN, Ali TOPAL, **M.S. Sureshkumar**, G. Polacco, *Classification on polymer modified images using textural features,* 5th Euroasphalt and Eurobitume Congress, Istanbul, Turkey, June 13-15, 2012 (submitted).

10. **M.S. Sureshkumar**, *Polymer Modified Asphalt Nanocomposites (PMAN): Flammability Properties,* International Conference on Functional Polymers (ICFP-2011), National Institute of Technology, Kozhikodu, India, Jan 28-30, 2011.

11. **M.S. Sureshkumar**, G. Polacco, *Polymer Modified Asphalt Nanocomposites (PMAN): Fuel Resistance,* International Conference on Advancement of Nanoscience and Nanotechnology (ICOANN-2010), Alagappa University, Karaikudi, India, NC-OP-07, pp. 42, Mar 01-03, 2010.

12. **M.S. Sureshkumar**, G. Polacco, *Polymer Modified Asphalt Nanocomposites (PMAN): Preparation and Characterization*, International Conference on Nanoscience and Nanotechnology (ICONN-2010), SRM University, Kattankulathur, India, pp. 40, Feb 24-26, 2010.

13. ***M.S. Sureshkumar***, F. Merusi, S. Filippi, G. Polacco, *Preparation and Characterization of EVA/Asphalt Nancomposites*, XIX Italian Conference Of Macromolecular Science Technology 2009, Milano, Italy, Sep 13-17, 2009.

14. **M.S. Sureshkumar**, Sara Filipi, Dario Biondi and Giovanni Polacco, *EVA/Asphalt Nanocomposites (EASN): Preparation and Properties*, International Conference on Nanotechnology and Advanced Materials (ICNAM) – 2009, held at University of Bahrain, Bahrain, NT-NC-2, 138, May 4-7, 2009.